Dissertation

Submitted to the

Combined Faculties for the Natural Sciences and for Mathematics

of the Ruperto-Carola University of Heidelberg, Germany

for the Degree of

Doctor of Natural Sciences

presented by

Hamidreza Hashemi, M.Sc. in Virology

born 6th March 1983 in Arak, Iran

Oral examination: 16th February 2017

Point Mutations in Nonstructural Coding Sequences of Rat H-1 Parvovirus and Consequences for Virus Fitness

Referees: Prof. Dr. Martin Müller

Prof. Dr. Ralf Bartenschlager

The present study was conducted in the lab of Dr. Christiane Dinsart, Division of Tumor Virology (Head: Professor Dr. Jean Rommelaere) between March 2014 and February 2017 and supported by a scholarship from the international Ph.D. program of the German Cancer Research Center (DKFZ) in Heidelberg.

Acknowledgment

Foremost, I would like to express my gratitude to my supervisor Dr. Dinsart for supporting me in all the time of research and writing of this thesis. Besides, I would like to thank Professor Jean Rommelaere for hosting me and giving me the opportunity to pursue my Ph.D. project in his division. A sincere thank you also goes to the members of my Thesis Advisory Committee; Professor Martin Müller, Professor Ralf Bartenschlager and Dr. Dirk Grimm for their insightful comments which guided me throughout this study. Very kind thanks go to the rest of my thesis defense committee; Dr. Volker Lohmann and Dr. Pierre-Yves Lozach. I thank my fellow labmates Alexandra Stroh-Dege, Renate Geibig, Carsten Geiß, Carles Cornet Bartolomé and Domenico Sorrentino, people in the lab of Dr. Jürg Nüesch: Clemens Bretscher and Claudia Plotzky, people in the lab of Dr. Antonio Marchini: Dr. Amit Kulkarni, Dr. de Oliveira, Dr. Junwei Li, Annabel Grewenig and Tiina Marttila. I would like to thank Ellen Burkard for taking care of the paperwork during my Ph.D., my friends in the lab of Dr. Marco Binder: Julia Wolanski, Sandra Bastian, Dr. Antje Reuter, Christopher Dächert, Dr. Joschka Willemsen and Jamie Frankish, the lab of Dr. Richard Harbottle: Matthias Bozza and Matthias Ehrbar, and all the lab members of Professor Martin Müller for their technical support and scientific discussions.

I would like to express my sincerest gratitude to my dear wife Dr. Somayeh Pouyanfard, not only for her scientific support but also for sharing all the moments with me and standing by my side through thick and thin.

I am also very grateful to my parents for encouraging me throughout my education and supporting me spiritually throughout my life. Last but not the least, I would like to express my deep appreciation for the endless support, kind and understanding spirit of my wife's family.

Summary

Some rodent parvoviruses including rat H-1PV virus are of particular importance for cancer therapy because of their intrinsic oncotropism owing to strict dependence on DNA replication machinery and other cellular factors that are provided by cells only when going through S phase of the cell cycle, a hallmark of transformed cells. Isolation of mutant viruses that replicate more efficiently in cancer cells has been used as a strategy to improve oncolytic properties of viruses. Previously in our lab, a fully infectious H-1PV mutant containing a 114 nt in-frame deletion in NS coding sequences (DelH-1PV) was analyzed by *Weiss et al*. This mutant exhibited key fitness features including enhanced infectivity *in vitro* and stronger anti-tumor activity *in vivo* compared to wt virus. Significant improvements in both early and late steps of the virus cycle were observed including a more efficient virus binding and uptake by host cells leading to earlier viral DNA replication, and earlier/faster nuclear export of infectious virions. In the current study, the effects of the above-mentioned deletion on virus fitness was further investigated by introducing point mutations in this region. The mutations clustered in the NS1/2-coding DNA sequence corresponding to the deletion sequence in DelH-1PV. Four mutants (H1-PM-I, H1-PM-II, H1-PM-III and H1-DM) were generated in which either NS2 (PM-II and PM-III) or NS1 and NS2(PM-I and DM) were modified and analyzed for their fitness phenotype. Our results show that the mutations PM-I, PM-II and DM improved some early steps of the infection cycle indicated by more efficient cell uptake of the virus particles. Viral DNA replication was stimulated by these mutations leading to higher production of progeny virions and better spread of the virus. To analyze the fitness effects of NS1 mutation (Y595H) independently of NS2, NS2-null derivatives were created. Our data showed that the $NS1^{Y595H}$ mutation stimulates viral DNA replication and spread in the absence of NS2. In contrast, PM-III mutation in NS2 (L153M) compromised virus replication and spread, indicated by a small plaque phenotype, lower yield and infectivity of the progeny particles. However, cellular binding and uptake of the virus particles were not impaired by this mutation. A strong *cis* effect of PM-III mutation on capsid production was observed at a post-transcriptional level. Altogether our results suggest that PM-III mutation may interfere with efficient translation of downstream open reading frame (capsid ORF) and efficient splicing of VP1/VP2 pre-mRNA leading to decreased and imbalanced production of the capsid proteins and consequently inefficient generation of pre-assembled capsids.

Zusammenfassung

Einige Nager-Parvoviren, darunter auch das H-1PV der Ratte, sind von speziellem Interesse für die Krebstherapie dank ihres intrinsischen Oncotropismus, der sie von der DNA-Replikationsmaschinerie abhängig macht und von anderen zellulären Faktoren, die von der Zelle nur während der S-Phase des Zellzyklus bereitgestellt werden – ein Kennzeichen transformierter Zellen. Die Isolation mutanter Viren mit gesteigertem Replikationspotential in Krebszellen wurde als Strategie verwendet, um die oncolytischen Eigenschaften des Virus zu verbessern. In einer vorhergehenden Arbeit unseres Labors untersuchten Weiss et al einen voll-infektiösen Mutanten von H-1PV, der eine 114 nt in-frame Deletion in der NS-kodierenden Sequenz (DelH-1PV) trug. Verglichen mit dem wt Virus zeigte diese Mutante entscheidende Fitness-Eigenschaften, darunter eine erhöhte Infektiosität *in vitro* und eine verstärkte anti-Tumor Aktivität *in vivo*. Signifikante Verbesserungen wurden beobachtet sowohl in frühen als auch in späten Schritten des viralen Zyklus, einschließlich einer effizienteren Bindung und Aufnahme durch Wirtszellen, was zu einer früheren DNA Replikation führte, und früherer/schnellerer Export von infektiösen Virionen aus dem Nucleus mit sich trug. In der aktuellen Studie wurden die Effekte der oben-beschriebenen Deletion auf die Fitness des Virus weiter untersucht indem Punktmutationen in diese Region eingeführt wurden. Die Mutationen befanden sich in der NS1/NS2-kodierenden DNA Sequenz, die der Deletions-sequenz im DelH-1PV entspricht. Vier Mutanten (H1-PM-I, H1-PM-II, H1-PM-III und H1-DM) wurden hergestellt, bei denen entweder NS2 (PM-II und PM-III) oder NS1 und NS2 (PM-I und DM) verändert wurden. Anschließend wurde der Fitness-Phänotyp der Mutanten untersucht. Unserer Ergebnisse zeigen, dass die Mutationen PM-I, PM-II und DM einige frühe Schritte des Infektionszyklus verbesserten, was sich durch eine effizientere Aufnahme der Virenpartikel äußerte. Die virale DNA Replikation wurde durch diese Mutationen gefördert, was zu einer erhöhten Produktion von Nachkommenviren und einer verbesserten Verbreitung des Virus führte. Um die Fitness-assoziierten Effekte der NS1 Mutation (Y595H) unabhängig von NS2 zu untersuchen, wurden NS2-null Mutanten hergestellt. Unsere Daten zeigten, dass die $NS1^{Y595H}$ Mutation in Abwesenheit von NS2 die virale DNA Replikation und die Verbreitung des Virus fördert. Die PM-III Mutation in NS2 (L153M) beeinträchtigte dagegen die virale Replikation und Verbreitung, was sich in einem Phänotyp von kleinen Plaques, geringerer Ausbeute und geringerer Infektiosität der Nachkommenviren äußerte. Allerdings wurde die zelluläre Bindung und Aufnahme der Virenpartikel nicht durch diese Mutation behindert. Auf post-transkriptioneller Ebene wurde ein starker *cis* Effekt der PM-III Mutation beobachtet, der sich auf die Produktion von Kapsiden auswirkte. Zusammengefasst weisen unsere Ergebnisse darauf hin, dass die PM-III Mutation eine effiziente Translation von downstream liegenden offenen Leserastern (Kapsid-OLR) und effizientes Splicing von VP1/VP2 pre-mRNA beeinträchtigt, was zu einer verringerten und unausgeglichenen Produktion von Kapsidproteinen führt und eine uneffiziente Herstellung von prä-assemblierten Kapsiden zur Folge hat.

Table of Contents

Table of Figures

Chapter 1 (Introduction)

Chapter 3 (Results)

Chapter 1

Introduction

1.1 Taxonomy of Parvoviruses

Parvoviruses are small, non-enveloped viruses with a linear, single-strand DNA (ssDNA) genome of about 5 kb that is assembled within an icosahedral capsid (18-26 nm). According to the latest (2015) report of International Committee of Taxonomy of Viruses (Cotmore et al., 2014), the family *Parvoviridae* (from *Parvus*-Latin for ‘‘small’’) contains two subfamilies: *Parvovirinae* and *Densovirinae*. The latter infect invertebrates and will not be described in detail. The *Parvovirinae* are divided into eight genera: *Amdoparvovirus, Aveparvovirus, Bocaparvovirus, Copiparvovirus, Dependoparvovirus, Erythroparvovirus, Tetraparvovirus and Protoparvovirus.* Human Bocaviruses has been associated with lower respiratory tract and gastrointestinal infections, predominantly in children (Kantola et al., 2011) and Erythroviruses include the B19 virus associated with the fifth disease in children (also known as slapped cheek syndrome) and transient aplastic crisis (TAC) in patients with sickle cell disease. The Dependoviruses include adeno-associated viruses (AAVs) which integrate into the host cell genome at specific sites and required co-infection of cells with a helper virus (adenovirus or herpesvirus) in order to have a productive replication. However, AAVs are not clearly associated with any pathology. The genus *Protoparvovirus* comprises important veterinary pathogens with a high mortality rate in young dogs and cats characterized by enteritis, panleukopenia and cerebellar ataxia, and porcine parvovirus is the most common cause of diagnosed porcine abortion causing serious economic losses in the swine industry (J. SZELEI, 2006). Rodent parvoviruses include mouse parvovirus 1 (MPV1), prototype and immunosuppressive strains of minute virus of mice (MVMp and MVMi respectively) and rat H-1 parvovirus (H-1PV). In order to

replicate their DNA, most parvoviruses require the host cell to go through S phase of cell cycle but they do not induce S phase entry. In case of AAVs, co-infection with a helper virus can stimulate S phase entry. The rat H-1PV, a member of the genus Protoparvovirus and closely related to MVM, was investigated in this study. The structure and molecular biology of parvoviruses described hereafter, is mostly focused on rodent parvoviruses MVM and H-1PV.

1.2 Virion Structure and Genomic Organization of Parvoviruses

1.2.1 Capsid Structure

Parvovirus virions are very small (18-28 nm in diameter), non-enveloped and uniquely dense and robust particles with the simplest form of icosahedral symmetry (T=1) (Figure 1). Three-dimensional capsid structures of protoparvoviruses including MVM and H1-PV have been resolved by X-ray crystallography (Agbandje-McKenna et al., 1998; Llamas-Saiz et al., 1996). The capsid is constructed from 2-3 forms of VP protein called VP1, VP2 and VP3. The largest capsid protein, designated VP1, has a molecular weight of 83 kDa and is found at 10 copies per capsid. Although VP1 is dispensable for capsid assembly and DNA packaging, it is absolutely required for infectivity (Tullis et al., 1993), since it carries a phospholipase A2 (PLA2) domain to breach the endosomal membrane (Farr et al., 2005; Girod et al., 2002; Zadori et al., 2001), and a conventional nuclear localization signal (NLS) made of clusters of basic amino acids which mediate the nuclear entry of the virus (Lombardo et al., 2002; Vihinen-Ranta et al., 2002). An N-terminally truncated form (142 amino acids shorter) of VP1 called VP2, with a molecular weight of 63 kDa, is the main structural component of the virions with 50 copies per capsid. The core structure of VP polypeptides in the capsid is based on eight antiparallel β-strands connected by large loops which constitute most of the capsid surface (Chapman and Rossmann, 1993) and are involved in host cell receptor interaction and form conformational neutralizing epitopes. Trimeric subunits of VP1 and VP2 are assembled into procapsids and ssDNA is packaged through a pore at one of the 12 five-fold axes which connect the surface and the interior of the capsid. Each

pore is located at the center of a cylinder structure which is created by juxtaposition of antiparallel β-ribbons from the surrounding VP subunits and plays crucial functions both at early and late phase of infection (Figure 1). Indeed, the pore is the extrusion portal for VP1 and VP2 N-termini during entry which is required for endosomal escape and successful transport of the particles to nucleus, and is also the portal for packaging and release of the viral genome. Interestingly, the entire genomic DNA is not contained within the capsid.

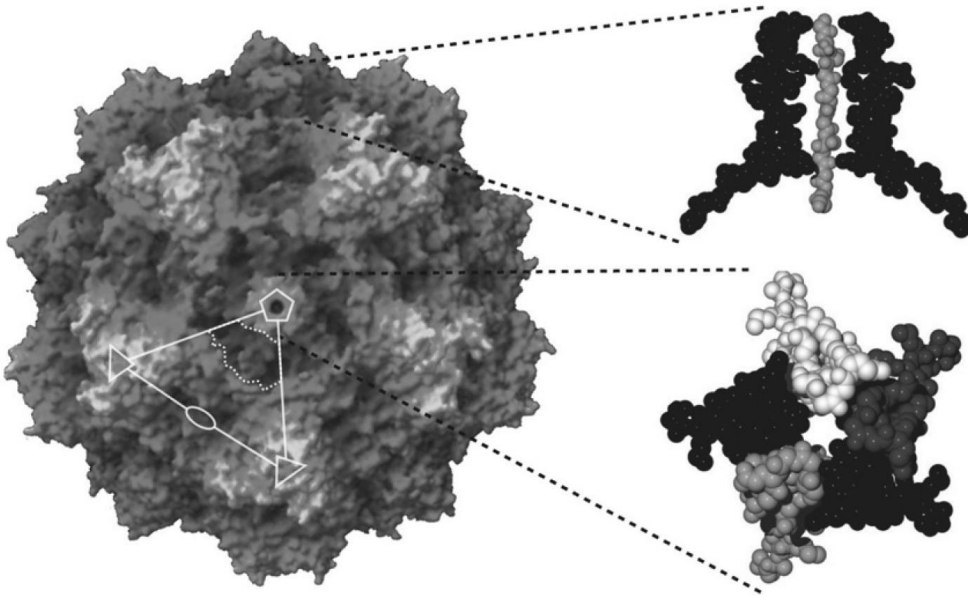

Figure 1. Morphology of the parvovirus particle. Left: space-filling model of MVM particle with a five-fold symmetry axis at center (pentagon). The three-fold spikes and a two-fold axis are indicated by triangles and an ellipse respectively. Within the five-fold axis, a cylinder containing a narrow central pore is seen, through which genomic DNA is packaged and one VP2 N-terminus is externalized subsequently which is cleaved to VP3 during virion entry. The five-fold axis is surrounded by a depression called “canyon” with an unknown function. Upper right: cross-section of the five-fold cylinder, showing only two of the five β-ribbons (lower right) which form the channel structure. The VP2 N-terminal residues within the pore are indicated in gray (Cotmore and Tattersall, 2007).

The DNA packaging proceeds in a 3’-to-5’ direction by helicase activity of NS1 protein, leaving a 5’-end sequence (about 24 nucleotides) called “tether” sequence projecting through the capsid shell. A single molecule of viral NS1 protein remains covalently attached to this end (Figure 2); however, the function of this sequence and attached NS1 is not clearly understood (Cotmore and Tattersall, 1989). The glycine-rich N-

terminal region (25 amino acids) from a single VP2 molecule per five-fold channel is externalized from DNA-full particles (Agbandje-McKenna et al., 1998; Kontou et al., 2005; Tsao et al., 1991) and not empty capsids (Cotmore et al., 1999) or virus-like particles (VLPs) (Hernando et al., 2000). Indeed, both VP1 and VP2 N-termini are completely sequestered within empty procapsids, but concomitant with packaging of ssDNA, a proportion of the serine-rich VP2 N-termini (1 molecule in each five-fold axis) are externalized at the virion surface and become accessible to protease digestion (leaving VP3) and antibodies (Cotmore and Tattersall, 2005a). These domains act as nuclear export signals, at least in some cells, to direct progeny virions out of the nucleus before cell lysis (Maroto et al., 2004). Furthermore, a deep depression called "canyon" surrounds each pore at five-fold axis but its function is not known (Figure 1).

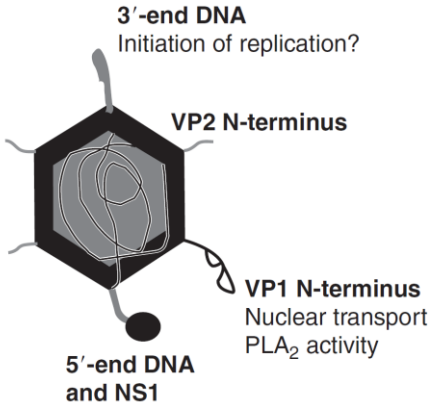

Figure 2. Schematic depiction of critical capsid structures. The phosphorylated N-termini of several VP2 subunits are externalized through the five-fold axes of full capsids and serve as export signals, at least in some cells. They are cleaved during entry of the virus particles by endosomal proteases. The N-terminal region of VP1 contains a domain with PLA2 activity that is critical for infectivity. This capsid-tethered domain is deployed during entry to breach the endosomal membrane which might release the virus into cytoplasm. Furthermore, the externalized VP1 N-terminus serves as a NLS to direct the incoming virions toward nucleus. A short DNA sequence (~24 nucleotides) at 5'-end of the virus genome is exposed on the surface of the capsid and one molecule of NS1 protein is covalently linked to it via a tyrosine residue. The capsid-tethered NS1 is removed during entry of the virus particles by endosomal nucleases. The 3'-end of the viral genome can be externalized *in vitro* after specific treatments and this might occur *in vivo* as well, resulting in DNA replication without complete capsid disassembly (Maija Vihinen-Ranta, 2006).

During productive infection, a substantial number of empty capsids and defective interfering (DI) particles are produced in addition to infectious virions. Full capsids go

through a “maturation” step which can be detected as a small change in the buoyant density of the particles from 1.45 to 1.41 g/cm3 (Figure 3). Parvovirus virions are remarkably robust and stable partly due to tight interaction of genomic DNA bases, mostly involving hydrogen bonds, with side chains from amino acids in the inner surface of the capsid (Agbandje-McKenna et al., 1998; Xie and Chapman, 1996). The virions can tolerate high temperatures and a wide range of pH from 3 to 9. However, they can be inactivated by formalin, β-propiolactone and oxidizing agents and mostly by UV.

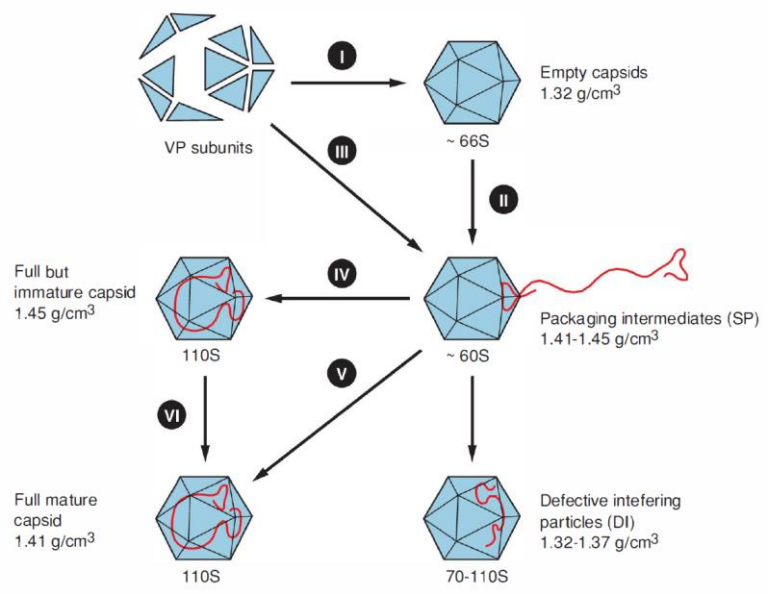

Figure 3. Parvovirus capsid assembly and DNA packaging. The VP1 and VP2 polypeptides are primarily assembled into heterotrimeric subunits which form empty capsids once transported into the nucleus. A fraction of empty capsids is filled up with progeny ssDNA that is displaced from replicative forms of DNA through helicase activity of viral NS or Rep proteins to form full particles with a slightly higher buoyant density (1.42-1.45 g/cm^3). During the course of infection, not only excessive amounts of empty capsids, but also particles with partial genomes called “defective interfering” (DI) particles are produced. Full capsids go through final maturation steps indicated by a small change in the buoyant density of the particles from 1 .45 g/cm^3 to 1 .41 g/cm^3 (Ke n n eth I . B e rn s 2013).

1.2.2 Genome Organization

Parvovirus genome consists of a linear ssDNA with palindromic telomeres known as inverted terminal repeats (ITRs) forming hairpin structures which range in size from approximately 120–420 bases and required for DNA replication. The ITRs vary

substantially across parvoviral genera in size, sequence and structure and can be symmetric (e.g. AAV2, B19) or asymmetric (e.g. MVM, H-1PV) and they provide most of the cis-acting elements required for viral genome replication and encapsidation. In the *Protoparvovirus* genus, the two terminal hairpins are different with respect to both sequence and secondary structure, thereby allowing differential replication initiation and encapsidation of two DNA strands (Figure 4). Also, in these viruses the left palindrome is usually shorter (120 nt) than the right one (250 nt). The folded structure of ITRs primes the conversion of ssDNA to dsDNA and plays a crucial role in DNA replication through a single-strand displacement mechanism termed “rolling hairpin replication”. While MVM and H-1PV package predominantly negative-sense DNA, LuIII virus (a related rodent *protoparvovirus*) and members of the *Dependovirus* and *Erythrovirus* genera, encapsidate strands of both polarities with approximately equal efficiency. This strand selectivity is not caused by any strand-specific packaging signal, but it is determined by differential rates of initiation from the two viral replication origins (Cotmore and Tattersall, 2005b). In most parvoviruses, the left half of the genome (3’-end of the negative-strand DNA) encodes non-structural proteins and the right half encodes capsid proteins. The organization and regulatory elements of genome of rat H-1PV is very similar to MVM (Figure 4).

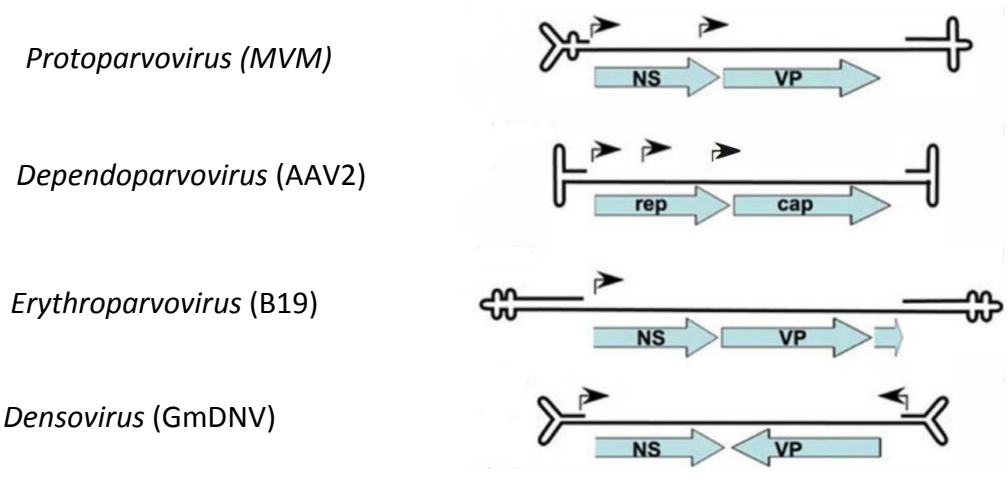

Figure 4. Genome organization of different subfamilies within the family *Parvoviridae*. The terminal hairpins, promoters (small arrows) and major open reading frames (large arrows) containing non-structural (NS) and capsid (VP) genes are shown (Kenneth I. Berns 2013).

In the *Protoparvovirus* genus, there are two overlapping transcription units under control of two promoters located at map units 4 and 38 (designated P4 and P38 respectively) and a single polyadenylation signal near the right end (5'-end in the negative-sense strand) of the genome (Figure 5). The viral proteins are encoded by three major transcripts called R1 (4.8 kb), R2 (3.3 kb) and R3 (2.8 kb). The R1 transcript is driven by the early constitutive p4 promoter and encodes the large nonstructural protein NS1. The small nonstructural protein NS2 is encoded by R2 mRNA produced from R1 through alternative splicing of the large intron (Qiu Jianming, 2006). The P4 promoter is a strong constitutive promoter and contains binding sites for cellular transcription factors such as CREB, E2F, Ets, SP1 (GC-box) and Smad4 (Ahn et al., 1989; Deleu et al., 1999; Dempe et al., 2010; Fuks et al., 1996; Gu et al., 1995; Perros et al., 1995) located upstream and downstream of a TATA box. In addition to binding to its recognition sequence on virus genome, SP1 also interacts with NS1. The capsid proteins as well as a late nonstructural protein called small alternatively translated (SAT) protein are encoded by R3 transcripts generated under control of P38 promoter (Zadori et al., 2005). This promoter overlaps with NS-coding sequences and in addition to core elements such as TATA- and GC-box contains a transactivation response (*tar*) element where NS1 protein binds and induces the expression of capsid proteins (Gu et al., 1992). The capsid of rodent parvoviruses such as MVM and H-1PV is composed of three proteins designated VP1, VP2 and VP3. The minor capsid protein VP1 is the largest in size and lowest in quantity and is expressed as an N-terminally extended form of VP2. During maturation of the full capsids, a peptide from the N-terminus of VP2 which is exposed outside the full (DNA containing) capsids, is cleaved proteolytically to form VP3. A common polyadenylation signal near the right end of the genomic DNA (nt 4908) controls termination of all viral transcripts.

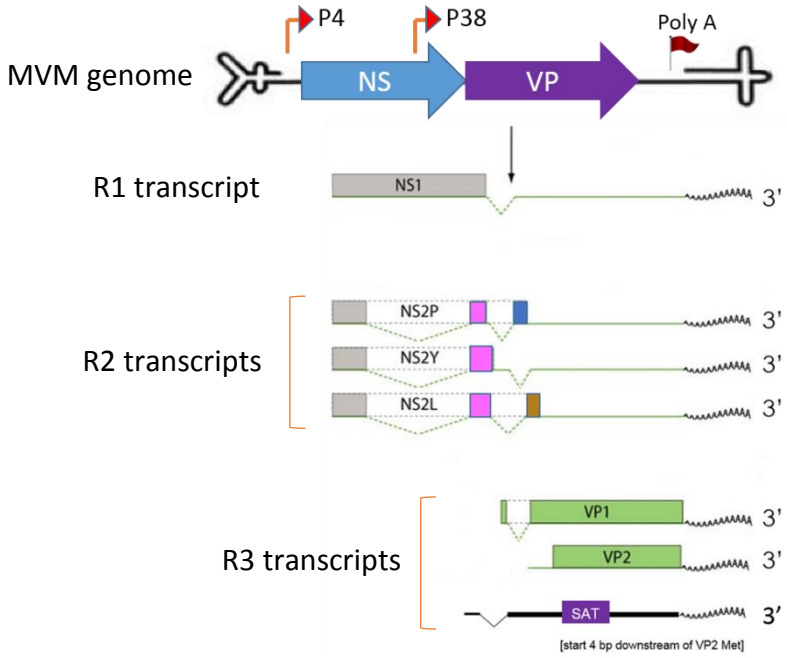

Figure 5. Transcripts generated from MVM genome. Three main transcripts called R1, R2 and R3 are transcribed from viral early P4 and late P38 promoters. The R1 encodes NS1 protein and a proportion of it is spliced to generate three forms of R2 transcripts via alternative splicing, expressing three C-terminally different isoforms of NS2 protein (NS2P, NS2Y and NS2L). The late mRNAs (R3) are transcribed under control of P38 promoter that is transactivated by NS1 protein. These mRNAs are translated into viral capsid proteins (VP1 and VP2) and a small non-structural protein called "SAT". All viral mRNAs are terminated at a single poly-adenylation site located at the right end of the genome.

1.3 Gene Expression of Rodent *Protoparvoviruses*

1.3.1 Non-Structural Proteins (NS1, NS2 and SAT)

Before viral transcription, the 3'-end hairpin structure primes complementary-strand DNA synthesis to generate a duplex replicative intermediate that serves as a template for viral transcription. This strictly restricts the parvovirus replication to actively proliferating cells. The early nonstructural proteins NS1 and NS2 are expressed from alternatively spliced mRNAs under control of constitutive P4 promoter in the left half of the genome (Figure 5). The splicing efficiency of the precursor mRNA (R1) and differential stability of these proteins determines their steady-state accumulation in infected cells. NS1 is a large phosphoprotein (672 aa, ~83 kDa) with a relatively long half-life (> 6h) which mainly accumulates in nucleus and has pleiotropic functions in the course of infection. In contrast to autonomous parvoviruses, large and small

nonstructural proteins of AAVs (Rep proteins) are produced from separate mRNAs under control of two distinct promoters. Both NS1 and NS2 proteins undergo post-translational modifications especially phosphorylation. However, the phosphorylation pattern of NS1 is believed to be temporally regulated in the course of infection. Cellular protein kinase C (PKC) plays a key role in regulation of different NS1 functions (e.g. helicase, ATPase, DNA binding and transcriptional activation) through phosphorylation of specific serine and threonine residues (Corbau et al., 2000; Nuesch et al., 1998a; Nuesch et al., 1998b). For instance, helicase activity of NS1 is regulated by phosphorylation at T435 and S473 by cellular PKC-λ (lambda) (Dettwiler et al., 1999; Nuesch et al., 2003). Recently, it was reported that acetylation maybe also involved in modulating NS1 functions particularly DNA binding, transactivation of P38 promoter and cytotoxicity (Li et al., 2013). An ATP-binding site in NS1 is involved in oligomerization of this protein (Nuesch and Tattersall, 1993). NS1 binds to the viral DNA site-specifically [$(ACCA)_{2-3}$] (Cotmore et al., 1995) and also unwinds the DNA downstream of the replication fork by its helicase activity (Nuesch et al., 1992; Wilson et al., 1991). This recognition site is not only present in origins of replication (in ITRs) and tar element (located upstream of P38 promoter) but is also found at several sites throughout the genome, at least once every hundred base pairs (Cotmore et al., 2007) and these are believed to have roles in viral chromatin structure and progeny ssDNA encapsidation (Kestler et al., 1999a). During DNA replication, NS1 introduces a site-specific nick in DNA via a *trans*-esterification reaction which leaves NS1 covalently bound to the 5'-end of the DNA via a "linking tyrosine" (Cotmore and Tattersall, 1989) and creates a new 3'-end that primes the DNA synthesis by cellular DNA polymerase δ in a unidirectional rolling circle mechanism. It is estimated that about 0.5% of the NS1 in MVM-infected cells is covalently attached to the 5'-ends of DNA replicative forms and progeny ssDNA (Cotmore and Tattersall, 1988). The genome-linked NS1 molecule and its tethered 5'-end genomic DNA sequence on the capsid exterior are cleaved off incoming virus particles during trafficking through endosomal compartment, most likely by lysosomal proteases and nucleases, and later on restored during DNA replication. In order to introduce the nick, NS1 requires interaction of a cellular

transcription factor called parvovirus initiation factor (PIF) with two “ACGT” sites on viral DNA (Christensen et al., 1997). This interaction partner binds the viral origin of replication in the left hairpin upstream of NS1 recognition site, resulting in formation of a ternary complex (NS1-PIF-DNA) essential for nicking reaction. Indeed, elimination of PIF-binding site from left hairpin of MVM genome is lethal to virus replication and results in accumulation of the 10kb dimeric replicative form (dRF) (Burnett and Tattersall, 2003). Through interacting with cellular factors involved in DNA replication such as the single-strand DNA-binding protein, RPA, NS1 usurps the cellular replication machinery for preferential amplification of the viral genome (Christensen and Tattersall, 2002). The DNA replication proceeds only in the S phase of the cell cycle in distinct sub-nuclear structures known as autonomous parvovirus replication (APAR) bodies (Bashir et al., 2001; Cziepluch et al., 2000) where a variety of viral (NS1, NS2) and cellular proteins (e.g. DNA polymerases α and δ, PCNA, RPA and cyclin A) come together. Also, a cellular protein called survival motor neuron (SMN) was shown to interact with NS1 and colocalize in these structures (Young et al., 2002). Through ATP-dependent binding to the so-called transactivation region (*tar* element) located upstream of P38 promoter (Lorson et al., 1996), mediated by its N-terminal DNA binding domain, NS1 also serves as a transcription factor which induces the expression of capsid proteins via its acidic C-terminal domain (Legendre and Rommelaere, 1994). Indeed, a multi-component transactivation complex is formed in which NS1 engages in several interactions with both general (*e.g*. TBP and TFIIA) and specific (*e.g*. SP1) cellular transcription factors. For instance, SP1 binds upstream of TATA box and directly interacts with NS1 bound to *tar* element of p38 promoter (Krady and Ward, 1995).

Upon infection of cells with H-1PV, a series of morphological changes (e.g. rounding and detachment of cells) called cytopathic effects (CPE) that are induced mainly by NS1 expression (Anouja et al., 1997). Also, infection with prototype strain of MVM (MVMp) has been shown to induce cell cycle arrest in a p53-dependent manner (De Beeck et al., 2001). However, the exact molecular mechanism(s) of the cell death by autonomous parvoviruses are not well understood. These viruses are generally

believed to induce different death pathways in different host cells. For example, MVMp kills murine fibroblasts (A9 cell line) through necrosis while the sole expression of nonstructural proteins of H-1PV can activate caspases and induce apoptosis in a permissive human monocyte cell line U937 (Rayet et al., 1998). It was suggested that NS1 can induce single-strand DNA breaks in the cellular chromatin and block the cell DNA replication (DeBeeck and CailletFauquet, 1997). Also, the sole expression of NS1 protein from H1PV was able to induce apoptosis in transformed human cells via accumulation of reactive oxygen species (ROS) (Hristov et al., 2010). Through accumulation of lysosomal Cathepsins in the cytosol of infected cells, H1PV was reported to trigger cell death in glioma cells (Di Piazza et al., 2007). Although a distinct cytotoxicity domain has not been found in NS1 protein, mutagenesis analysis of two consensus PKC phosphorylation sites within the C-terminal region of NS1 (T585 and S588) implicated this region in regulation of the cytotoxic properties of this protein in MVM infection of mouse cells (Daeffler et al., 2003). For MVM, direct interaction of NS1 with cellular enzymes such as the catalytic subunit of casein kinase (CKIIα) and tropomyosin has been suggested to mediate rearrangements and destruction of cellular microfilaments and interference with intracellular CKII signaling. Indeed, NS1 may act as an adaptor protein and bridge CKIIα and tropomyosin, altering phosphorylation pattern of tropomyosin which mediates cytoskeletal alterations and cell death (Nuesch and Rommelaere, 2006, 2007). Mammalian cells are frequently exposed to various kinds of intrinsic and extrinsic stresses such as reactive oxygen species (ROS), by-products of normal oxygen metabolism, and UV or ionizing radiation which can damage the DNA (e.g. double-strand DNA breaks) (Lindahl and Barnes, 2000). A complex pathway termed DNA damage response (DDR) has evolved to protect cells against lethal DNA damage and provide genomic stability (Jackson and Bartek, 2009; Polo and Jackson, 2011). Infection of cells with MVM (Adeyemi et al., 2010; Adeyemi and Pintel, 2014), H-1PV (Hristov et al., 2010) and human B19 parvovirus (Lou et al., 2012) has been shown to induce DDR, as suggested by phosphorylation of several factors such as H2AX (then called γ-H2AX), Chk2 and p53 which are recruited and colocalize with NS1 in APAR bodies within MVM-infected cells (Adeyemi et al., 2010).

Although expression of NS1 protein *per se* is involved in DDR, probably by ROS induction, nicking the cellular genomic DNA and resolving the viral concatemeric DNA replicative forms, at least in MVM, viral DNA replication is the main player in this process involving ATM signaling pathway. It is believed that DDR and ATM signaling pathway are hijacked by MVM for DNA replication.

In contrast to NS1, NS2 is a small protein (188 aa, ~25 kDa) which predominantly is localized in cytoplasm with only non-phosphorylated form found in nucleus (Cotmore and Tattersall, 1990b). It has a relatively short half-life (~1 h) and mostly accumulates during early phase of infection but is degraded quickly by proteasomes in a ubiquitin-independent manner, resulting in significant reduction in steady-state levels of this protein late in infection (Miller and Pintel, 2001). Three isoforms of NS2 protein which differ in their C-terminal hexapeptide sequences are generated from R2 primary transcript due to the use of two pairs of alternative 5' and 3' splice sites bordering the small intron. They are designated, in order of abundance, NS2P (major isoform), NS2Y (minor isoform) and NS2L (rare isoform), with NS2P and NS2Y being expressed at 5:1 ratio. However, the functional significance of NS2 regulation, and production of three isoforms of this protein needs to be determined. Although NS2 proteins are dispensable for productive virus replication in transformed human cells (Naeger et al., 1990), particularly NS2P isoforms is essential for productive replication in cells derived from its natural rodent host (Li and Rhode, 1991; Ruiz et al., 2006).

Several functions have been reported for NS2 protein such as capsid assembly (Cotmore et al., 1997), DNA replication (Naeger et al., 1990) and translation of viral mRNAs through interaction with 3'-UTR sequences (Li and Rhode, 1993; Naeger et al., 1993). Although small nonstructural proteins of AAV2 (Rep52/40) physically interact with capsids (Dubielzig et al., 1999) and are directly involved in packaging of single-stranded DNA via their helicase activity (King et al., 2001), no enzymatic activity or direct interaction with MVM capsids have been reported for NS2 polypeptides. Indeed, our knowledge about NS2 functions is deduced from phenotype characterization of NS2-null viruses when the protein is not expressed; hence the mechanism by which

NS2 exerts its functions, particularly in capsid assembly and DNA replication, is not well understood. A few cellular interaction partners have been identified for NS2 protein of MVM and H-1PV. In particular, NS2 binds a nuclear export factor termed chromosome region maintenance 1 (CRM1) also known as exportin-1, mediating nuclear egress of MVM progeny virions from mouse cells prior to cell lysis (Eichwald et al., 2002; Miller and Pintel, 2002b). Interestingly, supraphysiological nuclear export signal (NES) of NS2 interacts with CRM1 with a very high affinity, compared to regular leucine-rich NESs (Engelsma et al., 2008). Mutation of this NES to lower the affinity toward CRM1 renders the virus compromised in nuclear export. Since no direct interaction of NS2/CRM1 proteins with capsids has been reported, pleiotropic properties of CRM1 transporter must be indirectly involved in this process. In contrast, in human SV40-transformed cells, in which NS2 is dispensable, the capsids can be exported to cytoplasm in an NS2- and CRM1-independent manner. It was recently reported that MVM capsids carrying additional surface phosphorylations are flagged for nuclear egress prior to lysis of mouse cells (Wolfisberg et al., 2016).

When phosphorylated at T149, NS2 of MVM interacts with some members of 14.3.3 proteins, a family of conserved regulatory molecules expressed in all eukaryotic cells. This suggests that NS2 may modulate cellular signaling pathways since 14.3.3 proteins act as adaptors interacting with a several protein kinases and phosphatases. However, mutagenesis of T149 to a non-phosphorylable alanine resulted in a phenotype which was not distinguishable from wild-type MVMp in mouse and human cells *in vitro* (Brockhaus et al., 1996). The genome of all members of the genus *Protoparvovirus* harbor a small open reading frame (ORF) starting 4 or 7 nucleotides downstream of VP2 initiation codon. This ORF encodes a late nonstructural protein (~ 6 kDa) called small alternatively translated (SAT) protein from the same mRNA as VP2 using an alternative reading frame (Zadori et al., 2005). It is predicted to have a transmembrane helix with alternating glycine and hydrophobic residues (valine, alanine or leucine), seems to be post-translationally modified and localize in the membranes of endoplasmic reticulum (ER) and nucleus. Abolishing the expression of

SAT in porcine parvovirus (PPV), where the protein was first reported, resulted in a "slow-spreading" phenotype of the virus in cell culture. However, the mechanism of SAT contribution to virus replication and spread is not clear and requires further investigation (Zadori et al., 2005).

1.3.2 Structural Proteins (VP1, VP2 and VP3)

Capsid in most parvoviruses is composed of three overlapping proteins, designated VP1 (83 kDa), VP2 (63 kDa) and VP3 (60 kDa), except for human B19 virus where only VP1 and VP2 form the capsids. In protoparvoviruses (e.g. MVM and H-1PV), VP1 and VP2 are expressed from alternatively spliced mRNAs, hence VP1 is an N-terminal extension of VP2, containing additional 142 amino acids termed VP1-specific region (VP1SR). During virus internalization and trafficking through endosomal compartments, a stretch of 22-25 amino acids from VP2 N-terminus, which is only accessible on the surface of DNA-full capsids, is cleaved by a cellular chymotrypsin-like protease to generate VP3 (Mani et al., 2006; Paradiso, 1984; Tattersall et al., 1977; Tullis et al., 1992). This maturation step may also occur extracellularly after release of progeny virions and can be mimicked *in vitro* by incubating virus particles with various proteases. Apparently, the cleavage site in MVM is flexible; therefore it has been impossible to ablate proteolytic generation of VP3 by either mutagenesis of the putative cleavage site (Tullis et al., 1992) or protease inhibitors (Cotmore and Tattersall, 2007). Furthermore, even viral stocks lacking VP3 were equally infectious (Maroto et al., 2004). Hence, the function of VP2 to VP3 cleavage in the infection process is not yet understood. Although VP1 carries the same cleavage site as VP2, it is not accessible to proteolytic digestion in virions and remains totally sequestered within the capsid during the early stages of entry. The VP1 minor capsid protein and VP2 major capsid protein are expressed at a fixed ratio (1:5) in infected cells owing to regulated splicing of the small introns in R3 primary transcript. Indeed, MVM particles are composed of 60 protein subunits comprising 10 copies of VP1 protein. Although, VP2 can assemble and package viral ssDNA to form virus-like particles (VLPs), VP1 is essential for infectivity of virus particles. The unique N-terminal part of VP1 plays

critical roles in virus infectivity and production of progeny particles. This region contains 4 clusters of basic amino acids, designated BC1-4, which function as nuclear localization signals (NLS) essential for virus entry. For example, conjugation of VP1 N-terminal peptide to bovine serum albumin (BSA), a protein with exclusive cytoplasmic localization, resulted in nuclear transport. Also, microinjection of antibodies against this region into cytoplasm prior to virus inoculation blocked infection. Additionally, there is a non-conventional structural domain in the common region of VP1 and VP2 polypeptides, referred to as nuclear localization motif (NLM) which is likely involved in transport of VP2 oligomeric subunits into nucleus where capsids assemble. The unique N-terminal part of VP1 also harbors a highly conserved Ca^{2+}-dependent phospholipase A2 (PLA2) domain, composed of approximately 60 amino acids, that facilitates endosomal escape of the virus by modulating membrane lipids (Zadori et al., 2001), reminiscent of the adenovirus pVI capsid protein with endosomolytic activity (Wiethoff et al., 2005). However, N-terminus of VP1 is buried inside the virions and only exposed during entry. This indicates that virions go through important conformational transitions, most likely during endosomal trafficking, which are required for endosomal escape and subsequent nuclear transport. Interestingly, in some parvoviruses like B19 virus, the VP1 N-terminus is exposed on the capsids, which may indicate some unique differences in biology of this virus. Furthermore, the catalytic activity of PLA2 domains varies across parvovirus species, with the highest activity reported for porcine parvovirus (PPV) (Canaan et al., 2004). The VP2 N-terminus (2Nt) is highly phosphorylated at serine residues and is projected outside of virus particles through the 5-fold channel when ssDNA is packaged and serves as a nuclear export signal (NES) for progeny virions. As mentioned before, this part of VP2 is removed by cellular proteases during virus entry, leaving VP3 in particles. This removes the NES from VP2 N-terminus, so it was suggested that VP2 cleavage might be involved in intracellular trafficking of incoming virus particles towards nucleus (Maroto et al., 2004).

1.4 Life Cycle of Parvoviruses (Depicted in Figure 6 for *Protoparvoviruses*)

1.4.1 Binding to Cellular Receptor

Parvoviruses use different receptors to infect host cells. The parvovirus B19 binds globoside or erythrocyte P antigen (glycosphingolipid tetrahexoseceramide) to infect erythrocyte precursors and people who genetically lack this antigen are not susceptible to B19 virus infection. Moreover, the α5β1 integrin is known to act as a co-receptor for infection of these cells. The AAVs can have broad cellular tropisms and infect various hosts and more than one cell surface molecule may participate in the infection process. Several receptors and co-receptors have been described for AAV2 including heparan sulfate proteoglycan (HSPG), human fibroblast growth factor receptor 1 and αvβ5 integrin. Retargeting strategies have been used for different AAV serotypes to redirect transduction toward specific tissues for gene therapy purposes (Kotterman and Schaffer, 2014). Transferrin receptor (TfR) is used by canine parvovirus (CPV) and feline panleukopenia virus (FPV) to infect host cells in a species-specific manner which defines the host tropism of these two closely related viruses. Indeed, only a few capsid residues control the host range and tissue tropism of CPV, FPV and MVM strains (the fibrotropic MVMp and the lymphotropic MVMi), although the growth of MVMp in mouse lymphocytes has been shown to be additionally restricted at an early step after cell entry and before DNA replication (Previsani et al., 1997; Wrzesinski et al., 2003). Differences between canine and feline TfR especially glycosylation of Asn383 in canine TfR prevents FPV from infecting dog cells (Kaelber et al., 2012; Palermo et al., 2003). MVM and H-1PV capsids bind to a still not identified sialic acid-containing receptor(s) and the infection of the cells can be prevented by neuraminidase treatment. The sialic acid residue binds into the dimple-like depression at the capsid's two-fold axis. Affinity of the capsid binding to the receptor has been shown to regulate the plaque size of the virus *in vitro* and the virulence *in vivo* (Lopez-Bueno et al., 2006). Whether or not additional receptors and/or co-receptors are involved in MVM and H-1PV infection remains to be elucidated. Recently, using purified MVM particles as bait for immunoprecipitation and subsequent proteomic analysis of the enriched proteins, galectin-3 was found to play an important role in viral endocytosis and infectivity in mouse fibroblast cells (Garcin et al., 2013; Garcin et al., 2015). In an attempt to generate an entry-deficient H-1PV using 3D structure of MVM capsid, it was found that

a sialic acid-binding pocket in H1 virion also plays a key role in infection (Allaume et al., 2012; Halder et al., 2013).

1.4.2 Receptor-medicated Endocytosis and Endosomal Escape

Upon cell receptor binding, virus particles are taken up by endocytosis usually at clathrin-coated pits (e.g. CPV and MVM) followed by endosomal acidification. Treatment of cells by lysosomotropic agents such as ammonium chloride (NH_4Cl), chloroquine or bafilomycin A1 can block the infection, indicating a critical role of low endosomal pH in this process (Ros et al., 2002). The incoming virus particles undergo major structural arrangements that are required for VP1 N-terminus extrusion through 5-fold axes of the capsid to unleash its PLA2 domain and expose the nuclear localization signal. Also, during trafficking through the endosomal compartment or in the extracellular environment prior to entry, most VP2 N-termini which are exposed only on the surface of full capsids are proteolytically cleaved to VP3 by removing 22-25 amino acids (Paradiso, 1984; Ros et al., 2002). The internalized capsids can be detected in endosomes by antibodies for several hours indicating relatively long retention of the virus particles in this compartment before being released into cytoplasm and transported to the nucleus. Indeed, the particle-to-infectivity ratio of most parvoviruses seems to be high (100:1 to >1000:1), indicating that most virions taken up by the cell do not succeed to replicate (Harbison et al., 2008). The VP1 N-terminus includes a nuclear localization signal (NLS) and a Ca^{2+}-dependent phospholipase A2 (PLA2) activity which is essential for infection by breaching endosomal membrane resulting in escape of virus particles into cytoplasm. With the exception of the parvovirus B19 in which the N-terminus of VP1 is exposed on the surface, this domain is buried within the capsids and becomes exposed during cell entry. Interestingly, PLA2 activity varies between different parvoviruses with the highest enzymatic activity observed for porcine parvovirus (PPV) (Canaan et al., 2004), indicating differences in the biology of these viruses.

1.4.3 Intracytoplasmic Trafficking Prior to Nuclear Import

Before nuclear import, capsids are transported by active mechanism involving microtubules to a perinuclear region. This process can be blocked by treatment of cells with microtubule-depolymerizing drugs (e.g. nocodazole) or microinjection of anti-dynein antibodies into cytoplasm (Suikkanen et al., 2003a; Suikkanen et al., 2003b). Although there is no clear evidence of capsid ubiquitination or direct proteolytic digestion during internalization, some proteasome inhibitors can disrupt MVM and CPV infections (Ros et al., 2002; Ros and Kempf, 2004). However, the mechanism of proteasome involvement during MVM infection is not clear. It is not clear exactly where the incoming viruses penetrate the endosomal membrane and escape this compartment, but CPV infectivity can be blocked by intracytoplasmic injection of antibodies directed against intact capsids or VP1-specific region (VP1SR), indicating that capsids go through a cytoplasmic phase during the course of infection (Vihinen-Ranta et al., 2002; Vihinen-Ranta et al., 2000).

1.4.4 Nuclear Import of the Capsids

Capsid proteins of parvoviruses have to be transported into nucleus twice during virus life cycle: First, as trimeric assembly intermediates after *de novo* synthesis and second, during infection of the host cell when the incoming virions need to translocate into nucleus after uptake by receptor-mediated endocytosis. Intranuclear Injection of monoclonal antibodies recognizing conformational epitopes on AAV2 capsids can block the infection, indicating that intact or at least partially intact full particles enter the nucleus, probably by passing through the nuclear pore complex (NPC) (Sonntag et al., 2006). Similarly, CPV virions injected into the cytoplasm were able to translocate into the nucleus in a microtubule-dependent manner, where they were detectable by structure-specific antibodies and successfully initiated NS1 expression within 24 hours (Suikkanen et al., 2003a; Vihinen-Ranta et al., 2000). Indeed, the small diameter of parvovirus particles (260 Å) could theoretically allow their transport through the nuclear pores. However, there is no concrete evidence for such translocation mechanism. An alternative translocation strategy involving induction of transient disruptions in the nuclear membrane has been proposed (Cohen et al., 2006; Cohen

and Pante, 2005). For instance, microinjection of MVM particles into the cytoplasm of *Xenopus* oocytes was demonstrated to induce transient disruptions in the nuclear envelope (Cohen and Pante, 2005). The same morphological alterations were observed when MVM (Cohen et al., 2011) or AAV2 (Porwal et al., 2013) mutants with inactivated PLA2 motifs were used, indicating that the viral PLA2 is not responsible for nuclear envelope disruptions during entry. Although the mechanism by which parvoviruses alter NE integrity is not known, but cleavage of lamin-B by caspase-3 and lamin-A/C by PKC and cdk2 have been implicated in this process (Porwal et al., 2013).

1.4.5 DNA Replication and Production of Progeny Virus Particles

The parvoviral genome consists of a small linear ssDNA with terminal palindromes that fold into self-priming hairpin structures and contain most of the cis-elements required for DNA replication and encapsidation. Due to extremely small size of their genome, the DNA replication process in these viruses is strictly dependent on the factors (*e.g*. DNA polymerases, PCNA, RPA) provided by host cells going through the S phase of the cell cycle.

The viral ssDNA is converted to dsDNA primed by the 3'-end hairpin. The DNA replication proceeds via generation of monomeric and concatemeric duplex replicative forms that are finally processed into progeny ssDNA by nickase and helicase activities of NS1 protein. During infection, one VP1 and two VP2 polypeptides form a trimeric assembly intermediates in the cytoplasm. The VP1-VP2 heterotrimers are phosphorylated in the cytoplasm by cellular kinases from mitogen-activated protein kinase (MAPK) pathway such as Raf-1 kinase (Riolobos et al., 2010). They are then transported to the nucleus where they are further assembled into empty procapsids (Riolobos et al., 2006). Gil-Ranedo *et al* showed that the nuclear translocation of MVM capsid subunits is tightly regulated by the cell cycle (Gil-Ranedo et al., 2015). The progeny ssDNA is packaged through a channel at 5-fold axis of the capsid while it is concomitantly released from the intermediate duplex forms of DNA by NS1 via a strand displacement mechanism (Cotmore and Tattersall, 2014). Therefore, during virus

infection excessive amounts of empty capsids (~90%) are produced and only a small fraction package genomic DNA to produce virions.

1.4.6 Egress of Progeny Virions

Late in infection, progeny virus particles accumulated in the nucleus need to exit from infected cell. Although it is generally believed that nonenveloped viruses are released passively from infected cell due to membrane permeabilization and cell lysis, there is accumulating evidence that some small DNA viruses including MVM are actively transported into culture medium prior to cell lysis and subsequent passive release (Bar et al., 2013; Maroto et al., 2004). A large number of cellular and viral proteins and mRNAs (including mRNA and rRNA) are transported out of nucleus by interaction with an export receptor called chromosome region maintenance 1 (CRM1) or exportin-1 which normally binds short leucine-rich nuclear export signals (NES) on cargo proteins (Macara, 2001). The cargo-CRM1 complex is then carried out through nuclear pore complex (NPC) powered by Ran-GTP system, which can be inhibited by treatment of cells with the antifungal antibiotic leptomycin B (LMB). CRM1 associates with cargo proteins with high affinity in the presence of Ran-GTP in nucleus. Once in the cytoplasm, the GTP bound to Ran is hydrolyzed to GDP and cargo is released.

For MVM, two different pathways have been suggested to mediate the virus egress in mouse fibroblasts and human transformed cells. The route accessed by the virus in these cell lines relies on the degree of phosphorylation of VP2 N-terminus, a domain which is only exposed on the surface of the DNA-containing (full) particles and not empty capsids that are produced in excessive amounts in infected cells. In human transformed cells (NB-324K cell line), highly phosphorylated N-terminus of VP2 is predominantly involved in nuclear export of progeny virions independent of CRM1, while in mouse fibroblasts (A9 cell line) where VP2 is poorly phosphorylated, a CRM1-dependent mechanism mediates the virus exit (Maroto et al., 2004). The NS2 protein of MVM, preferentially in its nonphosphorylated form, is the only protein which has been shown to directly interact with CRM1 protein (Eichwald et al., 2002; Engelsma et

al., 2008; Miller and Pintel, 2002b). In contrast to classical NES signals with a low affinity for CRM1, NS2 benefits from a supraphysiological export signal which tightly binds CRM1 in the absence of Ran-GTP in cytoplasm, resulting in competitive inhibition of this cellular protein by its sequestration in perinuclear region (Engelsma et al., 2008). Although mutagenesis of key residues in CRM1-binding motif of NS2 or treatment of mouse cells with LMB results in nuclear retention of progeny particles, attempts to demonstrate an interaction of NS2 with capsid proteins were unsuccessful (Eichwald et al., 2002; Miller and Pintel, 2002b). A recent study using anion exchange chromatography and cellular fractionation identified 2 distinct populations of MVM progeny particles with different degrees of capsid surface phosphorylation (Wolfisberg et al., 2016). Interestingly, only mature virions with an externalized VP2 N-terminus and harboring additional surface phosphorylations showed nuclear export potential and were able to actively egress from infected mouse fibroblasts (A9 cell line) prior to cell lysis. Furthermore, phosphoserine residues at the N-terminus of VP2 were dispensable for this process but capsid surface phosphorylation was critically involved. Also, incoming capsids were stripped of the surface phosphorylations, which even further indicate their role in virion egress (Wolfisberg et al., 2016).

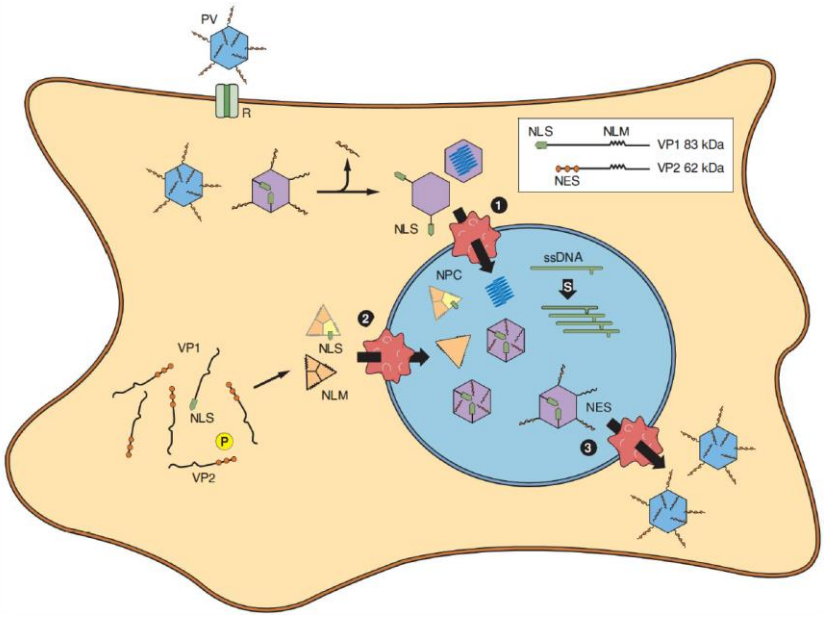

Figure 6. Life cycle of parvoviruses. Part (1) shows the very early steps after internalization of the virus particles including cleavage of VP2 N-terminus harboring a nuclear export signal (NES) and externalization of VP1 N-terminus carrying a nuclear localization signal (NLS). Part (2) illustrates the

formation of trimeric assembly intermediates through association of VP1 and VP2 proteins, followed by transport into the nucleus, where they are further assembled into empty capsids (procapsids). Part (3) shows the nucleo-cytoplasmic transport of the progeny DNA-containing particles, mediated by the phsophorylated N-terminus of VP2 protein functioning as a nuclear export signal (NES). Although CRM1-depdenent egress of progeny particles mediated by NS2 protein, is thought to be the major player in this step of infection in mouse cells (Kenneth I. Berns 2013).

1.5. Oncosuppressive and Oncolytic Effects of H-1PV

Replication-competent oncolytic viruses are being extensively considered as cancer bio-therapeutics due to their ability to infect and kill cancer cells, while sparing healthy cells, and provoke a systemic anti-tumor immune response which could potentially eradicate metastatic lesions (Kaufman et al., 2015; Marchini et al., 2015; Rommelaere et al., 2010; Russell et al., 2012b; Seymour and Fisher, 2016). Rodent parvoviruses including H-1PV are of particular importance because of their intrinsic oncotropism owing to tight dependence on DNA replication machinery and other cellular factors that are provided by cells only when going through S phase of the cell cycle, a hallmark of transformed cells (Cornelis et al., 1988; Deleu et al., 1999). Not only productive replication within cancer cells leads to cell lysis, but also sole expression of NS1, the main cytotoxic determinant of the virus, can result in cell cycle arrest and cell death (De Beeck et al., 2001; Hristov et al., 2010). The oncosuppressive properties of H1PV in various preclinical tumor models and effectiveness against tumors resistant to conventional therapies plus a unique safety profile owing to non-pathogenicity and lack of pre-existing immunity in humans, resulted in the launch of the first phase I/IIa clinical trial using H-1PV for treatment of patients with recurrent glioblastoma multiforme (GBM) (Angelova et al., 2015; Geletneky et al., 2015; Marchini et al., 2015; Nuesch et al., 2012; Rommelaere et al., 2010).

1.6 Aim of the Study

Isolation of mutant viruses that replicate more efficiently in cancer cells has been used as a strategy to improve oncolytic properties of viruses. For instance, fitness mutants have been selected by random mutagenesis of adenoviruses and serial passage of the pool of mutants in cancer cells using a procedure termed bioselection (Yan et al., 2003).

A similar experimental evolution approach has been successfully used for more rapidly evolving RNA viruses such as vesicular stomatitis virus (VSV) to adapt the virus to the features of cancer cells such as p53-deficiency (Garijo et al., 2014). Our laboratory previously isolated a naturally occurring fully infectious variant of H-1PV, designated H-1 dr virus, which was able to supplant the standard H-1PV strain (Faisst et al., 1995). This variant carries a large in-frame deletion (114 nt) in NS protein-coding sequences of the virus (Faisst et al., 1995). The deletion was introduced into an infectious clone of wild-type H1PV and a recombinant virus carrying this mutation was released for further analysis. The effects of the deletion on H-1PV replication was investigated in human transformed cells *in vitro* and *in vivo* (Weiss et al., 2012). The mutant virus harboring the deletion in NS-coding region (Del H-1PV) exhibited an enhanced infectivity *in vitro* and stronger anti-tumor activity *in vivo* compared to wild-type virus. Significant improvements in both early and late steps of the virus life cycle were observed including a more efficient virus uptake by host cells leading to an accelerated DNA replication process, and earlier/faster nuclear export of infectious virions (Weiss et al., 2012). This prompted us to further investigate the effects of the above-mentioned deletion on virus fitness by introducing point mutations in this region. The mutations were chosen on the basis of a study with MVM (Lopez-Bueno et al., 2004), a closely related murine parvovirus. MVMi variants were selected in mice with severe combined immunodeficiency (SCID) after long-term administration of a polyclonal antiserum against capsid (Lopez-Bueno et al., 2004). Surprisingly in these variants the mutations clustered in the NS-coding DNA sequence corresponding to the deletion sequence in DelH-1PV while sparing the capsid genes. These viruses were more virulent *in vivo* and replicated more efficiently in cell culture, as shown by higher production titers and larger plaques compared to those obtained with wild-type virus. A panel of H1PV mutants carrying the same point mutations as described for MVM was generated previously in our laboratory (Figure 7).

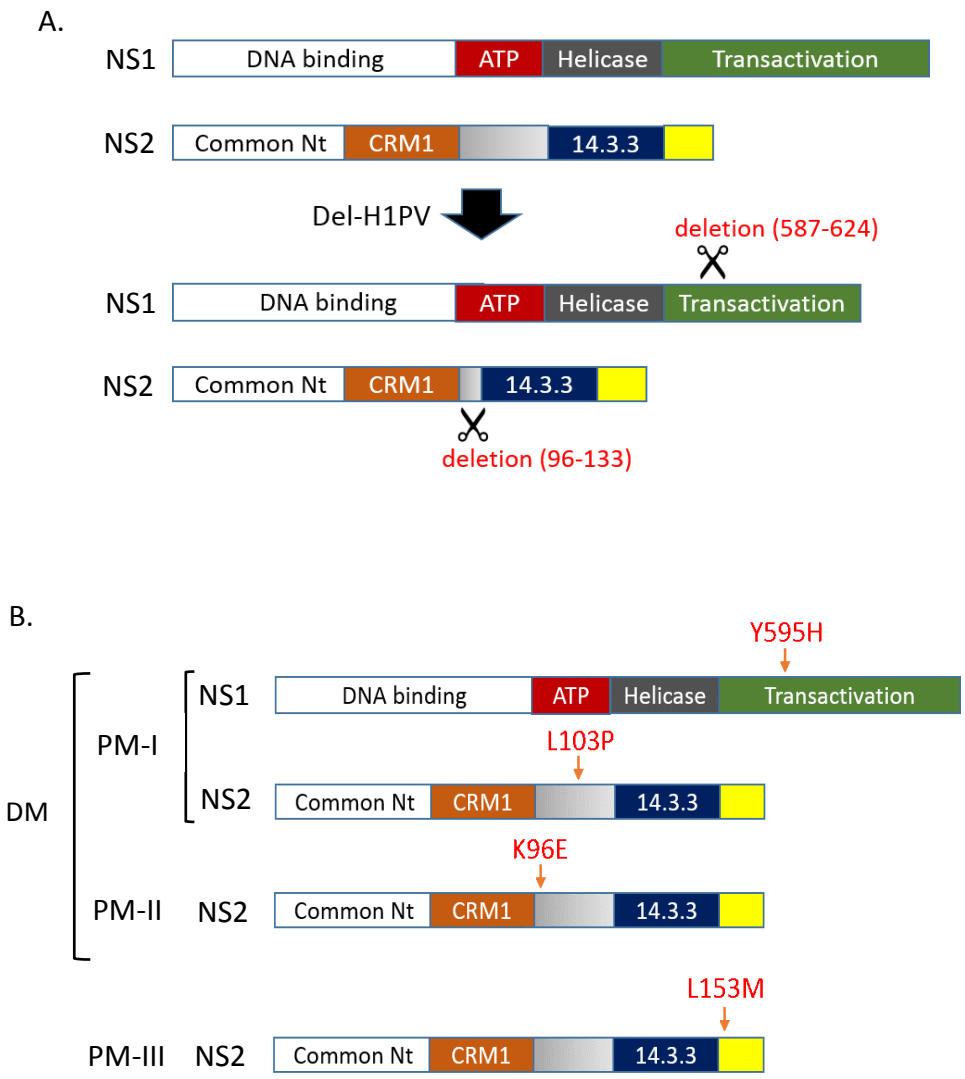

Figure 7. Illustration of the panel of H1PV mutants. (A) The Del-H1PV carries an in-frame deletion in both NS1 (587-624) and NS2 (96-133) proteins. (B) Depiction of the point mutations investigated in this study. Due to overlapping positions of NS1 and NS2 coding sequences, some of the point mutations affect both NS1 and NS2 proteins. PM-I virus carries two point mutations: Y595H in NS1 and L103P in NS2. PM-II mutation only affects NS2 (K96E) and the so-called double mutant (DM) virus harbors both PM-I and PM-II mutations. PM-III virus carries a point mutation (L153M) that only affects NS2 protein.

Since the mutations affect either NS2 or both NS1 and NS2 proteins, the aim of this study is to determine the relative contributions of both proteins to the fitness phenotype of the mutants and to analyze the step(s) of the viral infection cycle that are modulated by the modified NS1/NS2 proteins. Our results show that all the fitness mutations including PM-I, PM-II and DM improved the infectivity of the virus particles

indicated by more efficient uptake by the cells. Furthermore, DNA replication was stimulated by these mutations indicted by higher production of progeny virions, better spread of the virus and formation of larger plaques compared to WT virus. To analyze the fitness effects of NS1 mutation (Y595H) independent of NS2, NS2-null viruses were created in which NS2 protein expression was abrogated by mutagenesis of the splice acceptor site in NS2 mRNA precursor. Our data showed that the NS1 mutation contributes to better virus replication and spread.

In contrast, PM-III mutation in NS2 (L153M) compromised virus replication and spread, indicated by a small plaque phenotype, lower yield and infectivity of the progeny particles. However, cellular binding and uptake of the virus particles were not impaired due to this mutation. Because of overlapping position of NS-coding sequences and 5'-UTR (leader sequence) of the capsid mRNAs, a strong cis-acting effect this mutation may compromise the expression of the capsid proteins at a post-transcriptional level. We suggested that PM-III mutation probably interferes with efficient translation of downstream open reading frame (capsid ORF) leading to decreased production of progeny particles.

Chapter 2

Materials and Methods

2.1 Materials

2.1.1 Plasmid Vectors

Table 2.1 List of the plasmids used in this study. Abbreviations used in the plasmid nomenclature: WT: wild-type; PM: parvovirus mutant; DM: double mutant; NS1: non-structural protein 1; NS2: non-structural protein 2; Gluc: Gaussia luciferase; CMV: cytomegalovirus; P4: P4 promoter; P38: P38 promoter; Cyp: Cypridina luciferase; Y: Tyrosine; F: Phenylalanine; S: Serine; N: Asparagine; SAT: small alternatively translated protein

Note: All plasmids carry an ampicillin selection marker except for pBK-CMV-VP which carries a kanamycin selection marker

Plasmid	Description	Reference/ Supplier
pH1	Infectious DNA clone of wild-type H-1PV	(Weiss et al., 2012)
pDelH1	pH1 containing a 114bp deletion in NS-coding sequence (Del)	(Weiss et al., 2012)
pH1-PM-I	pH1 carrying the point mutation T2044C (PM-I)	Weiss (PhD thesis)
pH1-PM-II	pH1 carrying the point mutation A2022G (PM-II)	Weiss (PhD thesis)
pH1-PM-III	pH1 carrying the point mutation T2193A (PM-III)	Weiss (PhD thesis)
pH1-DM	pH1 carrying PM-I and PM-II mutations (DM)	Geiß (B.sc thesis)
pH1-NS2null	pH1 carrying the point mutation A1992C	This Thesis
pH1-DM-NS2null	pH1-DM carrying the point mutation A1992C	This Thesis
pH1-Del-NS2null	pDelH-1 carrying the point mutation A1992C	This Thesis
pChi-H1/Gluc	Infectious recH-1PV DNA clone, expressing Gaussia luciferase in replacement of viral capsid genes	Dempe 2012
pChi-H1-PM-III /Gluc	pChi-H1/Gluc plasmid carrying the PM-III mutation	This Thesis
pBK-CMV-VP	Helper plasmid expressing the capsid proteins VP1 and VP2 under the control of CMV promoter	(Kestler et al., 1999b)
pP4-NS	A plasmid expressing NS1/NS2 proteins under P4 promoter and BGH poly A signal	This Thesis

pP4-NS-PM-III	P4-NS carrying PM-III mutation	This Thesis
pP4-NS-DM	P4-NS carrying DM mutation	This Thesis
pP38-VP	Helper plasmid expressing VP1/VP2 proteins under the control of P38 promoter, contains a BGH poly A signal	This Thesis
pP38-VP-PM-III	pP38-VP carrying PM-III mutation and BGH poly A signal	This Thesis
pP38-Gluc	Plasmid expressing Gaussia luciferase under the control of P38 promoter; contains a BGH poly A signal	This Thesis
pP38-Gluc-PM-III	pP38-Gluc carrying PM-III mutation	This Thesis
pCMV-Cyp.luc	Plasmid expressing Cypridina luciferase under CMV promoter	Life Technologies
pH1-PM-III^{Silent}	pH1 carrying the silent mutation C2196T	
pP38-VP-PM-III^{Silent}	Plasmid expressing VP1/VP2 proteins under P38 promoter carrying a silent mutation and BGH poly A signal	This Thesis
pP38-Gluc-PM-III^{Silent}	Plasmid expressing Gaussia luciferase under P38 promoter carrying a silent mutation and BGH poly A signal	This Thesis
pH1-Y595F	pH1 carrying the mutation A2048T	This Thesis
pH1-SAT^{S18N}	pH1 carrying the mutation G2883A in SAT coding sequence	This Thesis
pH1-DM-SAT^{S18N}	pDM carrying the mutation G2883A	This Thesis
pH1-Del-SAT^{S18N}	pDelH1 carrying the mutation G2769A	This Thesis

2.1.2 Antibodies

Table 2.2 Antibodies used in this study. Abbreviations: NS1: non-structural protein 1; NS2p: non-structural protein 2 isoform P; GAPDH: Glyceraldehyde 3-phosphate dehydrogenase; WB: Western blot; HRP: horseradish peroxidase

Antibody	Host	Clonality	Dilution	Application/ Conjugate	Reference/Supplier
Anti-NS1	Rabbit	Polyclonal	1:2000	WB	Brockhaus 1996
Anti-NS2p	Rabbit	Polyclonal	1:1000	WB	(Wrzesinski et al., 2003)
Anti-H-1 VP1/VP2 peptide	Rabbit	Polyclonal	1:2000	WB	Kestler 1999
Anti-human GAPDH	Mouse	Monoclonal	1:3000	WB	Santa Cruz Biotech.
Anti-H1PV capsids	Rabbit	Polyclonal	1:400	Virus Neutralization	Neeb 1996 (Diplomthesis)
Anti-mouse IgG	Goat	Polyclonal	1:5000	WB/HRP	Promega
Anti-rabbit IgG	Goat	Polyclonal	1:5000	WB/HRP	Santa Cruz Biotech.

2.1.3 Cell Lines

Table 2.3 Cell lines used in this study. Abbreviations: MEM: minimal essential medium; DMEM: Dulbecco's modified Eagle medium. *Note: Both MEM and DMEM culture

media were supplemented with Penicillin (100 U/ml) and Streptomycin (100 µg/ml) from a 100X aqueous solution supplied by Life Technologies.

Cell Line	Description	Culture Medium
293-T	A derivative of HEK293 cell line (human embryonic kidney cell line transformed with Adenovirus 5) expressing SV40 large T-antigen	DMEM containing 10% FCS (Sigma)
NB-324K	Human embryonic kidney cell line transformed with SV40 T-antigen	MEM containing 5% FCS (Sigma)

2.1.4 Bacterial Strains

Table 2.4 Bacterial strains used in this study. Abbreviations: *E.coli*: *Escherichia coli;* SURE2: stop unwanted rearrangements

Bacterial Strain	Application	Supplier
E.coli SURE2®	Amplification of infectious wild-type and mutant H-1PV DNA clones	Agilent Tech.
E.coli Stellar Cells®	- Site-directed Mutagenesis - Amplification of pBK-CMV-VP, pP4-NS, pP38-VP and pP38-Gluc plasmids	Clontech

2.1.5 Antibiotics

Table 2.5 Antibiotics used for selection of bacterial clones in this study. All antibiotic solutions were stored at -20°C. Tetracycline and chloramphenicol solutions were protected from light.

Antibiotic	Working Concentration	Supplier
Ampicillin	100 µg/ml, stock solution in water (100 mg/ml)	Roche
Kanamycin	25 µg/ml, stock solution in water (50 mg/ml)	Merck Millipore
Tetracycline	12.5 µg/ml, stock solution in 70% ethanol (5 mg/ml)	Sigma
Chloramphenicol	175 µg/ml, stock solution in 100% ethanol (34 mg/ml)	Merck Millipore

2.1.6 Commercial Kits

Table 2.6 Commercial kits used in this study.

Kit	Application	Supplier
QIAprep® Spin Miniprep Kit	Small-scale isolation of plasmid DNA from bacterial culture (5 ml culture)	Qiagen
EndoFree Plasmid Maxi Kit	Large-scale isolation of endotoxin-free plasmid DNA from bacterial culture (250 ml culture)	Qiagen
QIAfilter Plasmid Mega Kit	Large-scale isolation of plasmid DNA from bacterial culture (500 ml culture)	Qiagen
QIAquick Gel Extraction Kit	Extraction of DNA from agarose gel	Qiagen
QIAamp MinElute Virus Spin Kit	Extraction of viral DNA from cell culture medium, cytoplasmic fractions and purified virus in Iodixanol	Qiagen
DNeasy Blood & Tissue Kit	Extraction of total cellular DNA and nuclear genomic DNA	Qiagen
RNeasy Mini Kit	Extraction of total cellular RNA	Qiagen
In-Fusion® HD Cloning Kit	Site-directed mutagenesis of plasmid DNA	Clontech
NE-PER Kit	Nuclear and cytoplasmic fractionation of cells	Life Technologies
Megaprime DNA labelling Kit	^{32}P-radioactive end labelling of VP-specific DNA probe for Southern blotting	GE Healthcare

2.1.7 Buffers and Solutions

Table 2.7 Buffers and solutions used in this study. Abbreviations: *E.coli*: *Escherichia coli;* PBS: phosphate buffered saline; BSA: bovine serum albumin; MEM: minimum essential medium; TAE: tris-acetate EDTA; EDTA: ethylene di-amine tetra-acetate; TGS: tris-glycine-SDS; SDS: sodium dodecyl sulfate; 2-ME: 2-mercaptoethanol; HBSS: Hank's balanced salt solution; HEPES: (4-(2-hydroxyethyl)-1-piperazineethanesulfonic acid); RNase A: ribonuclease A; APS: ammonium persulfate; SSC: saline sodium citrate; RIPA: radioimmunoprecipitation assay; DNA: deoxyribonucleic acid. Note: All the chemical reagents used were of very high purity (analytical grade).

Buffer/Solution	Formulation (and Reagent Supplier)	Application
Luria Bertani (LB) Broth	1% (w/v) Trypton, 1% (w/v) NaCl and 0.5% (w/v) Yeast extract in 1L water. Autoclaved and stored at RT.	*E.coli* culture
Bacto™ Agar	A 1.7% solution in water was autoclaved.	Plaque assay
Blocking Solution	10% (w/v) skim milk (Roth) and 0.2% (v/v) Tween-20 (Sigma) in 1X DPBS (AppliChem). Stored at 4°C.	Western blotting
Denaturation Solution	1.5 M NaCl (Sigma) and 0.5 M NaOH (Merck Millipore) in Milli-Q water. Stored at RT.	Southern blotting
Denhardt's Solution (100X)	2% (w/v) BSA (Roche), 2% (w/v) Ficoll 400 (Sigma) and 2% (w/v) Polyvinylpyrrolidone (PVP), sterilized by filtration and stored at -20°C.	Southern blotting

Overlay Medium	4 ml of 2X MEM (Life Technologies) (supplemented with 5% FCS, 100 U/ml of Penicillin and 100 µg/ml Streptomycin) and 3 ml of 2% Bacto™ agar (BD) per 6 cm plate	Plaque assay
TAE Buffer (50X)	2M Tris-base (Sigma), 57.1 ml glacial acetic acid (Merck) and 100 ml of 0.5 M EDTA (pH 8.0) (Merck) in 1L Milli-Q water. Stored at RT.	Agarose gel electrophoresis
TGS Buffer (10X)	0.25 M Tris, 1.92 M glycine and 1% SDS in 1L Milli-Q water, pH 8.3. Stored at RT.	SDS-PAGE electrophoresis
Laemmli Loading Buffer (4X)	278 mM Tris-HCl (pH 6.8), 44.4% glycerol (Sigma), 4.4% SDS (Sigma), 0.02% bromophenol blue (Merck) and 355 mM 2-ME (Sigma) in Milli-Q water. Stored at -20°C.	Denaturation and loading of cell lysates on SDS-PAGE gel
HBSS Buffer (2X)	280 mM NaCl, 10 mM KCl, 1.5 mM Na_2HPO_4, 50 mM HEPES (Roth) and 12 mM D-Glucose (Sigma), pH 7 in Milli-Q water. Sterilized by filtration (0.22 µm) and stored at -20°C.	Transfection of cell lines using calcium phosphate method
Hirt Extraction Buffer	10 mM Tris-base, 10 mM EDTA (pH 8), 0.6% (w/v) SDS, 100 µg/ml RNAse A (Qiagen, added before use), pH 7.4 in Milli-Q water. Stored at RT.	Extraction of low-molecular weight (episomal) DNA from mammalian cells
SSC (20X)	3 M NaCl and 300 mM trisodium citrate (Merck) in Milli-Q water, pH 7. Stored at RT.	Southern blotting
Hybridization Buffer	3X SSC, 1% (w/v) SDS, 5 mM EDTA and 10X Denhardt's solution in Milli-Q water.	Southern blotting
PBS-MK Buffer	1 mM $MgCl_2$ and 2.5 mM KCl in 1X PBS. Sterilized by filtration and stored at RT.	Virus purification
Iodixanol Solution (15%)	12 ml OptiPrep® (Sigma), 27 ml PBS-MK and 562 mM NaCl. Stored at RT and protected from light.	Virus purification
Iodixanol Solution (25%)	20 ml OptiPrep®, 28 ml PBS-MK and 0.01 µg/ml Phenol Red. Stored at RT and protected from light.	Virus purification
Iodixanol Solution (40%)	30 ml OptiPrep® and 15 ml PBS-MK. Stored at RT and protected from light.	Virus purification
Iodixanol Solution (55%)	40 ml OptiPrep®, 3.64 ml PBS-MK and 0.01 µg/ml Phenol Red. Stored at RT and protected from light.	Virus purification
Luria-Bertani (LB) Agar	1.5% (w/v) Agar-Agar in LB medium. Autoclaved, dispensed in Petri dishes and stored at 4°C.	*E.coli* culture
Neutral Red solution	0.33% (w/v) Neutral Red (Merck) in 1X PBS pH 7.2. Filtered through Whatman™ paper, sterilized by filtration, stored at 4°C and protected from light.	Plaque staining
NaCl (3M)	3 M NaCl in PBS-MK, sterilized by filtration and stored at RT.	Virus purification
Neutralization Buffer	1.5 M NaCl, 0.5 M Tris-HCl and 1 mM EDTA, pH 7.2 in Milli-Q water. Stored at RT.	Southern blotting
PBS (2X)	273.78 mM NaCl, 5.36 mM KCl, 9.76 mM KH_2PO_4, and 3.57 mM K_2HPO_4, pH 7.4. Autoclaved and stored at RT.	Plaque staining
PBS-MK Buffer	1 mM $MgCl_2$ and 2.5 mM KCl in 1X PBS. Sterilized by filtration and stored at RT.	Virus purification

Resolving gel, 10 %	375 mM Tris-base, 10% (v/v) Acrylamide/bis-acrylamide solution (Roth), 0.1% (w/v) SDS, 0.1% (w/v) APS (Bio-Rad), 0.05% (v/v) TEMED (Roth), pH 8.8.	SDS-PAGE electrophoresis
RIPA Buffer	150 mM NaCl, 10 mM Tris-base, 1 mM EDTA, 1% (v/v) NP-40, 0.5% (w/v) Sodium Deoxycholate (Sigma), 0.1% (w/v) SDS, pH 7.5 and EDTA-free protease inhibitor cocktail (Roche, added before use). Stored at 4°C.	Preparation of cell lysates for WB
Plaque Staining Medium	0.33% neutral red solution (2/32), 2X PBS (15/32), 1.7 % Bacto™ Agar (15/32)	Plaque staining
Proteinase K Buffer	20 mM Tris-base, 20 mM EDTA and 1% (w/v) SDS, pH 8.	Protein digestion before DNA extraction
V-TE Buffer	50 mM Tris-base and 0.5 mM EDTA, pH 8.7. Autoclaved and stored at RT.	Virus extraction
WB Washing Buffer	0.5% (v/v) Tween-20 in 1X PBS	Western blotting
Washing Solution Hyb-I	3X SSC and 1% (w/v) SDS in Milli-Q water	Southern blotting
Washing Solution Hyb-II	0.3X SSC, 1% (w/v) SDS in Milli-Q water	Southern blotting
WB Transfer Buffer-I	300 mM Tris-base and 20% (v/v) CH_3OH, pH 10.4	Western blotting
WB Transfer Buffer-II	25 mM Tris-base and 20% (v/v) CH_3OH, pH 10.4	Western blotting
WB Transfer Buffer-III	25 mM Tris-base and 40 mM Norleucin (Sigma), pH 9.4	Western blotting

2.1.8 Primers

Table 2.8 Primers used in this study. Abbreviations: NS: non-structural; SA: splice acceptor site; ITR: inverted terminal repeat; FAM: fluorescein amidite; MGB: minor groove binder; qPCR: quantitative PCR; F: forward; R: reverse

Primer Set	Sequence (5'-3')	Amplicon Size (bp)
P4-NS-XhoI-F P4-NS-NotI-R	5'-GTTCTACTCGAGATAAGCGGTTCAGAGAGTTTGAAACCAAG-3' 5'-AATAAAGCGGCCGCTCAAGGCTGTTCCCTGGTC-3'	2331
P38-XhoI-F P38.VP-NotI-R	5'-TATTAACTCGAGCATTACCGTGGTTAGAATAGGCTGTG-3' 5'-ATTAAAGCGGCCGCTTAGTATGTCATGTGAGGCACAG-3'	2820
P38-XhoI-F P38-BamHI-R	5'-TATTAACTCGAGCATTACCGTGGTTAGAATAGGCTGTG-3' 5'-TATATTGGATCCTAGTCCAAGGTCAGCTCCTCG-3'	579
VPs-qPCR-F VPs-qPCR-R	5'-ACATAACAGCTGGCGAGGACC-3' 5'-AAGCATCTAGCTGTGTCCCTCC-3'	157
GAPDH-qPCR-F GAPDH-qPCR-R	5'-AGCCTCAAGATCATCAGCAATGC-3' 5'-TGGTCATGAGTCCTTCCACGATAC-3'	103
PM-III^{Silent}-F PM-III^{Silent}-R	5'-CCCAACTTGGTCCGAGATCGAGG-3' 5'-TCGGACCAAGTTGGGCTCCGTTGAG-3'	7593

NS2-SA-F NS2-SA-R	5’-CGCTCGGTTCAATGCGCTCACC-3’ 5’-GCATTGAACCGAGCGAATTTATAGGAGTGTC-3’	7593
NS1-Y595F-F NS1-Y595F-R	CAAAACTTCGCTCTTACTCCACTTGCATC AAGAGCGAAGTTTTGGCTGAGAGGC	7593
H1-ITR-F H1-ITR-R	5’-GTTCTAGTCGACATAAGCGGTTCAGAGAGTTTGAAACC-3’ 5’-TATAGGGGATCCCTGAATAGACAGTAGTCCTTGTTCAT-3’	4825
H1-Seq-F1 H1-Seq-F2 H1-Seq-F3 H1-Seq-F4 H1-Seq-F5 H1-Seq-F6 H1-Seq-F7 H1-Seq-F8 H1-Seq-R	5’-AGCGAGGACATGGAATGGGAG-3’ 5’-ACCACTGCACAGGAAGCTAAG-3’ 5’-GAAAAGGCAGCAAACAGATTGAACC-3’ 5’-AACGAGGAGCTGACCTTGGAC-3’ 5’-AATCGCTAATGCTAGAGTTGAG-3’ 5’-GCACCAGCTCCTTACAGATACTAC-3’ 5’-AGCAGCACCAGAAAGGTACAC-3’ 5’-CCATCTGCAACTGGCAACATG-3’ 5’-GCCTCCAATCAGCACATGAC-3’	NA*
H1-qPCR-F H1-qPCR-R TaqMan® Probe	5´-GCGCGGCAGAATTCAAACT-3´ 5’-CCACCTGGTTGAGCCATCAT-3´ 5’-6-FAM-ATGCAGCCAGACAGTTA-MGB-3´	141
SB-VP-F SB-VP-R	5’- AGAGTTGAGCGATCAGCTGACGGAG-3’ 5’- GATGTTTGAGCTGCAGGTGTGTAAGG-3’	545

* NA: not applicable for sequencing primers.

2.2 Bacterial Culture and Plasmid Extraction

For small-scale purification of the plasmids, 5 ml of LB containing the appropriate antibiotics was inoculated with a single colony obtained after transformation and incubated overnight at 37°C. The bacterial cells were collected by centrifugation (Eppendorf) at 4000 rpm, 4°C for 10 min. The plasmid DNA was extracted using Miniprep kit (Qiagen) according to manufacturer’s instruction and stored at -20°C.

For large-scale amplification of plasmids carrying infectious DNA clone of H-1PV and the mutants, 20 ml of LB medium containing ampicillin and tetracycline were inoculated with transformed *E.coli* of SURE2 strain (table 2.4) and incubated for a few hours at 37°C with vigorous shaking. 500 µl of the starting culture was added to 500 ml of LB medium containing the same antibiotics and incubated overnight at 37°C. The following morning, chloramphenicol was added to the culture medium and incubation continued for 4-6 hours in order to increase the plasmid copy number in the cells. The culture was centrifuged (Thermoscientific Sorvall) at 6000 xg, 4°C for 10 min to pellet

the bacterial cells. The pellet was stored at -20°C until DNA extraction by Mega or Maxiprep kit according to manufacturer's instructions (Qiagen). In order to prepare transfection-grade plasmid, endo-free Maxiprep kit was used to avoid cytotoxic effects of bacterial LPS (endotoxin).

2.3 Site-Directed Mutagenesis

To generate H-1PV mutants described in this study, point mutations were introduced into the infectious DNA clone of the virus using In-Fusion® cloning kit according to manufacturer's instructions (Clontech). Briefly, inverse PCR reactions were performed on the infectious molecular clone of H-1PV using the appropriate pairs of overlapping primers and a high-fidelity PCR mix (CloneAmp HiFi PCR Premix, Clontech) in a thermocycler (Eppendorf) as recommended by the manufacturer (Clontech). To degrade the input plasmid DNA, the PCR products were incubated with DpnI restriction enzyme overnight at 37°C, separated by agarose gel electrophoresis and extracted using gel extraction kit (Qiagen). 100 ng of each purified linear DNA was used in In-Fusion reaction according to manufacturer's instruction followed by transformation into *E.coli* Stellar strain and plating on agar plates containing ampicillin. Several single colonies were screened for the correct plasmid clone by sequencing using the appropriate sequencing primers based on the mutagenized region (table 2.8). Positive clones were digested by EcoRI/StuI enzymes and the 1293 bp inserts sub-cloned into the infectious molecular clone pH1 in order to avoid mismatches in other regions of the viral genome. The final constructs were then used to transform the recombination-deficient E.coli SURE2 strain for large-scale amplification as described above (section 2.2) followed by transfection into 293-T cells to produce the virus stocks (section 2.4).

2.4 Virus Production from Infectious DNA Clones by transfection of 293-T Cells

To produce master stocks from H-1PV mutants, $5x10^6$ 293-T cells were seeded into 15 cm plates 16 hours before transfection. For each virus stock the plasmid 15 µg DNA and 250 mM calcium chloride (final concentration) were mixed in a tube followed by addition of an equal volume of 2XHBSS buffer and incubation at RT for 20 min. Finally, 2250 µl of the mixture was added dropwise to each plate of the cells without aspirating

the culture medium. The cells were incubated at 37°C, 5% CO_2 for 72 hours before proceeding with virus extraction and purification (section 2.5).

2.5 Virus Extraction and Purification

To extract the virus particles from 293-T cells after transfection or NB-324K cells after infection, cells were scraped in the culture medium and transferred to 50 ml falcon tubes. After centrifugation at 4000 rpm and 10°C for 15 min, the cell pellet was washed once with 10 ml of 1x PBS, suspended in 10 ml of V-TE buffer (table 2.7) and subjected to 3 freeze-thaw cycles at -20°C and RT to release the virus particles. The cell lysate containing the crude virus stock was clarified by centrifugation at 4000 rpm and 10°C for 15 min and transferred to a polypropylene ultracentrifuge tube (Quick-Seal®, Beckman Coulter). The crude virus sample was underlaid with 4 steps of Iodixanol solutions in order of increasing density (15%, 25%, 40% and 55%). The centrifugation was performed at 50,000 rpm and 10°C for 2.5 hours using a 50.2 Ti rotor (Beckman Coulter). The layer containing the full viral particles (40% Iodixanol) was extracted and stored at 4°C until further analysis.

2.6 Titration of DNA-Containing (Full) and Infectious Particles

The DNA-containing (full) and infectious virus particles were quantified using quantitative PCR (qPCR) and plaque assay respectively. To titrate full particles, 10 µl of the virus suspension was diluted in 0.9% NaCl to a final volume of 200 µl and viral DNA was extracted using QIAamp MinElute Virus Spin Kit (Qiagen). The viral DNA was eluted in 100 µl Milli-Q water and stored at -20°C until further analysis. A TaqMan® qPCR was used to quantify the copy number of the viral genome using a standard curve created by serial dilutions (in Milli-Q water) of XhoI-linearized pH1. Briefly, a pair of primers specific for NS1 coding sequence and a dual-labelled (6-FAM and MGB at 5’ and 3’ ends respectively) TaqMan® probe (table 2.8) specific to the amplicon (141 bp) were mixed in equimolar amounts with 2X TaqMan Universal PCR Master Mix (Life Technologies) and 2 µl of the viral DNA or the standard sample in a final volume of 20 µl. The PCR reaction was performed in white 96-well plates (Hard-Shell® PCR plates, Bio-Rad) for 40 cycles in a qPCR thermocycler (CFX96 Touch™ Real-Time PCR, Bio-Rad).

Infectious viral particles were quantified using a standard plaque assay on NB-324K cells, as previously described (ref). Briefly, 5x105 NB-32K cells in MEM medium supplemented with 5% FCS were seeded in 6 cm plates and incubated overnight at 37°C, 5% CO2. The virus samples were serially diluted (10-fold) in MEM medium without supplements and 400 µl of virus dilutions were inoculated to NB-324K cells in duplicates for 1 hour at 37°C. The inoculum was aspirated and the cell monolayer was covered with 7 ml of a semi-solid overlay medium (table 2.7) and left under laminar flow hood to solidify. The plates were incubated at 37°C, 5% CO2 for 5 days when the plaques were developed. In order to stain the plaques, at day 4 the plates were covered with 3 ml of a semi-solid overlay medium containing neutral red dye (table 2.7) and incubated overnight at 37°C. After fixation with 3.7% formalin solution plaques were counted. The virus titer was calculated using below equation and reported as plaque-forming unit per ml (PFU/ml):

Virus Titer (PFU/ml) = Mean number of plaques in duplicate plates x 2.5 x dilution factor x 1/ml

In order to measure the size distribution of the plaques, plaque assays were performed in 15 cm plates. The infection and staining procedure were done similarly but the number of cells seeded for infection ($3x10^6$), volume of infection (2.5 ml), overlay medium (50 ml/plate) and staining overlay medium (21 ml/plate) were increased proportionately. The size of the plaques was measured using ImageJ software.

2.7 Analysis of Viral Protein Expression by Western Blotting

The viral protein expression was assessed in NB-324K cells both after viral infection and transfection of the infectious DNA clones. 24 hours before infection $2.5x10^5$ NB-324K cells were seeded in 2 ml of complete MEM in 6-well plates. The cells were infected at a MOI of 2225 viral genome copies/cell (equivalent to 1 PFU/cell for WT virus) for 1 hour at 37°C followed by addition of 2 ml of complete MEM. One hour after incubation at 37°C allowing virus internalization, anti-capsid neutralizing serum (1:400) was added to the culture medium to prevent secondary infections by progeny virions. At various times post infection, the culture medium was aspirated and the cells were washed once with cold PBS. Whole cell lysates were prepared by adding 250 µl of cold RIPA

buffer containing a protease inhibitor cocktail (table 2.7), collected in pre-chilled tubes on ice and clarified by centrifugation at 14000 rpm, 4°C for 15 min (Eppendorf). The supernatants were boiled in 4X Laemmli buffer and stored at -80°C until further analysis. Equal volumes (35 µl) of the lysates were loaded per well and separated on a 10% SDS-PAGE gel (60 V overnight) followed by semi-dry transfer to a nitrocellulose membrane (GE Healthcare, 0.45 µm). The membrane was blocked for 1 hour at RT and incubated in the primary antibody (Table 2.2) overnight at 4°C. The antigen-antibody interaction was detected using a HRP-conjugated secondary antibody and the protein bands were detected using enhanced chemiluminescence (Western Lightning® Plus-ECL, PerkinElmer). Images were captured using the "sequential integrate" setting of an ECL imaging system (Intas Science Imaging, GmbH). The cellular GAPDH was used as loading control. To analyze protein expression after transfection, $7x10^5$ NB-324K cells were seeded into 6 cm plates 24 hours before transfection with a mix containing 5.5 µg plasmid DNA, 8.25 µl Lipofectamine® 3000 and 11 µl P3000™ reagent and Opti-MEM™ in a total volume of 250 µl per well according to the manufacturer's instructions (Life Technologies). The transfection medium was removed 5 h after incubation at 37°C and fresh complete medium was added to the cells.

2.8 Analysis of Viral DNA Replication by Southern Blotting

To analyze viral DNA replication, $1.6x10^6$ NB-324K cells were seeded on 10 cm plates 24 hours before infection or transfection. The infection was performed in 1 ml of MEM without supplements at a MOI of 1 PFU/cell for 1 hour at 37°C followed by addition of 10 ml complete MEM. The incubation was continued for 1 hour, the medium was aspirated, cells were washed once with 10 ml of 1X PBS and 10 ml of complete MEM containing anti-capsid neutralizing serum (1:400) was added to block secondary infection cycles. At progressive time points after infection, the cells were scraped in culture medium and harvested by centrifugation for 15 min at 4000 rpm, 10°C. The cell pellet was washed with 5 ml of PBS and suspended in 200 ml of PBS for total DNA extraction using DNeasy® Blood & Tissue kit (Qiagen) as recommended by the manufacturer. Finally, equal volume of total DNA was loaded on 1% agarose gel

containing ethidium bromide (Roth) and separated by electrophoresis. After soaking in denaturation and neutralization buffers (table 2.7), the gel was equilibrated in 20X SSC buffer for 15 min and the DNA bands were transferred in 20X SSC buffer (table 2.7) to a positively charged Nylon® membrane (PerkinElmer) using an upward capillary system overnight. The DNA bands were UV cross-linked to the membrane (Stratalinker® 1800, Agilent Technologies) using the auto cross-linking setting of the apparatus. To detect the viral DNA, a hybridization step was performed using a ^{32}P-labbeled VP-specific DNA probe as described before (Weiss et al., 2012). The VP-specific probe was prepared by PCR amplification of a 545 bp region of pH1 plasmid (Table 2.1) using SB-VP-F and SB-VP-R primers (Table 2.8) and Q5 high-fidelity DNA polymerase (NEB) following the cycling conditions recommended by the manufacturer (NEB). The amplicon (545 bp) was separated on 2% agarose gel followed by purification using QIAquick® Gel Extraction Kit (Qiagen). To prevent non-specific binding of the probe to the membrane, a blocking step was performed using prehybridization solution containing 0.2 mg of heat-denatured herring sperm DNA (Roche) per mL for 1 h at 65°C with continuous shaking. The ^{32}P-labelled DNA probe was heat denatured at 100°C for 10 min (Thermomixer, Eppendorf), cooled on ice for 5 min and added to the hybridization solution at 65°C with continuous shaking for 16 hours. In order to remove non- and unspecifically bound probes, the membrane was washed twice for 30-60 min and once for 15-30 min with washing solutions of different salt concentrations. After air-drying, the membrane was wrapped in plastic (Saran) and exposed to a radiosensitive film (Kodak) at -80°C in the presence of an intensifying screen.

The viral DNA replication was also analyzed after transfection of infectious DNA clones of the viruses. Briefly, $1.6x10^6$ NB-324K cells were seeded in 10 cm plates 24 hours before transfection. Transfection of the cells was performed with a mixture containing 14 µg of plasmid DNA, 21.7 µl Lipofectamine® 3000, 28 µl P3000™ reagent and Opti-MEM™ in a total volume of 250 µl per plate according to manufacturer instruction (Life Technologies). The transfection medium was removed after 5 hours incubation at 37°C and fresh complete medium was added to the cells. At desired time points after

transfection, the culture medium was aspirated and the cells were washed once with PBS. The cells were scraped in PBS and collected by centrifugation at 1500 rpm, 10°C for 15 min (Eppendorf). The cell pellet was suspended in 500 µl of Hirt extraction buffer containing RNase A (100 µg/ml, Qiagen) and incubated for 5 min at RT (table 2.7). To digest the proteins, the cell lysate was transferred to 1.5 ml tube (Eppendorf) and 1 mg/ml of proteinase K (Roche) was added followed by incubation at 37°C for at least 6 hours. High molecular weight cellular DNA was precipitated by adding NaCl to a final concentration of 1 M and overnight incubation at 4°C. After centrifugation for 1 h at 13000 rpm, 4°C (Eppendorf), viral DNA was recovered from the supernatant by phenol/chloroform extraction and ethanol precipitation. Finally, the DNA pellet was dissolved in 100 µl of Milli-Q water and its concentration was determined spectrophotometrically at λ=260 nm using a NanoDrop® (Thermoscientific). To selectively degrade the input methylated plasmid DNA, 25 µl of the DNA was incubated with 2 µl of the methylation-dependent restriction enzyme DpnI at 37°C overnight. The separation of viral DNA replicative forms by agarose gel electrophoresis, Southern blotting and hybridization procedures were performed subsequently as described above.

2.9 Construction of Mutant H-1PV-based Vectors Expressing Luciferase Reporter

In order to test the effects of the point mutations such as PM-III on the expression of P38-driven transcripts, a H-1PV-based vector was used which carries Gaussia luciferase under P38 promoter in replacement of the capsid genes (pChi-H1/GLuc) as described before (Dempe et al, 2012). A fragment containing the PM-III mutation was excised out from an infectious DNA clone of the virus (pH1-PM-III plasmid) using EcoRI and StuI enzymes and replaced the wild-type sequence in pChi-H1/GLuc vector to create pChi-H1/Gluc plasmid (Table 2.1).

2.10 Construction of Split Plasmid Vectors from H-1PV for Co-Transfection Studies

Due to overlapping positions of the NS1 and NS2 C-terminal coding sequences with P38 promoter and consequently 5'-UTR of the capsid mRNAs, the point mutations in these proteins could potentially influence the capsid gene expression through *cis*-acting

effects. In case of PM-III mutant in which the capsid production is severely compromised, it was tempting to see if the mutation has any *cis*-acting effect on expression of VP1 and VP2 proteins. For this purpose, a split vector system was created as depicted below. In this system, one plasmid encodes wild-type NS1/NS2 proteins under P4 promoter (pP4-NS) and the other one expresses the capsid proteins under control of wild-type (pP38-VP) or mutant P38 promoter sequence (pP38-VP-PM-III). For reporter gene analysis, wild-type or mutant P38 promoter sequences were cloned into a promoter-less vector containing *Gaussia* luciferase gene and BGH poly A signal to create pP38-Gluc and pP38-Gluc-PM-III plasmids respectively (Table 2.1).

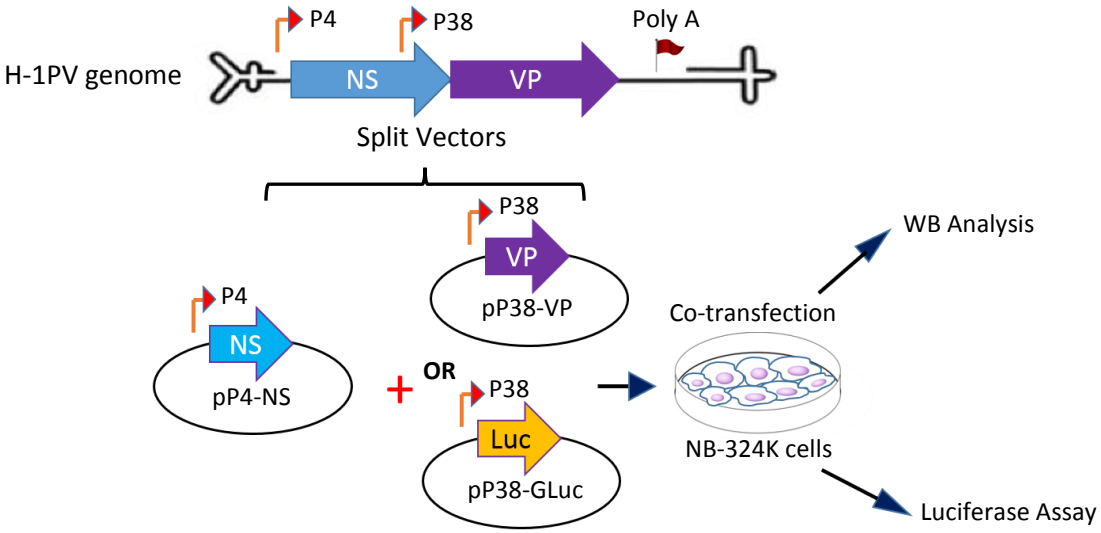

To create these plasmids (table 2.1), a fragment of the viral genome encompassing the P4 promoter and the NS1/NS2 coding sequence was PCR amplified from an infectious DNA clone of the virus using P4-NS-XhoI-F and P4-NS-NotI-R primers (table 2.8) and a high-fidelity DNA polymerase (Q5® DNA polymerase, NEB) following cycling conditions recommended by the manufacturer (NEB) in a thermocycler (Eppendorf). Briefly, 1 ng of plasmid DNA was added to a mix containing 0.5 µM forward and reverse primers, 200 µM dNTPs (NEB) and 2 mM Mg^{2+} in a final volume of 50 µl. The PCR product was purified using PCR Clean-Up kit (Qiagen) and digested with XhoI and NotI enzymes (NEB). The DNA insert was separated on 1% agarose gel and eluted from agarose using QIAquick® Gel Extraction Kit (Qiagen). A vector was prepared by removing *Gaussia*

luciferase gene from pMCS-*Gaussia* plasmid (Life Technologies) using XhoI and NotI enzymes and ligated to P4-NS and P38-VP inserts. To construct the reporter vectors expressing *Gaussia* luciferase under control of P38 promoter (pP38-Gluc plasmids), a region covering P38 promoter was PCR amplified from the infectious DNA clone of the viruses using P38-XhoI-F and P38-BamHI-R primers (Table 2.8). The PCR product was purified, digested with XhoI and BamHI enzymes (NEB) and cloned upstream of *Gaussia* luciferase gene in a linearized pMCS-*Gaussia* vector (Life Technologies).

2.11 Co-Transfection of H-1PV Split Vectors for Capsid Expression and Luciferase Assay

In order to test the *cis*-acting effects of the point mutations on the expression of the capsid gene, $2.7x10^5$ N-234K cells were seeded in 6-well plate (Greiner Bio-One) 24 hours before transfection. A mixture of pP4-NS (500 ng/well) and pP38-VP or pP38-VP-PM-III plasmid (2 µg/well) was co-transfected using LFA®3000 (Life Technologies) according to the manufacturer instruction. The cell lysates were harvested in 250 µl RIPA buffer containing a cocktail of protease inhibitors and the expression of the capsid proteins (VP1/VP2) was assessed by Western blotting as described before (section 2.7). To analyze the luciferase expression, $1x10^5$ NB-324K cells were seeded per well of in a 12-well plate (Greiner Bio-One) 24 hours before transfection. A mixture of pP4-NS (195 ng/well) and pP38-GLuc or pP38-GLuc-PM-III plasmids (780 ng/well) plus pCMV-*Cypridina* (25 ng/well) were co-transfected. The activity of *Gaussia* and *Cypridina* luciferase in the cell culture medium was measured separately using the specific substrates Coelenterazine and Vargulin (also known as *Cypridina* luciferin) respectively (NanoLight™ Technology). At desired time points, 60 µl of the culture medium was transferred to a 1.5 ml tube (Eppendorf) and stored at -80°C until measurement. To measure the luciferase activity, 25 µl of the sample was pipetted into 2 wells of a white 96-well plate (Greiner Bio-One). Eighty microliter of the substrate solution (1 µM Coelenterazine or Vargulin) was added and luciferase activity was measured after 1 min using a Luminometer (PerkinElmer). The *Gaussia* luciferase activity values were

normalized to *Cypridina* values for variations in cell viability and/or transfection efficiencies.

2.12 Quantification of the Capsid mRNAs by SYBR® Green Reverse Transcriptase PCR (qRT-PCR)

The capsid (VP1 and VP2) mRNAs were measured after co-transfection of pP4-NS and pP38-VP vectors (section 2.11) using SYBR® Green quantitative reverse transcriptase PCR (qRT-PCR). At desired time points, the culture medium was discarded and the cells were washed once with PBS. The cells were lysed in the well using the cell lysis buffer, homogenized by QIAshredder® (Qiagen) and total RNA was extracted using RNeasy Mini Kit (Qiagen). Finally, the RNA was eluted in 50 µl of nuclease-free water (Life Technologies) and the concentration was measured spectrophotometrically at λ=260 nm using a NanoDrop® (Thermoscientific). The quality of the RNA was assessed by absorbance ratio of A260/A280 and on a 1% agarose gel from integrity of the cellular ribosomal RNA bands (28S rRNA and 18S rRNA) followed by snap-freezing on dry ice and storage at -80°C until further analysis. Before RT reaction, RNA samples were treated with RNase-free DNase-I (NEB) to get rid of residual co-purified cellular and viral DNA. For this purpose, 2 µg of total RNA was digested with 2 units of the RNase-free DNase-I in a total volume of 20 µl for 60 min at 37°C in a thermomixer (Eppendorf). To inactivate the DNase-I before RT reaction, EDTA was added to final concentration of 5 mM and the mixture was incubated at 75°C for 10 min and then snap chilled on ice to melt the RNA secondary structures. The first DNA strand (cDNA) was synthesized from 15 µl of the heat-treated RNA using 200 units of Moloney Murine Leukemia Virus Reverse Transcriptase (M-MLV RT, Promega), 1 µg of random primers (Promega) and an RNase inhibitor (RNasin®, Promega) in a reaction volume of 25 µl according to the manufacturer instruction. The RT reaction was performed at 37°C for 60 min in a thermocycler (Eppendorf) followed by heat-inactivation of the RT enzyme at 90°C for 5 min. The sample volume was increased to 40 µl by adding 15 µl of nuclease-free water and stored at -20°C until synthesis of the second strand cDNA. To synthesize the second strand of the cDNA, 4 µl of cDNA was mixed with a 2X SYBR® Select Master Mix

(Life Technologies) supplemented with VP-specific primers (table 2.8) or GAPDH (as reference mRNA) primers at a final concentration of 10 µM in a qPCR thermocycler (CFX96 Touch™ Real-Time PCR, Bio-Rad). The relative capsid mRNA concentration to cellular GAPDH, reported as expression fold change, was quantified using the comparative Ct method and $2^{-\Delta\Delta Ct}$ equation as below:

$\Delta Ct_{(test\ sample)} = Ct_{(VP,\ test\ sample)} - Ct_{(GAPDH,\ test\ sample)}$

$\Delta Ct_{(mock\ sample)} = Ct_{(VP,\ mock\ sample)} - Ct_{(GAPDH,\ mock\ sample)}$

$\Delta\Delta Ct = \Delta Ct_{(test)} - \Delta Ct_{(mock)}$

Fold Change Expression of Capsid = $2^{-\Delta\Delta Ct}$

2.13 Bioinformatic Analysis of the 5' Untranslated Region (5'-UTR) of the Capsid mRNA

The secondary structures of the 5'-UTR sequences of the capsid mRNAs (VP1 and VP2) from H-1PV (GenBank: JX505432.1; nucleotides 1892-2188) and from MVMi (lymphotropic strain of minute virus of mice; GenBank: X02481.1; nucleotides 1983-2279) were analyzed by *in-silico* prediction approach using the default settings of the RNAfold® WebServer at University of Vienna. The structures were reported as minimum free energy (MFE) encoding base pair probabilities.

3. Analysis of different Steps of H-1PV Infection Cycle

3.1 Virus Binding (Adsorption) to Host Cells

$5x10^5$ NB-324K cells were seeded in 6-well plate and incubated for 16 hours at 37°C, 5% CO2 to allow the cell attachment. Before virus infection, the plates were chilled at 4°C for 15 min to prevent virus internalization. The culture medium was aspirated and the cells were inoculated at 4°C with WT or mutant viruses at a MOI of 2225 virus genomes/cell in 250 µl of MEM with gentle rocking for 1 hour. The inoculum was transferred into a 1.5 tube (Eppendorf) and stored at -20°C until DNA extraction with QIAamp MinElute Virus Spin Kit (Qiagen) to measure unbound viral particles. To determine the amounts of membrane-bound virus particles, cells were scraped in 200

µl of PBS, transferred into a 1.5 tube and stored at -20°C until DNA extraction with DNeasy Blood & Tissue Kit (Qiagen). The viral genome copy numbers in the samples were quantified using TaqMan® qPCR as described before (section 2.6).

3.2 Virus Uptake and Nuclear Transport

After 1 hour incubation at 4°C for virus adsorption (section 3.1), the cell cultures were incubated at 37°C to allow internalization of the bound virus particles. At various time points, the culture medium was removed and the cell monolayer was washed with 5 ml of PBS. To remove the residual membrane-bound virus particles and to detach the cells, 500 µl of trypsin-EDTA solution (0.25% trypsin, 1 mM EDTA) was added to the cell culture followed by incubation at 37°C for 5 min. The reaction was stopped by adding 900 µl of complete MEM (5% FCS) and the cell suspension was transferred into a 1.5 ml tube (Eppendorf). The cells were collected by centrifugation at 300xg, 4°C for 3 min (Eppendorf) and the cell pellet was washed once with 1 ml of cold PBS. The cytoplasmic and nuclear fractions were then prepared using NE-PER Nuclear and Cytoplasmic Extraction Kit (Life Technologies). Briefly, the cell pellet was resuspended in 100 µl of ice-cold Cytoplasmic Extraction Reagent I (CER I) containing a cocktail of protease inhibitors (Roche) followed by vigorous vortexing and incubation on ice for 10 min. The CER II reagent was added to the mixture and vortexed. After a short incubation on ice (1 min), the cells were centrifuged at 14000 rpm, 4°C for 5 min to pellet the intact nuclei. The supernatant was collected as the cytoplasmic fraction and stored at -20°C until DNA extraction using QIAamp MinElute Virus Spin Kit (Qiagen). The nuclei were washed once with 1 ml of ice-cold PBS, suspended in 200 µl of ice-cold PBS and stored at -20C until DNA extraction using DNeasy Blood & Tissue kit (Qiagen). The viral genomes in the cytoplasmic and nuclear fractions were quantified using TaqMan® qPCR as described above (section 2.6).

3.3. Analysis of the Late Steps of H-1PV Infection Cycle

The viral DNA replication and nuclear exit of the progeny virions and their pre-lytic release into the culture medium were investigated by cellular fractionation and virus

titration. The cell seeding, infection and cellular fractionation were performed as described in section 3.2. In addition to the cytoplasmic and nuclear fractions, the viral genome copies were also quantified in the culture medium after DNA extraction with QIAamp MinElute Virus Spin Kit (Qiagen) following the manufacturer protocol.

4. Isolation and Characterization of a Novel H-1PV Fitness Mutant (H1-SAT^{S18N})

During amplification of wild-type H-1PV in NB-324K cells, a novel fitness mutant emerged in the virus stock showing a large plaque phenotype. This variant was isolated from four individual plaques picked using a sterile Pasteur pipette, transferred into 2.5 ml of MEM and incubated at 4°C until use. Each viral suspension was used to infect $5x10^6$ NB-324K cells in a 15 cm plate. Five days after infection, the cells were scraped in the culture medium and transferred into a 50 ml falcon tube. The cells were centrifuged at 1500 rpm, 10°C for 15 min, the supernatants discarded and the cell pellet suspended in 2.5 ml of MEM followed by 3x freeze-thaw cycles to lyse the cells. The cell lysates were inoculated to $5x10^6$ NB-324K cells to further amplify the virus particles. When cytopathic effects were observed, as indicated by cell rounding and detachment, the cell-associated virus particles were harvested by low speed centrifugation, the cell pellet was resuspended in 1 ml of MEM and the clarified lysates stored at 4°C until further analysis.

The viral genomes were extracted from clarified lysates using QIAamp MinElute Virus Spin kit (Qiagen) and the entire viral genomic DNAs (excluding terminal hairpins) were PCR amplified using a high-fidelity DNA polymerase (Q5® DNA polymerase, NEB) and appropriate primers (H1-ITR-F and H1-ITR-R) (table 2.8). The viral genomes were sequenced using H1-Seq-F1 to H1-Seq-F8 primers (table 2.8) by Sanger sequencing method (GATC Biotechnology, Germany). A single point mutation (G2763A based on H-1PV genome sequence with GenBank annotation JX505432.1) was found in the late non-structural protein (SAT) of all the virus clones tested, except in one clone that produced the same plaque size as the wild-type and was used as control. This mutation introduces an amino acid substitution (S18N) in the SAT protein, while being a silent mutation in the capsid sequence (GAG-to-GAA; both encoding glutamic acid). Finally a

DNA fragment encompassing the mutation was PCR amplified (2820 bp) using the appropriate primers (P38-XhoI-F and P38.VPs-R) and cloned into the MfeI and HindIII sites of the infectious molecular clones pH1, pDel-H1 and pDM. The final constructs were verified by sequencing and restriction analysis, and transfected into 293-T cells to produce virus stocks as described before (section 2.4). The mutant viruses were further amplified in NB-324K cells at low MOI (0.003 PFU/cell), purified on Iodixanol gradient (section 2.5) and titrated by TaqMan® qPCR and plaque assay (section 2.6).

Chapter 3

Results

3.1 Point Mutations in the NS Protein Coding Sequence Affects the Fitness of H-1PV

Isolation of fitness mutants is being investigated as a strategy to augment therapeutic efficacy of oncolytic viruses. An experimental approach called bioselection has been employed successfully for adenoviruses (Yan et al., 2003) and vesicular stomatitis virus (Garijo et al., 2014). Previously in our lab, a fully infectious variant of H-1PV designated H-1 dr virus was reported to supplant the standard H-1PV strain (Faisst et al., 1995). This mutant carries a large in-frame deletion (114 nt) in NS protein-coding sequences of the virus (Faisst et al., 1995). In an attempt to increase oncolytic properties of H-1 virus, Weiss *et al*. introduced this deletion in a molecular clone of H-1PV and investigated its effects on virus replication in human transformed cells *in vitro* and *in vivo* (Weiss et al., 2012). This deletion substantially enhanced the virus fitness in cell culture and resulted in more efficient oncolytic properties *in vivo* (Weiss et al., 2012). This prompted us to further investigate the region subject to deletion by introducing point mutations. Four mutations originally reported to increase the fitness of the H-1PV-related parvovirus MVMi (Lopez-Bueno et al., 2004), were previously introduced in H-1PV molecular clone (see Materials and Methods, Table 2.1). When produced as viruses these mutants showed substantially different plaque phenotypes compared to wt virus. Similar to DelH-1PV (Weiss et al., 2012), H1-PM-I, H1-PM-II and H1-DM mutants enhanced the virus fitness, as indicated by a large plaque phenotype. Surprisingly, H1-PM-III mutant showed an attenuated phenotype (in contrast to the fitness phenotype described for MVMi), with impaired virus replication and poor spread, resulting in formation of smaller plaques compared to wt. Figure 1A illustrates the plaque phenotype of wt (H-1PV), H1-DM and H1-PM-III viruses. The sizes of 178 plaques and their frequency were measured from scanned pictures of 15 cm plates

using ImageJ software. As shown on Figure 1B, all the viruses gave rise to a mixture of small and large plaques. However, a higher frequency of large plaques and a lower frequency of small plaques was observed for H1-DM mutant compared to wt virus. In contrast, H1-PM-III mutant showed a significantly higher frequency of small plaques and lower frequency of large plaques.

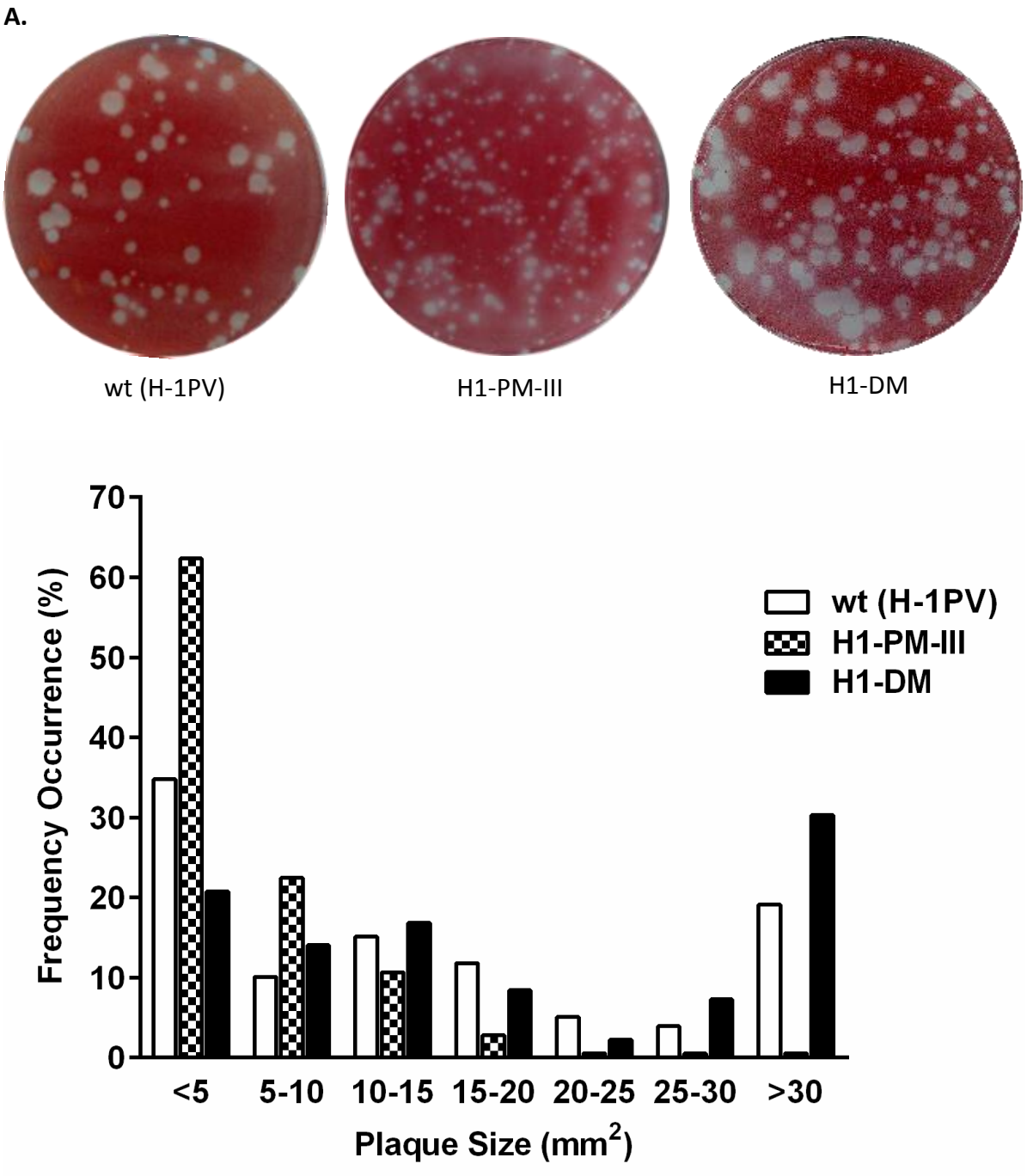

Figure 1. Plaque phenotype of the mutants. (A) $5x10^6$ NB-324k cells were infected with H-1PV (wt), H1-DM and H1-PM-III viruses at a MOI of 0.003 PFU/cell followed by virus purification. Plaque assays were performed in 15 cm dishes. (B) Sizes of plaques were determined from scanned pictures of the plates

using the Java-based image processing software ImageJ. Plaque sizes are given in mm^2 and frequency of occurrence is expressed as percentage of total number of plaques analyzed (n=178).

Furthermore, H1-PM-I, H1-PM-II and H1-DM mutants yielded more progeny DNA-containing particles which were more infectious than wt H-1PV, as indicated by lower particle-to-infectivity (P:I) ratio. The P:I ratio of the virus stocks was measured 5 days post infection at a low MOI of (0.003 PFU/cell) to allow serval rounds of virus amplification. The virus particles were harvested from the cells and titrated by plaque assay to measure the infectious particles (virions) and by qPCR to measure total yield of the genome-containing (full) particles. Figure 2A shows the titers of infectious viruses and Figure 2B, the titers of DNA-containing particles in these stocks. As shown in Figure 2A, H1-PM-I, H1-PM-II and H1-DM produced higher titers of infectious progeny virions while PM-III yielded less infectious progeny virions than wt H-1PV. Similarly, the yield of total DNA-containing particles was higher for H1-PM-I, H1-PM-II and H1-DM mutants, compared with wt, while H1-PM-III produced lower titers (Figure 2B). This resulted in ∼4-fold lower P:I ratios (Figure 2C) for H1-PM-I, H1-PM-II and H1-DM viruses and ∼4-fold higher P:I ratio for PM-III mutant. Furthermore, the virus titers and infectivity of H1-PM-I, H1-PM-II and H1-DM mutants were comparable.

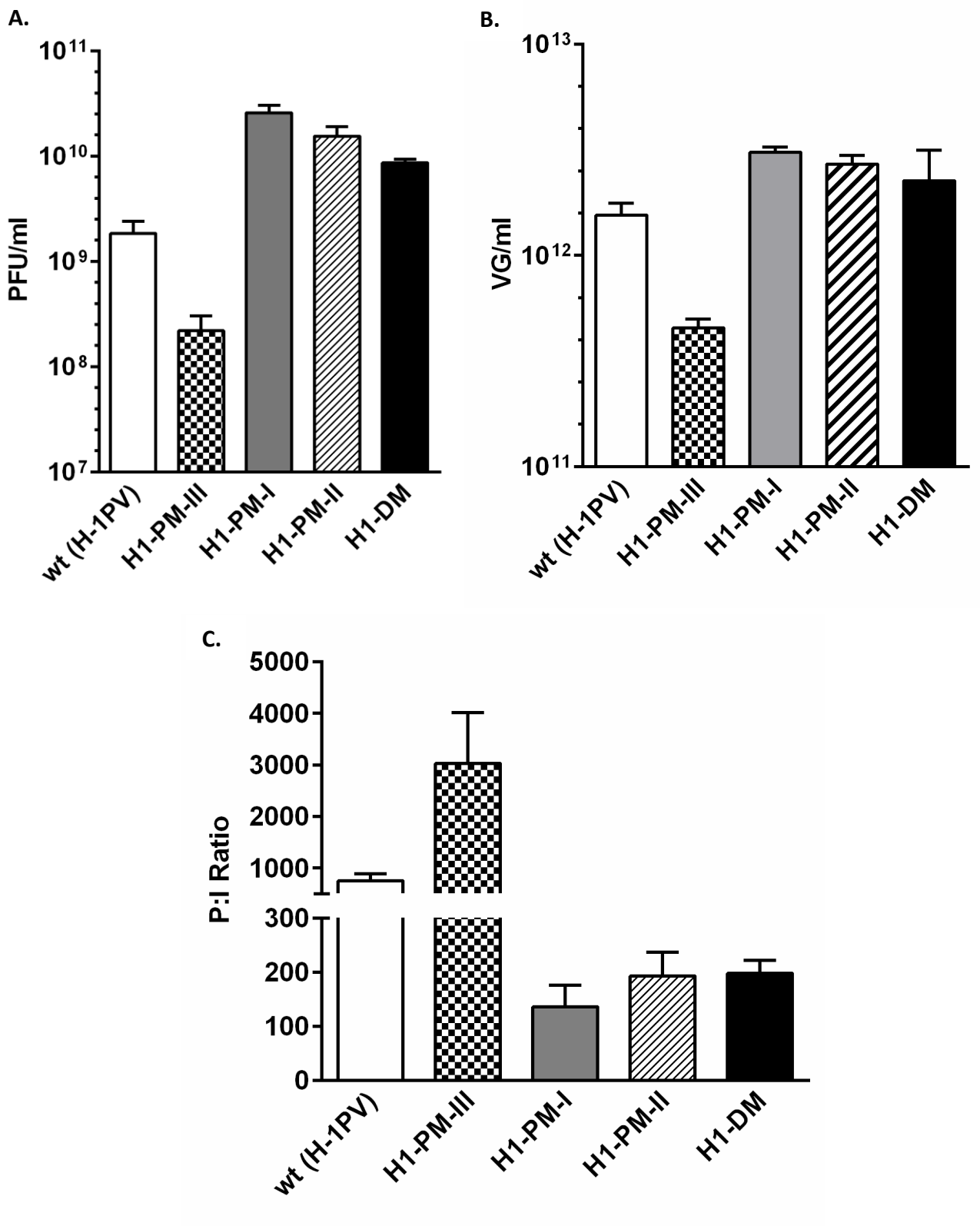

Figure 2. Point mutations in NS-coding sequence affect the yield and infectivity of progeny particles. $5x10^6$ NB-324K cells were infected with wt (H-1PV), H1-PM-III or H1-DM virus at a low MOI (0.003 PFU/cell) to allow further rounds of infection. Five days after infection, the viruses were purified and both full and infectious particles were measured in the virus stocks. Mean ± SD of three independent

measurements of a representative virus stock is shown. (A) Infectious particle titers were measured by plaque assay. (B) Total yield of genome-containing (full) particles was measured by qPCR. (C) Particle-to-infectivity ratio of the virus stocks.

This indicates that the point mutation(s) introduced in the corresponding region of DelH-1PV mimics the fitness features of the deletion variant such as: improved yield and infectivity of progeny virus particles, resulting in large plaque phenotypes of these viruses. Interestingly, the opposite scenario was observed for H1-PM-III mutant which carries a single amino acid substitution (L153M) in NS2, slightly downstream of the deletion region (aa 96-133), although this mutation conferred a fitness phenotype on MVM, a H-1PV-closely related parvovirus (Lopez-Bueno et al., 2004).

3.2 Expression of Viral Proteins After Infection of NB-324k Cells

We next wanted to investigate the effects of these point mutations on the expression of the viral proteins. Viral protein expression was analyzed after infection of NB-234K cells with the mutants at a multiplicity of infection (MOI) of 2225 genome copies/cell (same number of full viral particles). After infection, anti-capsid neutralizing serum was added to the culture medium to prevent further rounds of infection. Total cell lysates were prepared 16 and 20 h post-infection and the accumulation of viral proteins was analyzed by Western blotting using cellular GAPDH as loading control (Section 2.7). As shown in Figure 3A and B, the expression of all viral proteins (structural and non-structural proteins) was significantly increased after infection with H1-PM-I, H1-PM-II and H1-DM viruses, compared with wt. In contrast, H1-PM-III mutant produced substantially lower amounts of the capsid proteins VP1 and VP2 (∼40% of wt) when equal number of full particles was used to infect the cells. Yet, compared with wt, similar levels of NS1, the viral protein required to transactivate the P38 promoter that directs the expression of the viral capsids, accumulated after infection with PM-III (Figure 3B and E). Interestingly, quantification of the signal intensities of the bands showed a ratio VP2:VP1 of 5:1 for H1-PM-I, H1-PM-II and H1-DM, as also known for H-1PV, while this ratio was around 20:1 for PM-III (Figure 3C and D). This indicates that PM-III mutation reduces not only the overall capsid expression after infection, but also

it has a stronger effect on VP1 expression, leading to an imbalanced ratio of VP2:VP1. However, the steady-state levels of nonstructural proteins were comparable to wt virus. This indicates that the diminished accumulation of the capsid proteins is not caused by a delay in expression of NS1, the protein required for induction of capsid promoter (P38).

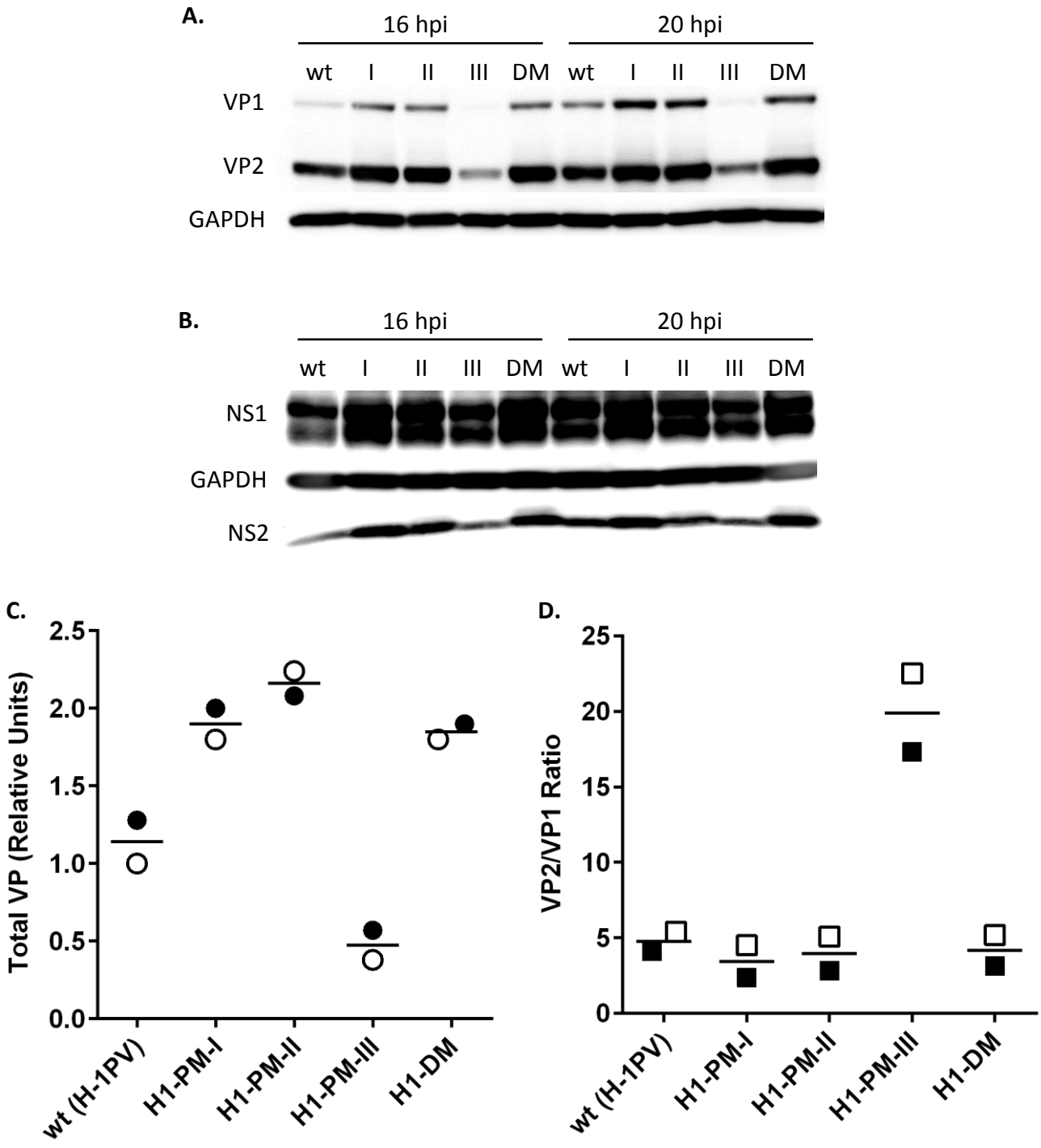

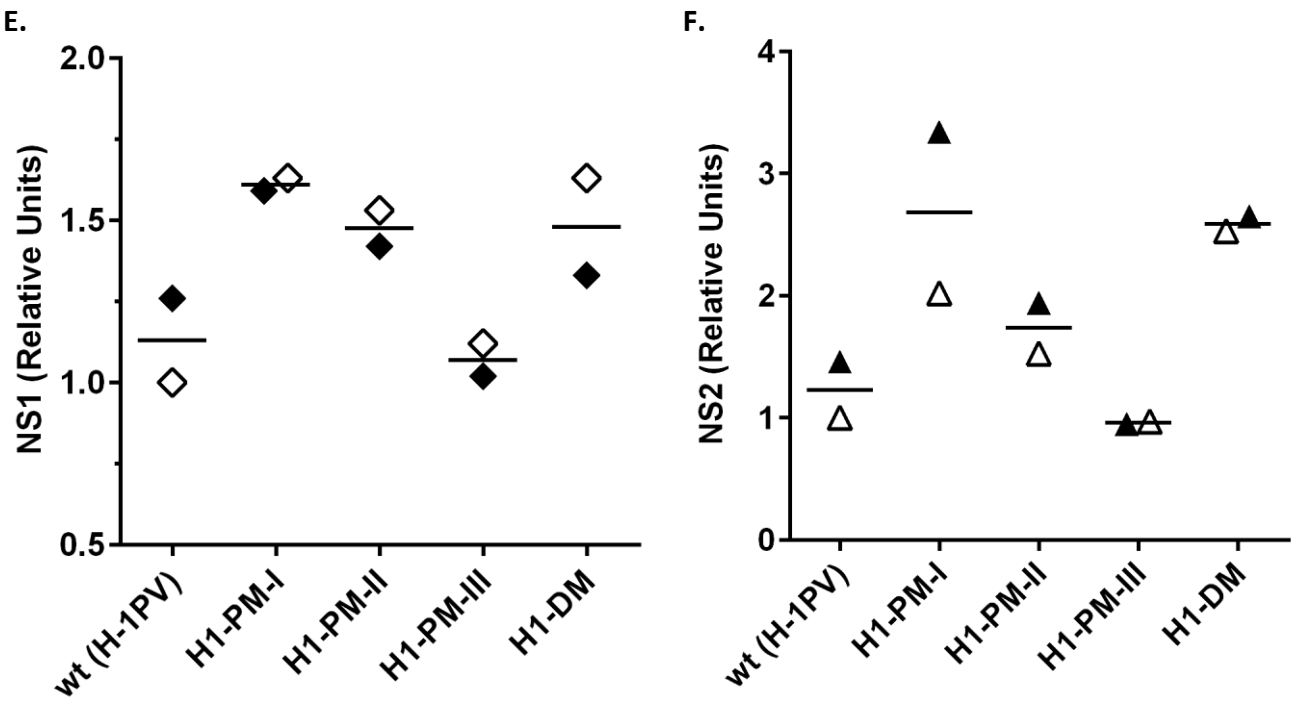

Figure 3. Viral protein accumulation in a single infection cycle with equal number of genome-containing particles. $5x10^5$ NB-324K cells were infected at MOI of 2225 VG/cell in the presence of anti-capsid neutralizing serum added to the culture medium 2 hpi. Whole cell lysates were prepared 16 and 20 h post-infection. 10 µg of total protein lysates were separated on a 10% SDS-PAGE gel and detection of the proteins was performed using primary antibodies specific for NS1, NS2p and VP and horseradish peroxidase-conjugated secondary antibodies and specific interactions revealed by enhanced chemiluminescence (ECL). Protein band densities were quantified by Lab-1D software. (A, B) Western blotting of viral proteins (structural VP1/2 and nonstructural NS1 and NS2). Lanes I, II, III and DM stand for H1-PM-I, H1-PM-II, H1-PM-III and H1-DM mutants respectively. (C, D) Densitometric quantification of capsid proteins VP1 and VP2 (relative units) and their ratio. (E, F) Quantification of NS1 and NS2 proteins. Empty and filled symbols indicate the samples collected at 16 and 20 hpi respectively. Mean of the values is indicated by a line. All protein quantifications were normalized to the density of the corresponding wt protein at 16 hpi.

As mentioned in the introduction part, VP2 is the main component of the capsid structure (50 copies/particle) and VP1 is the minor protein (10 copies/particle). Although VP2 protein alone can assemble into virus-like particles (VLPs) and package ssDNA (Willwand and Hirt, 1993), VP1 is essential for infectivity of the virus particles (Tullis et al., 1993). A small intron flanked by so-called D1-A1 splice junctions, separates the first and second VP1 exons and is naturally excised out less efficiently than VP2

small intron (Clemens and Pintel, 1988; Schoborg and Pintel, 1991). Figure 4 shows the position of the small introns in capsid mRNAs.

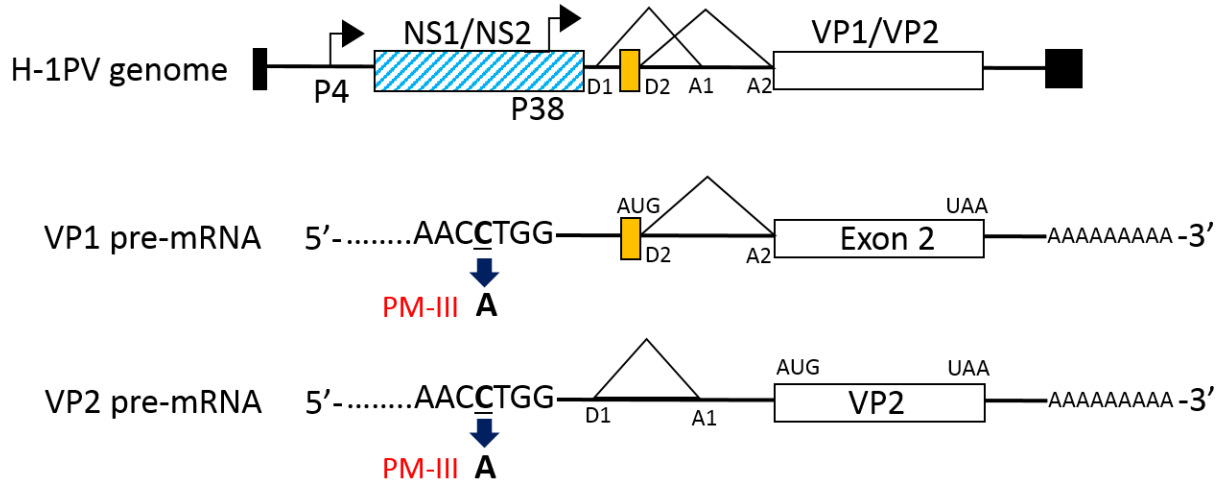

Figure 4. Organization of the small introns in H-1PV capsid transcripts. Top scheme shows the genome organization of the virus. P4 and P38 promoters are indicated with arrows. D1-A1 and D2-A2 indicate splice donor and acceptor sites of VP2 and VP1 respectively. The small orange rectangle shows the first exon of VP1 pre-mRNA (middle scheme). The VP2 pre-mRNA (bottom scheme) consists of a single exon for which the AUG initiation codon and UAA stop codon have been indicated. PM-III mutation (C-to-A) in 5'-UTR of VP1/VP2 mRNA is located 125 nt upstream of VP1 splice donor site (D2) and 89 nt upstream of VP2 splice donor site (D1).

This maintains the VP2 and VP1 mRNAs and subsequently proteins at 5:1 ratio. The increased ratio of VP2:VP1 in addition to the total amount of these proteins suggests that VP1 expression might be more severely affected by PM-III mutation, maybe due to an interference with VP1 mRNA splicing. Supporting this, when the inoculum was adjusted for the infectivity of the virus particles (MOI of 1 PFU/cell), the levels of VP2 after infection with PM-III were similar to wt, but did not restore the VP2:VP1 ratio to 5:1 (Figure 5A B and C). This indicates that PM III mutation affects more specifically the production of VP1 even if the accumulation of both VP2 and VP1 proteins is reduced. The capsid proteins expressed by H1-PM-I and H1-DM viruses accumulated to slightly higher levels compared to wt virus at 20 hpi (Figure 5B, filled symbols) and the ratio VP2:VP1 in H1-PM-I, H1-PM-II and H1-DM-infected cells was similar to wt (Figure 5C).

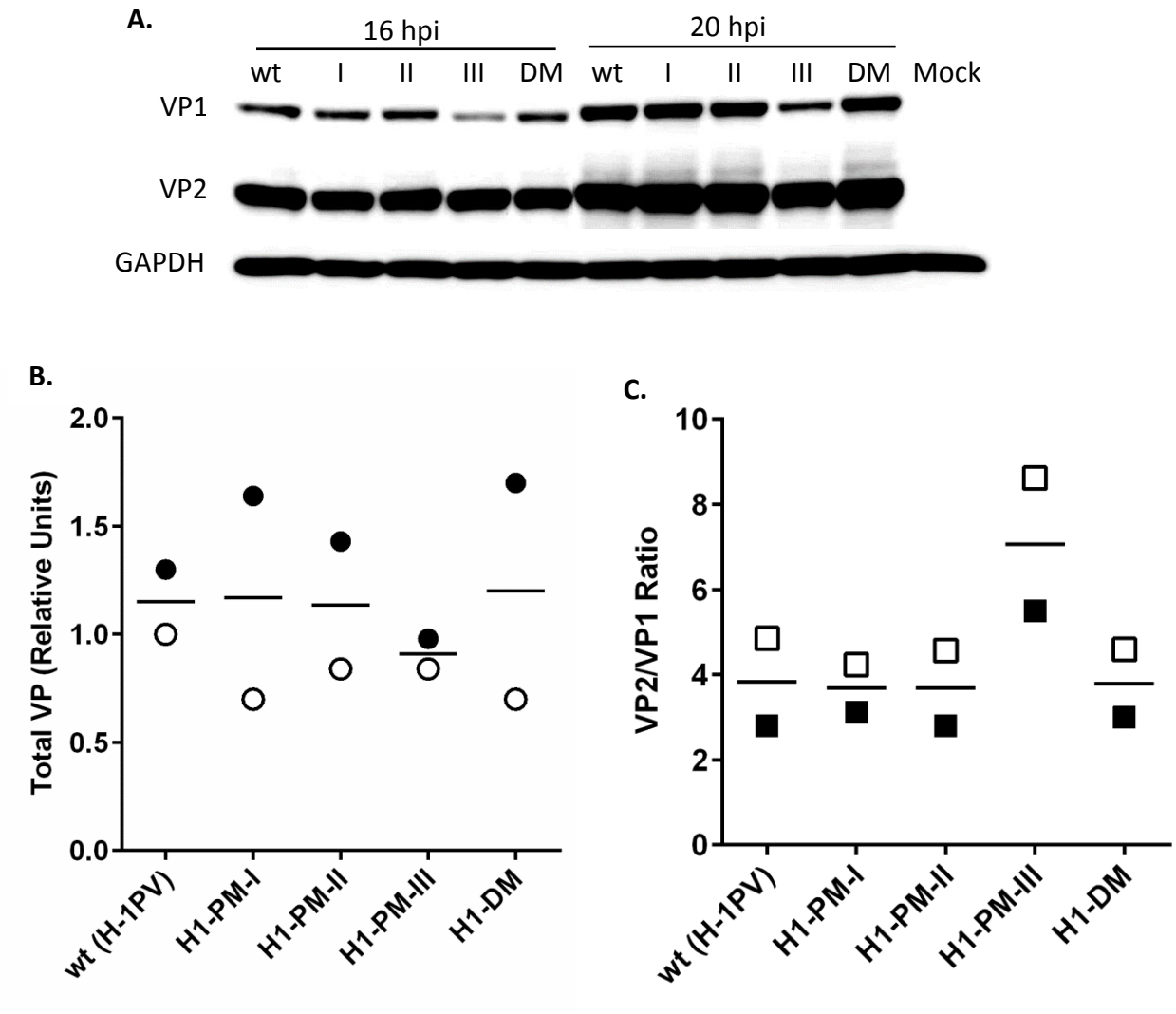

Figure 5. Viral protein levels after infection with equal infectious units (1 PFU/cell) of the virus particles. (A) $5x10^5$ NB-324K cells were infected with wt (H-1PV) or H1-PM-I, H1-PM-II, H1-PM-III and H1-DM mutant viruses at a MOI of 1 PFU/cell followed by addition of an anti-capsid neutralizing serum to the culture medium 2 hpi to prevent further rounds of infection. Whole cell lysates and Western Blotting were prepared as for Figure 3. Lanes I, II, III and DM stand for H1-PM-I, H1-PM-II, H1-PM-III and H1-DM mutants respectively. (B, C) Total accumulation of the capsid proteins VP1 and VP2 after densitometric quantification of the bands using Lab-1D image analysis software and expressed as relative units to the wt corresponding band at 16 hpi. Figure C indicates the ratio of VP2:VP1 levels. Empty and filled symbols show the values at 16 and 20 hpi respectively.

As shown in Figure 6, increasing the MOI to 3 PFU/cell further confirmed these observations.

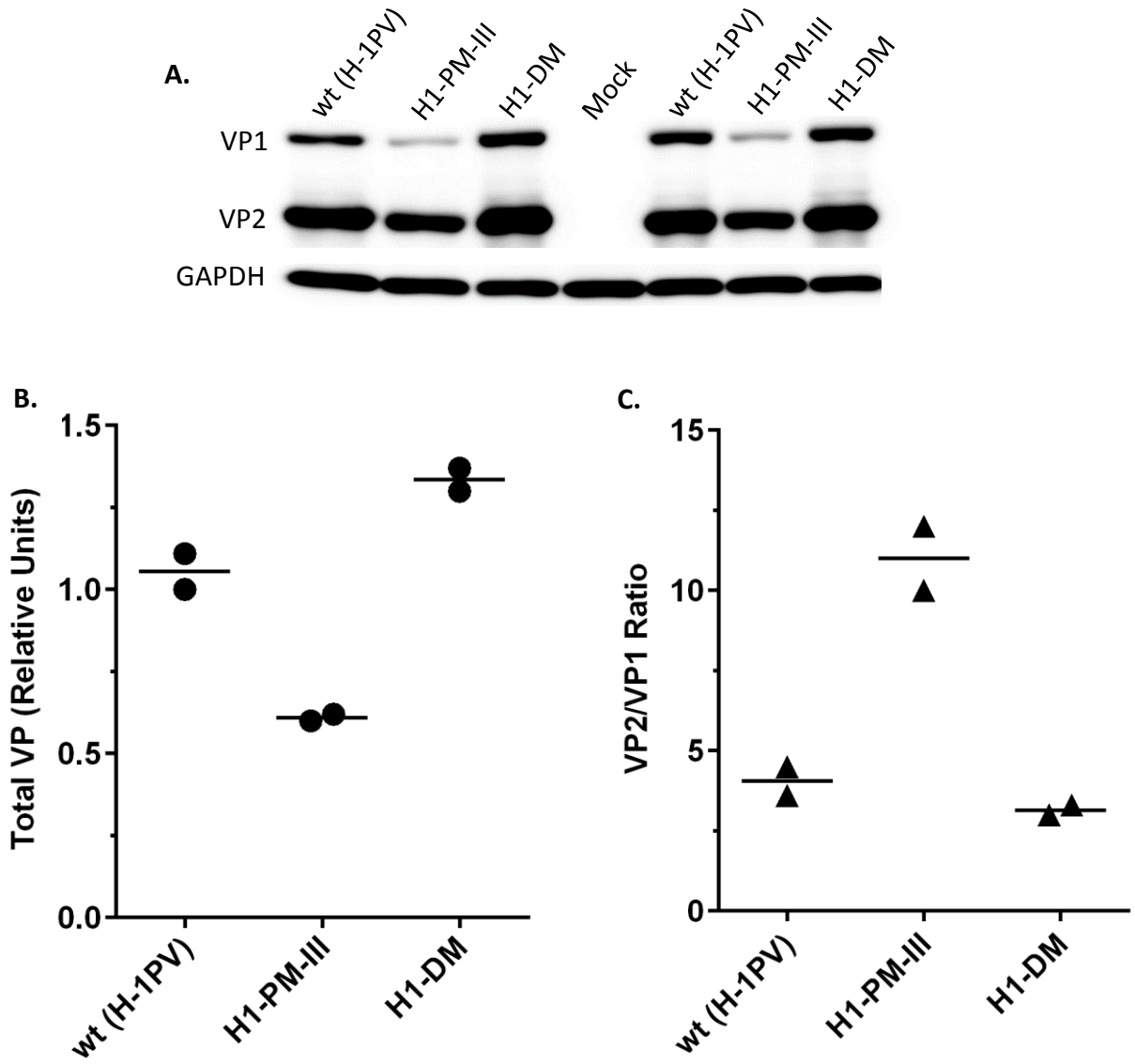

Figure 6. Viral protein levels after infection with a MOI of 3 PFU/cell. $5x10^5$ NB-324K cells were infected with wt (H1-PV) virus or H1-PM-I, H1-PM-II, H1-PM-III and H1-DM mutants at a MOI of 3 PFU/cell followed by addition of anti-capsid neutralizing serum to culture medium. (A) Whole cell lysates and Western Blotting were prepared 22 hpi as for Figure 3. Results of two independent experiments are shown. (B) Total accumulation of capsid proteins expressed as relative units to wt. The densities of the protein bands were quantified by Lab-1D software. (C) Mean ratio of VP2:VP1 levels.

In another approach, to circumvent the early steps of the infection preceding gene expression, such as virus uptake, transport to the nucleus, decapsidation and conversion of viral ssDNA to dsDNA, infectious molecular DNA clones of wt (pH1 plasmid) and of the mutants (pH1-PM-III and pH1-DM plasmids) were transfected into NB-324K cells followed by addition of anti-capsid neutralizing serum to the culture

medium to prevent secondary infections (Figure 7). Supporting the data obtained after infection with the same number of infectious virus particles (1 PFU/cell and 3 PFU/cell), the levels of both capsid proteins was significantly lower after transfection of pH1-PM-III (50% of pH1 VPs, Figure 7A and B). Slightly higher amounts of the capsid proteins were produced by pH1-DM compared to pH1 (Figure 7A and B).

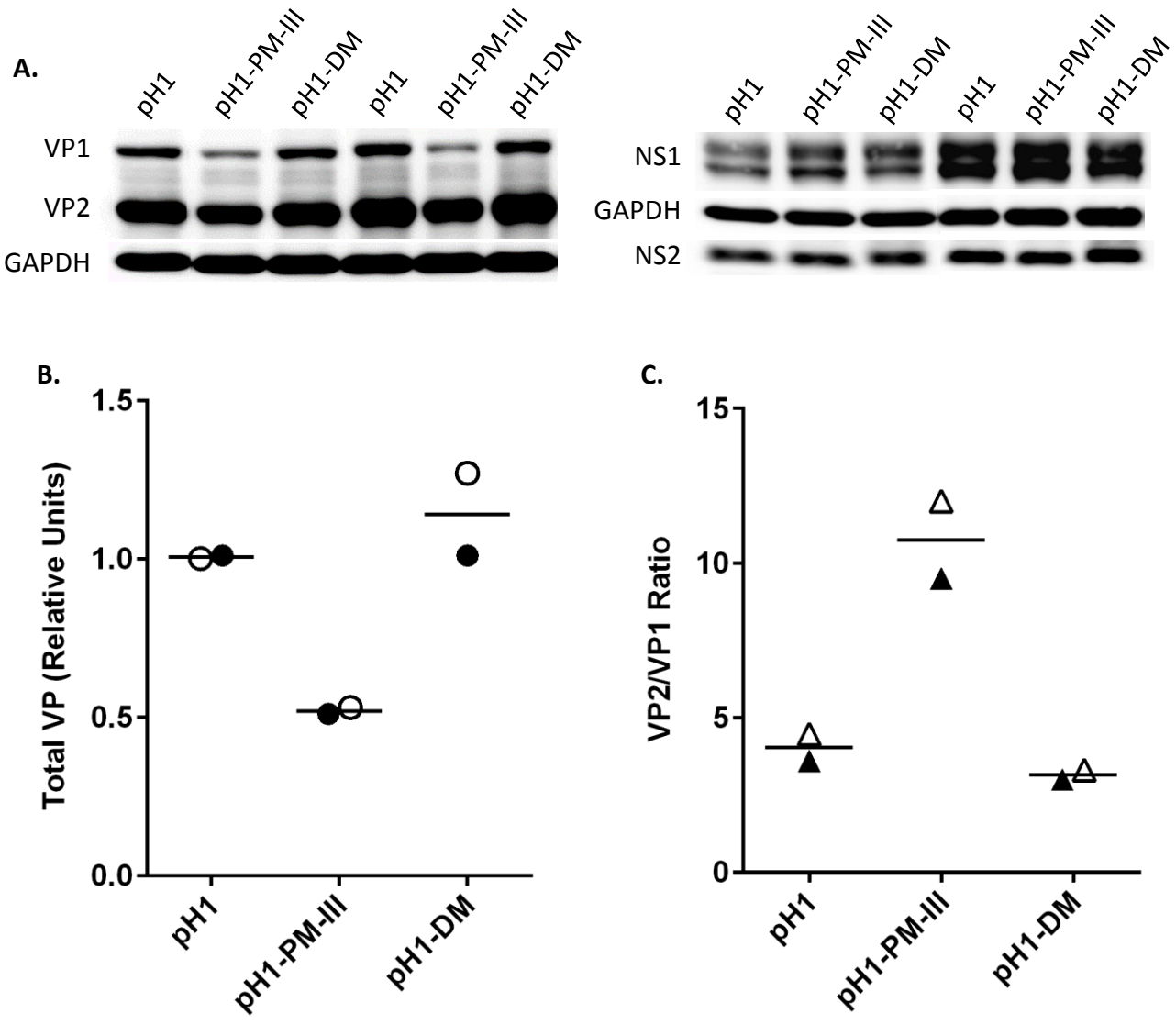

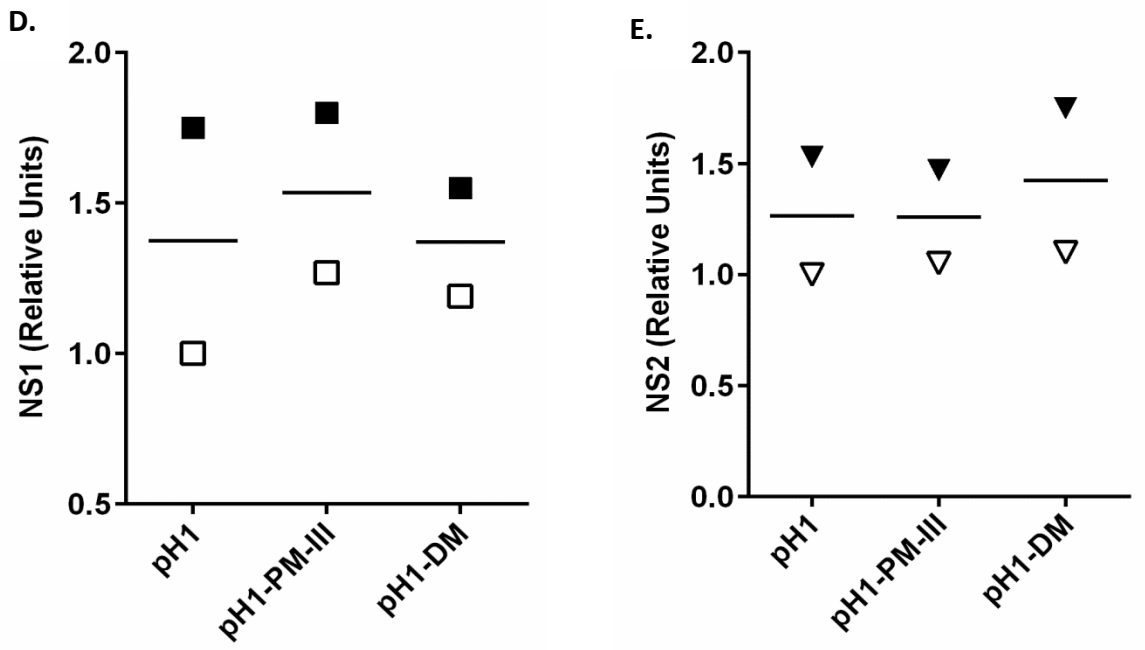

Figure 7. Western blot analysis of viral protein levels after transfection of infectious DNA clones of the viruses. (A) $7x10^5$ NB-324K cells were transfected with 5.5 µg of pH1, pH1-PM-III and pH1-DM plasmids using LFA®3000 reagent. Whole cell lysates were prepared and the expression of the capsid proteins, NS1, NS2 and cellular GAPDH (as loading control) was analyzed by Western blotting as described for Figure 3. The results after 16 (empty symbols) and 24 h (filled symbols) are shown. (B, C) Total amount of VP1 and VP2 proteins was quantified by densitometric analysis of the bands using Lab-1D software and expressed as relative units to the wt band at 16 hpi. (C) Ratio of VP2:VP1 levels. (D, E) Accumulation of NS1 and NS2 proteins is presented as relative units to the wt bands at 16 hpi. Mean values are indicated by a line.

Furthermore, the ratio of VP2:VP1 proteins after pH1-DM transfection was comparable to pH1, and was about 2-fold increased after transfection with pH1-PM-III (Figure 7C). As shown in Figure 7D and E, NS1 and NS2 proteins were efficiently produced by the cells receiving pH1-PM-III plasmid. This indicated that diminished capsid production was not due to decreased steady-state levels of NS1, the protein required for induction of P38 promoter, or lower transfection efficiency of pH1-PM-III construct compared to pH1. Taken together, this data indicates that the reduced capsid accumulation after H1-PM-III infection is unlikely due to (a) defect(s) in the early steps of the infection and can be recapitulated by transfection of pH1-PM-III, when a duplex viral genome is delivered to the cells.

3.3 Viral DNA Replication is Modified by NS1/NS2 Mutations

As mentioned in the introduction part, the incoming viral genome must be converted into dsDNA which is then amplified in concatemeric forms. Parvovirus DNA replication requires essential functions of NS1 (e.g. helicase and nickase) and cellular DNA replication machinery (e.g. DNA polymerase and PCNA). The concatemeric double-stranded forms of DNA are resolved to monomeric genome-length duplexes (mRF) which are unwound and packaged as progeny, negatively-oriented, ssDNA inside preassembled empty capsids. Having determined that the expression of viral proteins is altered in cells infected with the mutants, either decreased (H1-PM-III) or increased (H1-PM-I, H1-PM-II and H1-DM) compared with wt (H-1PV), we next wanted to evaluate whether or not this is concomitant with differences in conversion of ssDNA to dsDNA and subsequent accumulation of intermediate replicative forms of viral DNA. For this purpose, the viral DNA replicative forms were analyzed by Southern Blotting on virus-infected NB-324K cells. $1.6X10^6$ cells were infected with H-1PV or mutant viruses (H1-PM-I, H1-PM-II, H1-PM-III and H1-DM) at a MOI of 1 PFU/cell and anti-capsid neutralizing serum was added to prevent secondary infections. Total DNA was extracted using DNeasy Blood & Tissue kit (QIAGEN) and the viral replicative forms were analyzed by Southern blotting using a radioactive ^{32}P-labeled VP-specific DNA probe (Section 2.8). Figure 8A shows the accumulation of viral monomeric replicative form (mRF, 5 kbp band), dimeric replicative form (dRF, 10 kbp band) and single-stranded DNA (ssDNA) 16 and 20h post-infection. The intensity of the bands corresponding to mRF and dRF was stronger than wt for all three mutants H1-PM-I, H1-PM-II and H1-DM as can be seen 16 hpi (Figure 8A left panel). The ssDNA, which was visible at 20 hpi, accumulated stronger for the mutants H1-PM-I and H1-DM (Figure 8A, middle panel). Interestingly, although H1-PM-III virus produced mRF and dRF replicative forms similar to wt, the progeny ssDNA was strikingly impaired (Figure 8A, middle panel). Indeed, the intensity of H1-PM-III ssDNA band after infection at a MOI of 1 PFU/cell was below the detection level of the Southern blotting (Figure 8A, left panel) and appeared only very weakly when the MOI was increased up to 3 PFU/cell (Figure 8A, right panel).

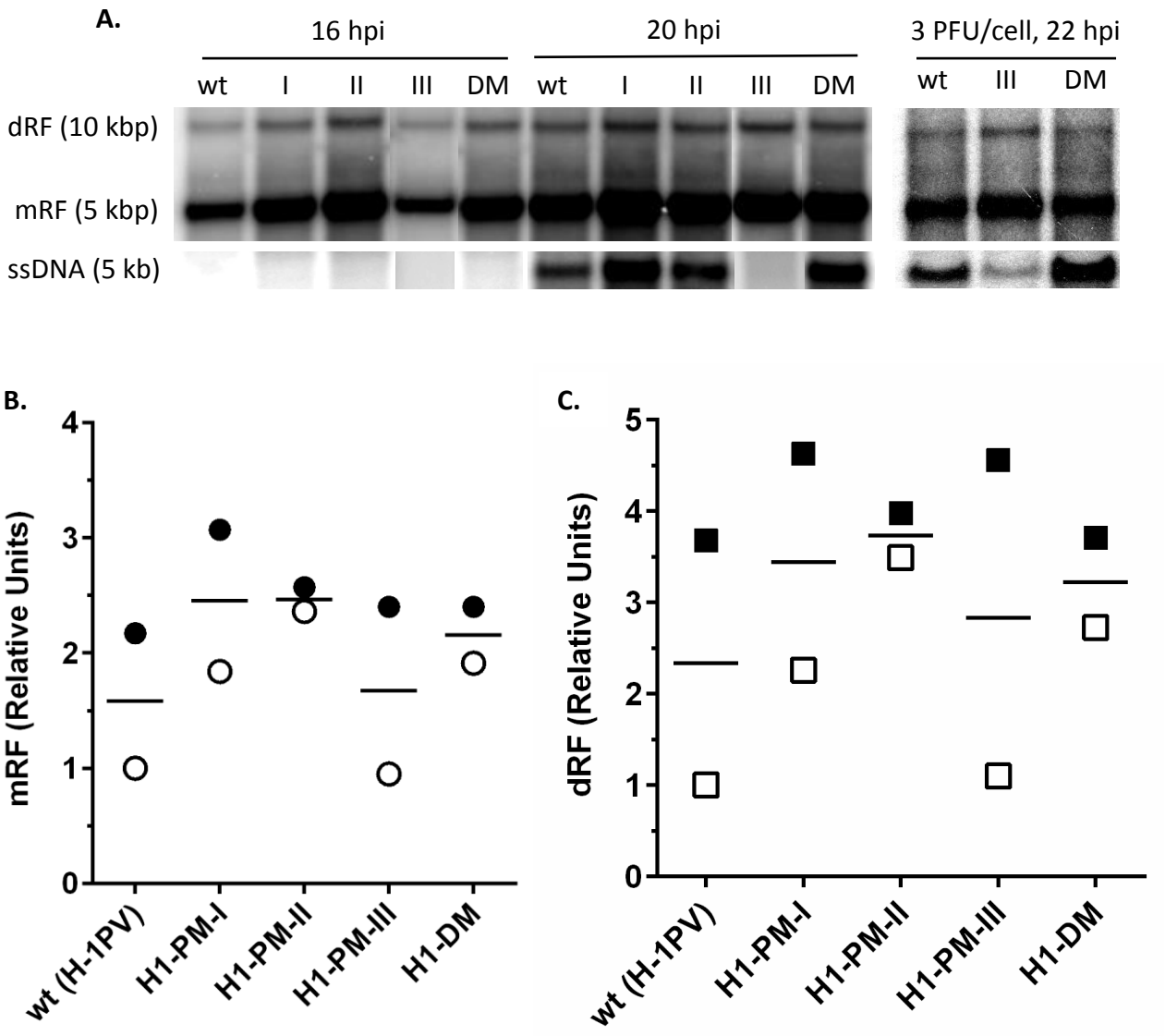

Figure 8. Southern blot analysis of viral DNA replication after infection with equal infectious units of virus particles. (A) $1.6x10^6$ NB-324K cells were infected at MOI of 1 PFU/cell (A, left panel) or 3 PFU/cell (A, right panel) with wt (H-1PV) and the mutants. Total DNA was extracted and viral DNA was analyzed by Southern blotting using a ^{32}P-labeled VP-specific probe. (A) Lanes I, II, III and DM stand for H1-PM-I, H1-PM-II, H1-PM-III and H1-DM mutants respectively. The bands corresponding to monomeric and dimeric replicative forms of viral DNA are indicated as mRF and dRF respectively. (C, D) Densitometric quantification of monomeric (mRF) and dimeric replicative forms (dRF) at 16 (empty symbols) and 20 hpi (filled symbols). All the quantifications were normalized to wt mRF and dRF at 16 hpi referred to as 1.

After transfection with the plasmids pH1-PM-III and pH1, similar levels of the DNA replicative form mRF were observed 22h post transfection after digestion of the input plasmids with DpnI enzyme (Figure 9A and B). However, in this assay, dRF could hardly

be seen, irrespective of the plasmids, and DpnI restriction fragments of the plasmids masked the viral ssDNA band.

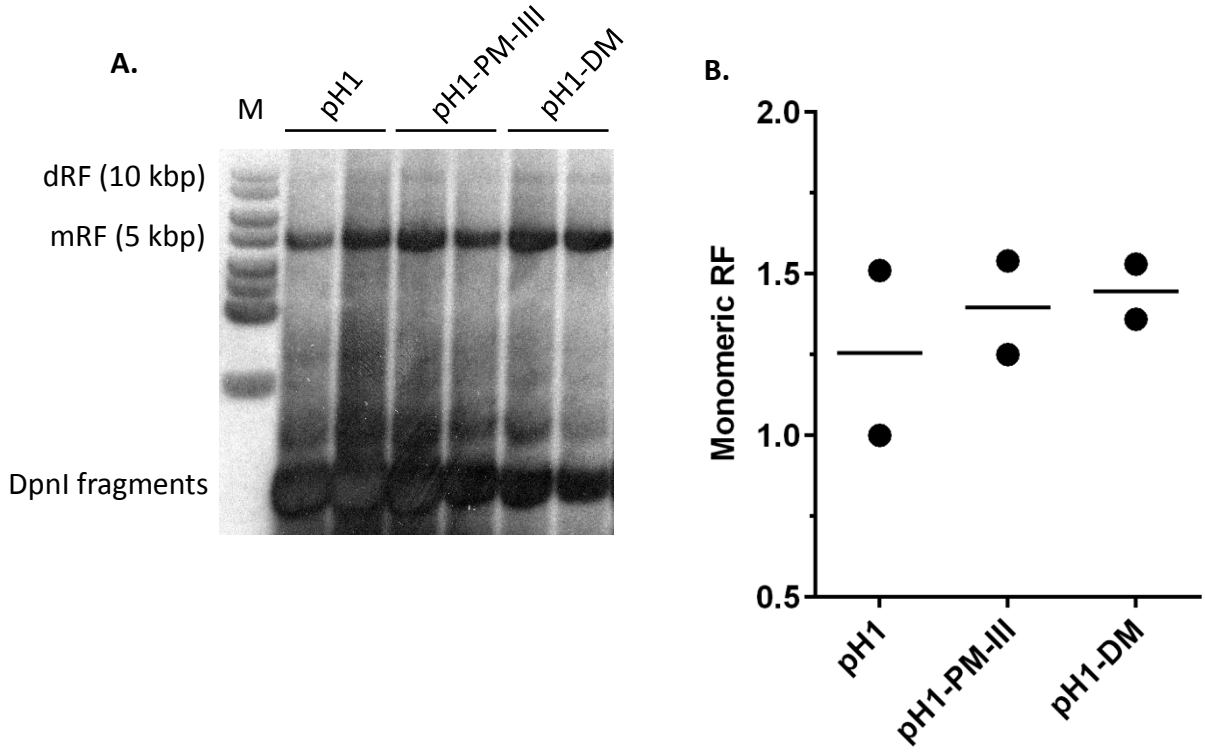

Figure 9. Replication of viral DNA upon introduction of infectious DNA clones. $1.6x10^6$ NB-324K cells were transfected with 14 µg of pH1 (wt), pH1-PM-III and pH1-DM plasmids using LFA®3000 reagent. After 22 h the cells were lysed in Hirt buffer and the cellular genomes were salted out at 4°C followed by precipitation of low molecular weight episomal DNA from the supernatant. The input plasmid was selectively digested with DpnI restriction enzyme and the viral DNA replicative forms were revealed by Southern blotting using a radioactive ^{32}P-labeled VP-specific DNA probe. (A) Southern blot of two independent transfections is shown. dRF and mRF indicate dimeric and monomeric replicative forms respectively. M lane indicates 1kb DNA marker. Lanes III and DM stand for pH1-PM-III and pH1-DM plasmids respectively. (B) The densities of mRF bands were quantified by ImageJ software. All the values were normalized to mRF wt band.

4.1 Protein Expression Encoded by the Viral R3 mRNA is Impaired in H-1-PM-III Mutant

We next wanted to determine whether the decreased accumulation of VP proteins after infection with PM-III was specific for the capsid proteins. To address this question, PM-III mutation was grafted into a H1-based vector encoding *Gaussia* luciferase in replacement of capsid genes under P38 promoter (pChi-H1-PM-III/GLuc, Section 2.9).

In order to normalize for transfection efficiency, the pChi-H1-PM-III/Gluc and pChi-H1/Gluc plasmids were co-transfected with pCMV-Cyp.luc vector into 2.7x10^5 NB-324K cells. Secreted luciferase activities were measured in the cell culture medium and the *Gaussia* luciferase activity was normalized to *Cypridina* luciferase values. The activity of *Gaussia* luciferase, expressed as relative light units (RLU), was normalized to that from *Cypridina* luciferase. As shown in Figure 10, the plasmid vector harboring the PM-III mutation showed around 2-fold less reporter expression compared to the wt vector. This is in agreement with the results obtained for capsid protein expression when the infectious DNA clone of PM-III (pH1-PM-III plasmid) was transfected into the cells (Figure 7B) or after infection with the same infectious units of the mutant virus (Figure 6B).

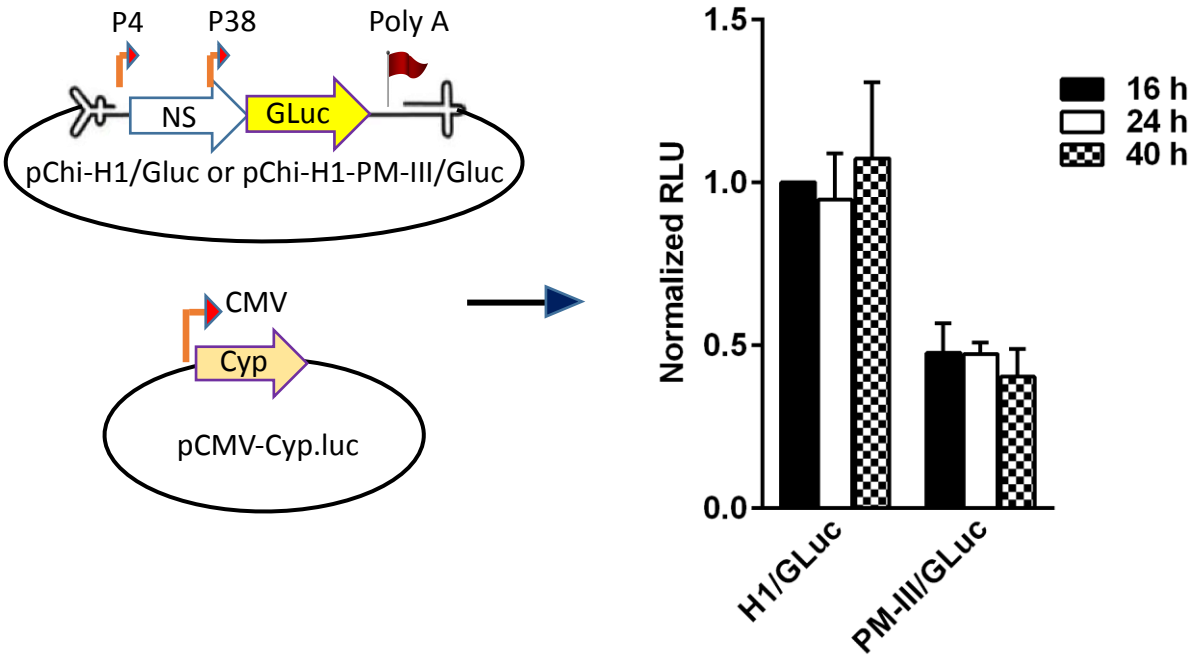

Figure 10. Luciferase reporter expression after transfection of NB-324k cells with pChi-H1-PM-III/GLuc. (Left panel) A H1-based vector containing the PM-III mutation was constructed in which the *Gaussia* luciferase cDNA is cloned in replacement of the capsid genes under the P38 promoter (pChi-H1-PM-III/GLuc). 1x10^5 NB-324K cells were co-transfected with 975 ng of either wt control (pChi-H1/Gluc) or pChi-H1-PM-III/GLuc vectors and 25 ng of pCMV-Cyp.luc, a plasmid encoding naturally secreted *Cypridina* luciferase under CVM promoter to normalize for transfection efficiency. Activities of both luciferases were measured in cell culture medium 16, 24 and 40 h after transfection as described in Materials and Methods (Section 2.11). *Gaussia* luciferase values were normalized to those from *Cypridina* luciferase and expressed as relative light units (RLU) to the control (wt). H1/Gluc and PM-

III/GLuc indicates pChi-H1/GLuc and pChi-H1-PM-III/Gluc plasmids respectively. Mean ± SD of three independent experiments is shown.

Although some post-translational modifications or instability of the viral capsids resulting from PM-III mutation cannot be ruled out, the reduced luciferase activity observed after transfection with pChi-H1-PM-III/GLuc plasmid suggests that the impaired accumulation of capsid proteins in H1-PM-III-infected cells (Figure 3, 5 and 6) and pH1-PM-III transfected cells (Figure 7) is not specific for VP proteins. We hypothesize that PM-III mutation most likely affects either the levels of R3 transcripts and/or *de novo* synthesis of their encoded proteins.

4.2 PM-III Mutation Acts *in Cis* on the Expression of Capsid Proteins

The overlapping position of the NS-coding sequences and 5'-UTR region of the capsid mRNA prompted us to investigate *cis*-acting effect(s) of the nucleotide substitution(s) introduced by PM-III and DM mutations on expression of the capsid proteins. For this purpose, split constructs were created from pH1 (wt), pH1-PM-III and pH1-DM infectious DNA clones (Section 2.10). In this dual vector system, P4-NS and P38-VP expression cassettes are carried by separate plasmids. Different combinations of pP4-NS, pP38-VP and their mutant derivatives were co-transfected into NB-324K cells and the levels of capsid proteins were analyzed by Western blotting. As shown in Figure 11A (Lane 2&5), capsid expression was decreased when pP38-VP-PM-III plasmid was co-transfected with either wt pP4-NS (Lane 2) or mutant pP4-NS-PM-III vector (Lane 5), compared with co-transfection of wt pP38-VP construct with either wt pP4-NS (Lane 1) or mutant pP4-NS-PM-III (Lane 4). In contrast, DM mutations did not alter expression of the capsid proteins, when pP38-VP-DM vector was co-transfected with either wt pP4-NS (Lane 3) or mutant pP4-NS-PM-III construct (Lane 6). Indeed, PM-III mutation exhibited a strong *cis*-acting effect on the capsid expression (Figure 11A, Lanes 2&5) and compromised the accumulation of VP1 and VP2 proteins (~30% less than wt) (Figure 11B, pP38-VP-PM-III compared to pP38-VP). Furthermore, in agreement with the gene expression observed post-infection (Figure 3, 5 and 6) and transfection of

infectious clones (Figure 7), the VP2:VP1 ratio was more than 2-fold increased when the capsid proteins were produced by pP38-VP-PM-III plasmid compared to pP38-VP (wt) construct (Figure 11C) By contrast, when pP4-NS-PM-III was used to transactivate pP38-VP no *trans* effect of PM-III mutation (L153M in NS2) was observed on the accumulation of the capsid proteins (Figure 11A, Lane 4). As shown in Figure 11D, quantification of the R3 transcripts by qRT-PCR did not show any decrease caused by PM-III mutation in pP38-VP-PM-III. This suggests that the impaired capsid production in H1-PM-III mutant is not caused either by altered transactivation of the P38 promoter or by the mutation of NS2 protein in pP4-NS-PM-III and/or instability of R3 transcripts. It is noteworthy that the primers used in the qRT-PCR reaction were designed for the common coding region of VP1 and VP2 transcripts, hence cannot distinguish unspliced and spliced forms of the capsid R3 mRNAs. As mentioned earlier in introduction part, VP2 is the major capsid protein and is present at ~50 copies per capsid while VP1 is the minor component and is present at ~10 copies per capsid. As depicted in Figure 4, P38 promoter generates R3 pre-mRNAs which are alternatively spliced at D1-A1 or D2-A2 junctions to generate VP2 and VP1 mRNAs respectively. In fact, the VP2:VP1 ratio (5:1) is maintained at mRNA level, where more efficient excision of VP2 small intron at D1-A1 junctions compared to VP1 small intron at D2-A2 junctions results in higher yields of VP2 protein (Clemens and Pintel, 1988; Schoborg and Pintel, 1991). The data obtained with the split vectors strongly suggest that *cis*-effects of PM-III mutation at a post-transcriptional level interfere with production of capsid proteins and more prominently VP1, leading to impaired generation of preassembled capsids.

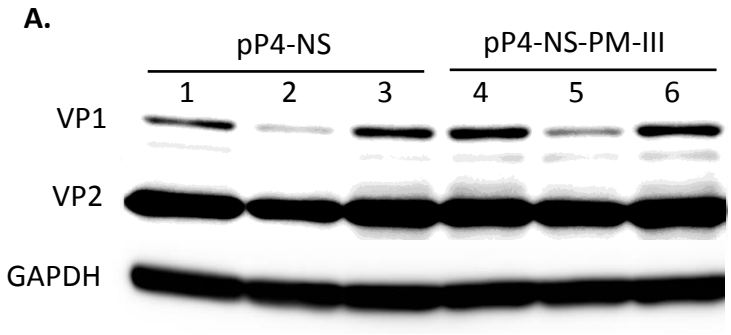

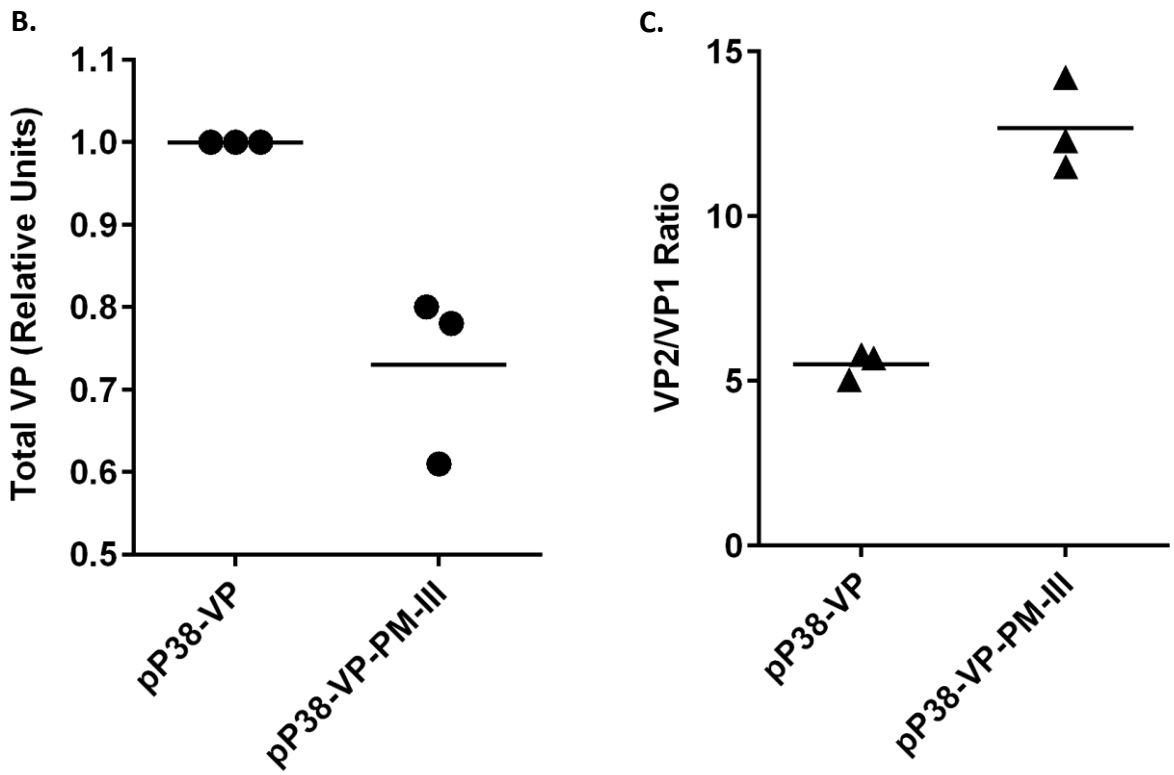
B.
Total VP (Relative Units)
1.1
1.0
0.9
0.8
0.7
0.6
0.5
pP38-VP
pP38-VP-PM-III
C.
VP2/VP1 Ratio
15
10
5
0
pP38-VP
pP38-VP-PM-III

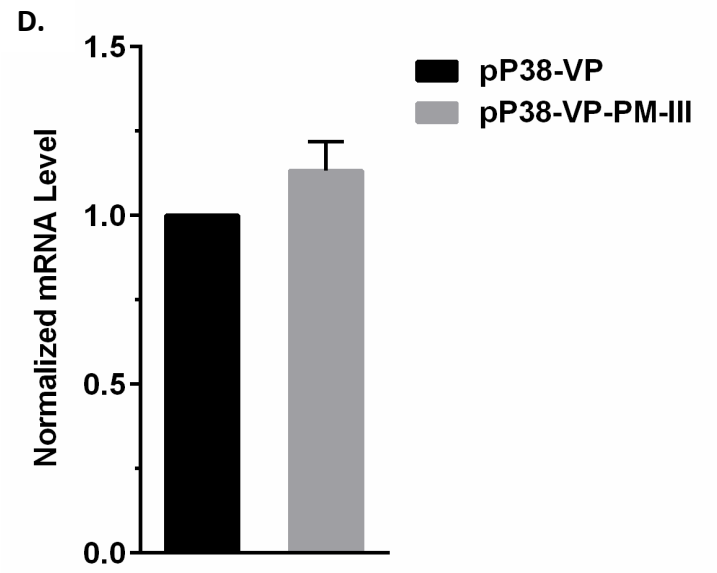
D.
Normalized mRNA Level
1.5
1.0
0.5
0.0
pP38-VP
pP38-VP-PM-III

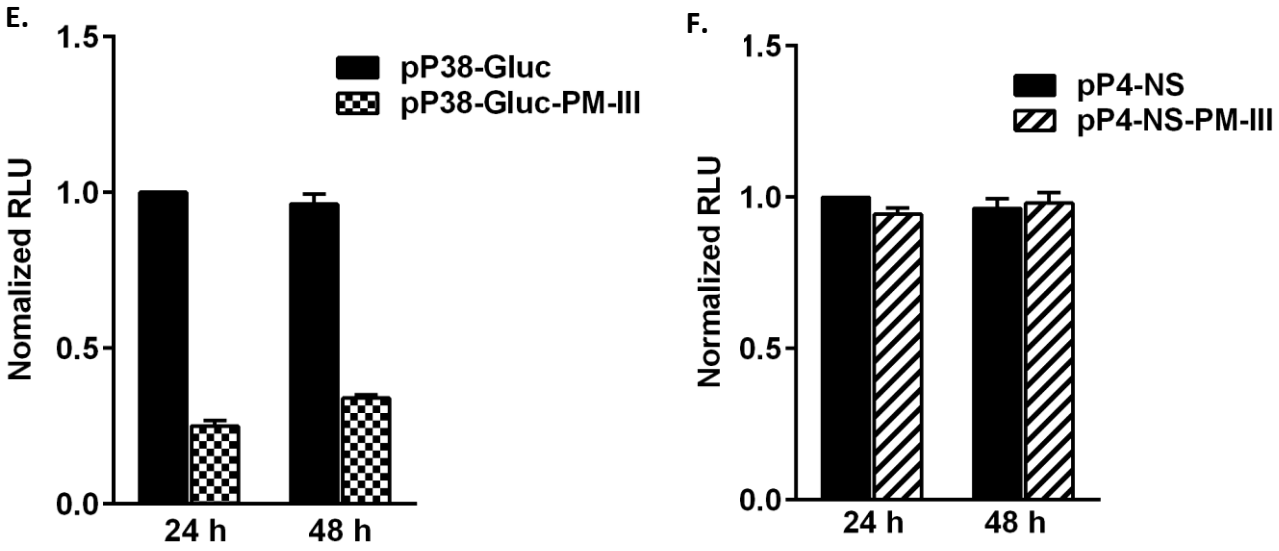

Figure 11. *Cis*-acting effect of PM-III mutation on capsid expression by split vectors. 0.5 µg of plasmids carrying P4-NS expression cassettes either wt (pP4-NS) or mutant-derived: pP4-NS-PM-III and pP4-NS-DM, were co-transfected with 2 µg of pP38-VP expression cassettes either in their wt form (pP38-VP) or containing the mutations pP38-VP-PM-III and pP38-VP-DM, into $2.7x10^5$ N-234K cells using LFA®3000 reagent. Lanes 1&4 indicate pP4-NS and pP38-VP, 2&5: pP4-NS and pP38-VP-PM-III, 3&6: pP4-NS and pP38-VP-DM co-transfection. (A) 24 hours after transfection, capsid proteins and cellular GAPDH were analyzed from transfected cell extracts by Western blotting. (B, C) Densitometric quantification of the capsid protein bands expressed by pP38-VP, pP38-VP-PM-III and pP38-VP-DM. The results are expressed as mean of three independent transfection experiments normalized to wt band. (C) Ratio of VP2:VP1 proteins. (D) Relative quantification of total R3 transcripts encoding VP1 and VP2, from samples co-transfected with pP4-NS and pP38-VP or pP38-VP-PM-III plasmids using cellular GAPDH mRNA as reference. Results are expressed as normalized to intensities pP38-VP/GAPDH =1. (E) *Cis* effects of PM-III mutation on reporter gene expression. $1x10^5$ NB-324K cells were co-transfected with 195 ng of wt (pP4-NS) and 780 ng of pP38-Gluc or pP38-Gluc-PM-III and 25 ng of pCMV-Cyp.luc (expressing *Cypridina* luciferase as normalizing reporter) plasmid. Finally, *Gaussia* and *Cypridina* activities were measured in the culture medium 24 and 48 h after transfection. (F) The reporter induction capacity of NS expression cassette derived from PM-III mutant. The pP38-Gluc plasmid was co-transfected with either pP4-NS or pP4-NS-PM-III vectors. In both E and F, *Gaussia* luciferase values were normalized to those from *Cypridina* luciferase and expressed as relative light units (RLU) to the values obtained for wt vectors. Mean ± SD of three independent experiments is shown.

The expression of Gaussia luciferase (Gluc) by pP38-Gluc devoid of the small introns (Figure 4) showed that P38-driven gene expression is affected by *cis* effects of PM-III mutation even in the absence of a splicing event. Indeed, ~70% lower luciferase activity was observed when P38 promoter contained the PM-III mutation (pP38-Gluc-

PM-III) compared to the wt sequence (pP38-Gluc) (Figure 11E), while the levels of Gluc were similar to wt when either pP4-NS or pP4-NS-PM-III were co-transfected with pP38-Gluc (wt) construct (Figure 11F). The *cis* effect of PM-III mutation (C-to-A) on the expression of P38-driven transcripts is likely due to a post-transcriptional effect, generating a small ORF upstream of VP1 and VP2 initiation codons, in a favorable Kozak context (G at +4 and A at -3 position, relative to A in ATG) which could repress downstream translation of R3 mRNAs (wt: AAC**C**TGG and PM-III: AAC**A**TGG).

These observations were further confirmed by the analysis of gene expression after infection of NB-324K cells with a NS2null derivative of H-1PV (H1-NS2null virus). In this assay the expression of NS2 protein is absent due to the introduction of a mutation in the splice acceptor site of NS2 large intron, thereby preventing the synthesis of R2 mRNA which encodes NS2. The capsid proteins accumulated efficiently in the nucleus and the cytoplasm (Figure 12A, B and C), although substantially lower yield of progeny virions was achieved in a single round of infection compared to wt virus (Figure 12D). It is known that NS2 is dispensable for virus replication cycle but reduces the virus production in non-host cells. However, whether a defect in the assembly of the capsids or generation of ssDNA and genome packaging caused the lower yield of NS2null progeny virions was still unclear.

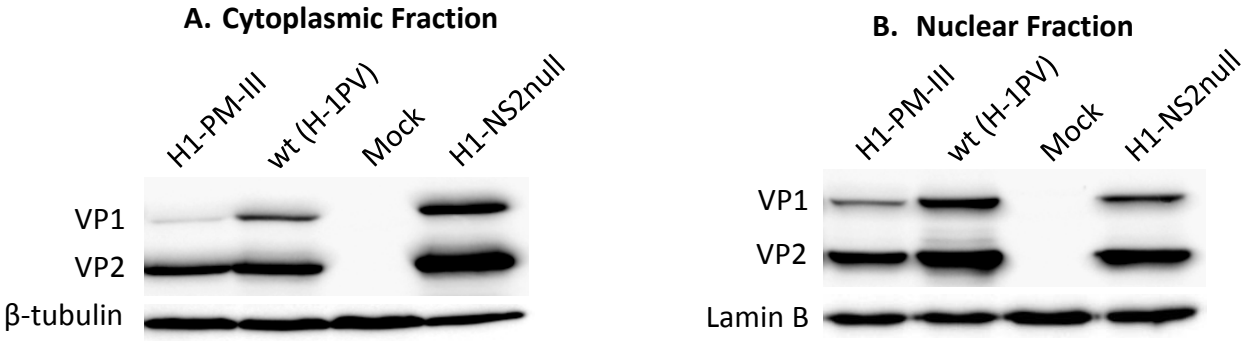

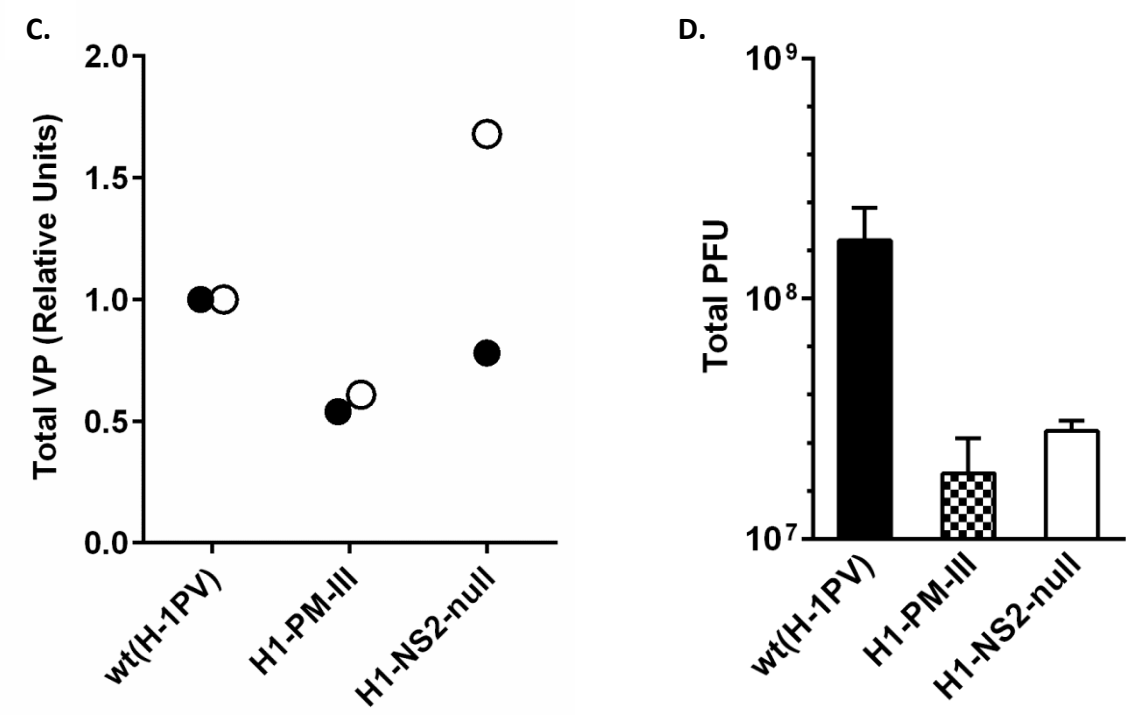

Figure 12. Accumulation of the capsid proteins and yield of progeny virions in H1-NS2null and H1-PM-III-infected cells. (A, B) $5x10^5$ NB-324K cells were infected with wt (H1PV), H1-PM-III and a NS2-null derivative of wt virus (H1-NS2null) at a MOI of 3 PFU/cell followed by addition of anti-capsid neutralizing serum to culture medium to prevent further rounds of infection. Cytoplasmic and nuclear fractions were prepared 20 hpi and their capsid protein content was analyzed by Western blotting as for Figure 3. A and B indicate cytoplasmic and nuclear fractions respectively, for which β-tubulin and lamin B were used as specific loading controls. (C) Total accumulation of capsid proteins VP1 and VP2 is shown in cytoplasmic (empty circles) and nuclear (filled circles) fractions after normalization to the values obtained for wt proteins. (D) Total yield of progeny virions obtained after infection of $5x10^5$ NB-324k cells with 3 PFU of wt (H-1PV), H1-PM-III and H1-NS2null viruses. Mean ± SD of duplicates from two independent plaque assays are shown.

4.3 A Silent Mutation Eliminates *Cis* Effects of the PM-III Mutation on Capsid Expression and Restores the wt Phenotype

As mentioned before, PM-III mutation has strong *cis* effects on the translation of R3 transcripts (Figure 11). This was independent of the splicing of the downstream small introns in VP1 and VP2 pre-mRNAs (Figure 11E) and of the PM-III mutation in NS2 protein (Figure 11F). The *cis* effect on capsid (Figure 13B and C) and reporter gene expression (Figure 13E) was eliminated and both were restored to wt levels when PM-III mutation AAC**A**TGG was substituted with AAC**T**TGG. It is worth mentioning that AAC**T**TGG sequence eliminates the initiation ATG codon, creates a nucleotide

substitution at 5'-UTR of the (wt) capsid mRNAs and restores the amino acid sequence of the mutant NS2 protein to wt (L153). Indeed, this construct was called "silent" due to restoration of the amino acid sequence of the mutant NS2 protein to wt. H-1PV carrying the silent mutation showed a plaque phenotype similar to the wt virus (Figure 13A). After co-transfection of pP38-VP-PM-III^{Silent} and pP4-NS constructs into NB-324K cells, not only total accumulation of the capsid proteins but also the ratio of VP2:VP1 expression by pP38-VP-PM-III^{silent} was similar to wt construct (pP38-VP) (Figure 13C and D). Also, as shown in Figure 13E, the luciferase activity after co-transfection of pP38-Gluc-PM-III^{Silent} and pP4-NS constructs into NB-324K cells, was similar to pP38-Gluc (wt) construct.

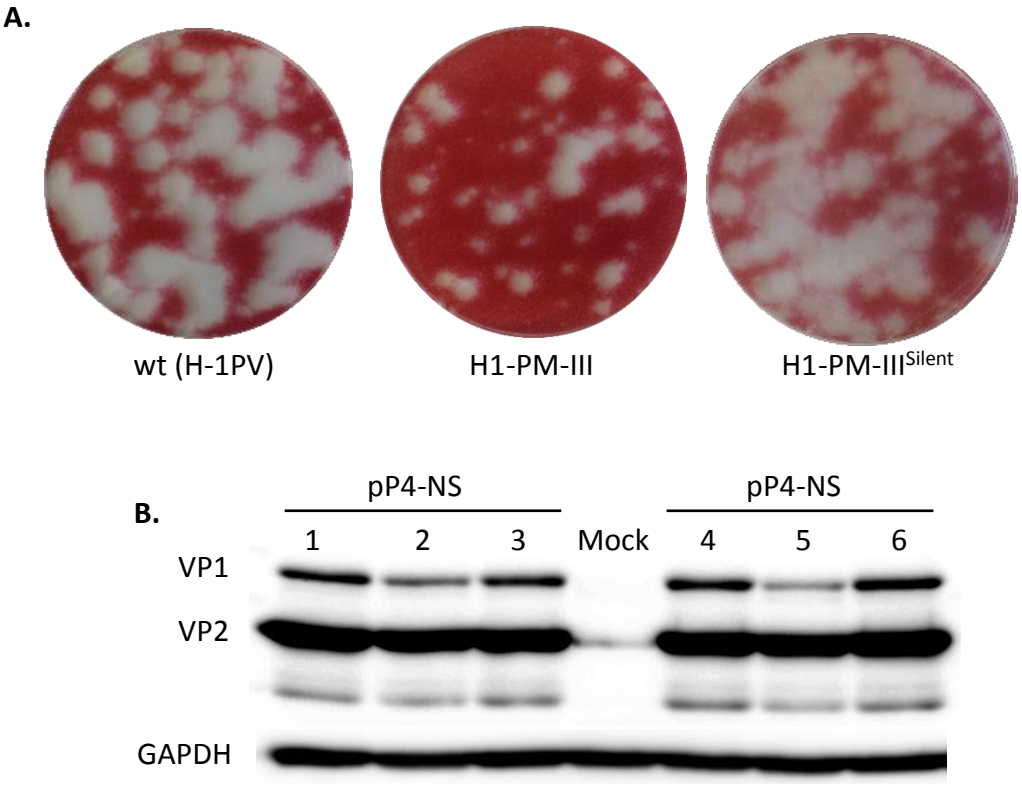

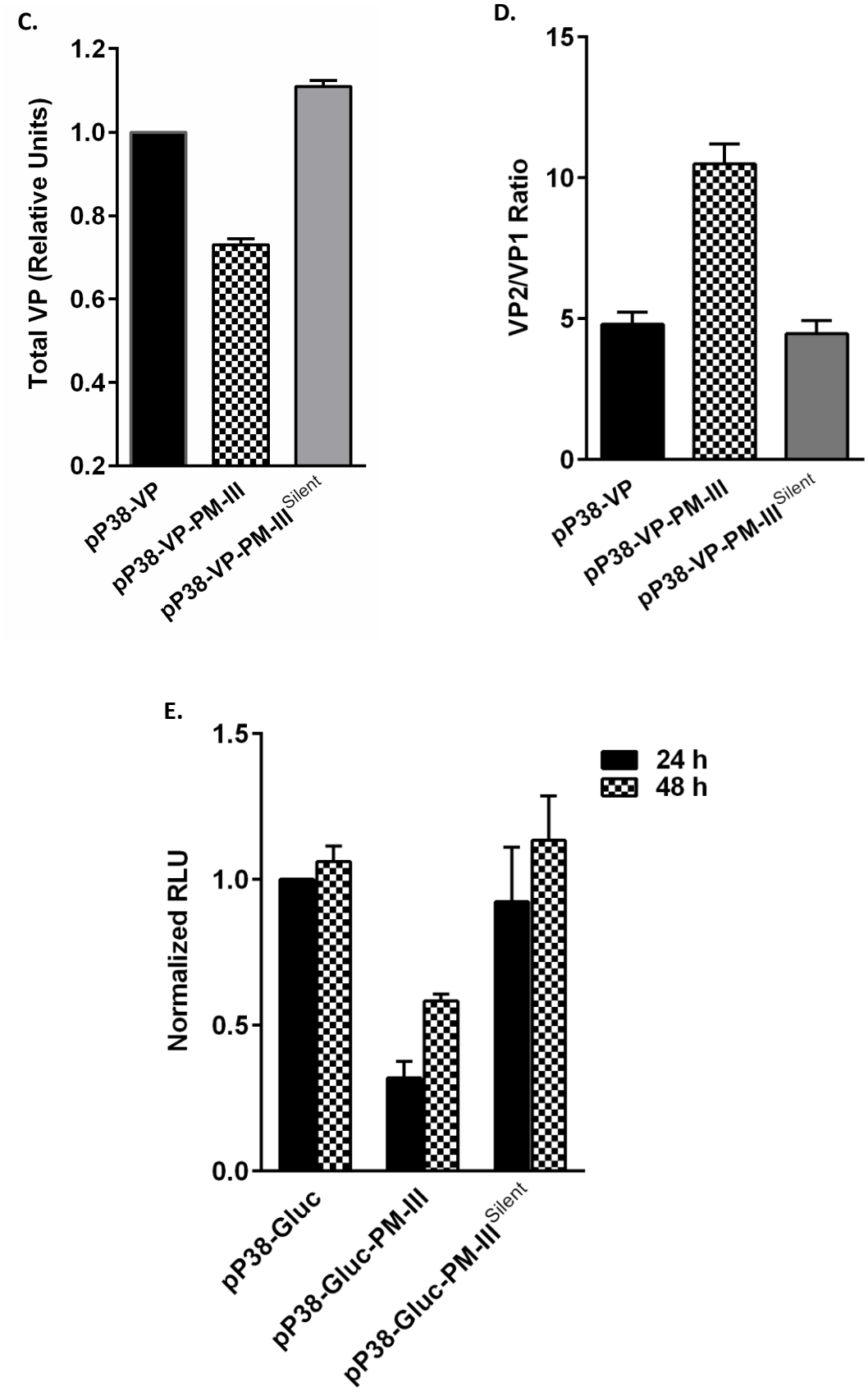

Figure 13. A silent mutation at PM-III position (L153) restores wt phenotype. (A) A silent mutation (A-to-T) was introduced in pH1-PM-III plasmid to generate pH1-PM-III^{Silent}. The silent mutant virus stock was produced after transfection of 293-T cells and titrated by plaque assay in NB-324K cells. (B) *Cis*

effects of the silent mutation on capsid expression were analyzed after co-transfection of 2 µg of pP38-VP (Lanes 1&4), pP38-VP-PM-III (Lanes 2&5) or pP38-VP-PM-III^{Silent} (Lanes 3&6) plasmids with 0.5 µg of the inducer vector (pP4-NS) into 2.7x10^5 NB-324K cells. Whole cell lysates were prepared 22 h post-transfection and capsid proteins were analyzed by Western blotting. Cellular GAPDH was used as loading control. Results of two independent transfections are shown. (C, D) Total accumulation of capsid proteins and VP2:VP1 ratio are shown as mean ± SD of two independent transfection experiments. (E) *Cis* effects of the silent mutation on reporter gene expression. 1x10^5 NB-324K cells were co-transfected with 780 ng of pP38-Gluc, pP38-Gluc-PM-III and pP38-Gluc-PM-III^{Silent} constructs, 195 ng of the inducer plasmid (pP4-NS) and 25 ng of pCMV-Cyp.luc (expressing *Cypridina* luciferase as normalizing reporter) plasmid. Both *Gaussia* and *Cypridina* luciferase activities were measured in the culture medium 24 and 48 h after transfection. Mean ± SD of three independent transfections is shown.

These results further confirmed that reduced expression of VP1 and VP2 proteins and increased ratio of VP2:VP1 are caused by a *cis* effect of PM-III mutation in 5'-UTR of R3 transcripts. However, this experiment does not rule out a possible contribution of NS2 mutated in PM-III (L153M), since NS2 is wt in the "silent" mutant. An interesting scenario with respect to *cis* effects of PM-III mutation would be a "double hit" hypothesis: 1. The C-to-A substitution creates an upstream initiation codon in a favorable Kozak context and this may repress downstream reinitiation of ribosomes at both VP1 and VP2 mRNAs, leading to diminished expression of both capsid proteins or luciferase. Also, as it will be shown in Figure 15 and Supplementary Figure 2, it cannot be excluded that PM-III induces modifications in the secondary structures of the capsid mRNAs 5'-UTR sequence, which could affect for instance translation efficiency of the mRNAs.

2. The more drastic *cis* effects of the mutation on VP1 compared to VP2, probably through interference with proper splicing of VP1 small intron or stronger, results in an imbalanced molar ratio of the capsid proteins (>2-fold higher ratio of VP2:VP1 compared to wt). It is also tempting to attribute the stronger *cis* effect of PM-III mutation on VP1, to the fact that the small upstream ORF created by this mutation overlaps with VP1 ORF and not VP2. Indeed, VP2 initiation codon is located far downstream (395 nt) of the PM-III ORF stop codon (Supplementary Figure 1), while VP1 ORF starts 14 nt upstream of PM-III ORF stop codon and in a different reading

frame (frame +2) (Figure 14). The overlapping position and different reading frames of VP1 and PM-III ORF may cause a stronger interference with translation of VP1 compared to VP2, even if the splicing of small introns in capsid mRNAs is not impaired by this mutation. In fact, the ribosomes terminating translation of ORF-1 created by PM-III mutation, need to translocate upstream to reinitiate translation of ORF-2 (VP1). Another possibility for ribosomes to access VP1 ORF is leaky scanning, where a proportion of scanning ribosomes fail to initiate at the AUG and continue scanning to next AUG. However, the efficacy of leaky scanning is highly dependent on the context of upstream AUG (Kozak, 2002). Therefore, the strong Kozak context of PM-III ORF could diminish the efficacy of this process, leading to strong repression of VP1 translation.

```
H-1PV  ACCAUCUCUGACUCCGAGAAGUACGCCUCUCAGCCAAAACUACGCUCUUACUCCACUUGC 60
MVMi   ACCAUUCACGACACCGAAAAGUACGCCUCUCAGCCAGAACUAUGCACUAACUCCACUUGC 60
       *****    *** **** ****************** ***** ** ** ***********
       AUCGGACCUUGCGGACCUAGCUCUAGAGCCUUGGAGCACACCAAAUACUCCUGUUGCGGG 120
       AUCGGAUCUCGAGGACCUGGCUUUAGAGCCUUGGAGCACACCAAAUACUCCUGUUGCGGG 120
       ****** ** * ****** *** ************************************
       CACUGCAGCAAGCCAAAACACUGGGGAGGCUGGUUCCACAGCCUGCCAAGGUGCUCAACG 180
       CACUGCAGAAACCCAGAACACUGGGGAAGCUGGUUCCAAAGCCUGCCAAGAUGGUCAACU 180
       ******** ** *** ********** ********** ********** ** *****
       GAGCCCAACCUGGUCCGAGAUCGAGGCGGAUUUGAGAGCUUGCUUCAGUCAAGAACAGUU 240
       GAGCCCAACUUGGUCAGAGAUCGAGGAGGAUUUGAGAGCGUGCUUCGGUGCGGAACCGUU 240
       ********* ***** ********** ************ ****** **   **** ***
       GGAGAGCGACUUCAACGAGGAGCUGACCUUGGACUAAGGUACA 283
       GAAGAGAGACUUCAGCGAGCCGCUGAACUUGGACUAAGGUACG 283
       * **** ******* ****  ***** ***************
```

PM-III mutation

```
 M   V   R   D   R   G   G   F   E   S   L   L   Q   S   R   T   V
AUG GUC CGA GAU CGA GGC GGA UUU GAG AGC UUG CUU CAG UCA AGA ACA GUU

 G   E   R   L   Q   R   G   A   D   L   G   L   R   Y   N   G   T
GGA GAG CGA CUU CAA CGA GGA GCU GAC CUU GGA CUA AGG UAC AAU GGC ACC
                                                    M   A   P

 S   S   #
UCC AGC UAA AAG AGC UAA A
  P   A   K   R   A   K
```

Figure 14. (Top panel) Nucleotide Sequence alignment of wt 5'-UTR region of the VP1 mRNA of MVMi and H-1PV. The nucleotide sequences were aligned using default settings of Clustal Omega online tool. Identical regions are shown with asterisks. Two AUGs located upstream of VP1 initiation codon in MVMi are underlined. The AUG flanked by a favorable Kozak context is indicated with red letters with -3 (A) and +4 (G) nucleotides (relative to A in AUG as +1 nt) in italic. The blue box encloses the position of PM-III mutation where CUG in wt is mutated to AUG. (Bottom Panel) A small ORF is created upstream of VP1 initiation codon, indicated by AUG and stop codon (#) in red letters. The C-terminal peptide derived from NS2 protein (NS2Y isoform) encoded by this ORF is shown. The VP1 ORF starting 5 codons upstream of PM-III ORF stop codon (UAA) is underlined (frame +2). For sequence of VP2 mRNA 5'-UTR, see supplementary Figure 1.

4.4 *In Silico* Predicted Structure of R3 Transcript 5'-UTR is Modified by PM-III Mutation

So far, our results show that PM-III mutation has a cis-acting effect on the expression of the capsid proteins most likely at a post-transcriptional level. As mentioned before in the introduction part, PM-III was originally isolated as a fitness mutant which was selected in mice during long-term replication of MVMi (Lopez-Bueno et al., 2004). In contrast, an attenuated virus was obtained when this mutation was introduced in the same region of H-1PV genome. This prompted us to compare the nucleotide sequence of the leader sequence of the capsid mRNA in these two closely related parvoviruses. For this purpose, the nucleotide sequences were aligned using Clustal Omega online tool. As shown in Figure 14 and Supplementary Figure 1, the nucleotide sequences of leader regions of VP1 and VP2 mRNAs derived from H-1PV and MVMi are 15% and 10% different respectively. Interestingly, in MVMi, two upstream initiation codons (AUG) are found in VP1 mRNA leader sequence and one of them is located in a favorable Kozak context (G at +4 and A at -3 position relative to A in AUG codon) (Figure 14). Also, as shown in Supplementary Figure 1, there is no upstream AUG in leader sequence of VP2 mRNA derived from H-1PV while one AUG is found in a non-optimal Kozak context in MVMi (A at +4 and C at -3 position relative to A in AUG codon). Upstream open reading frames (uORFs) are prevalent in the 5'-UTR sequence of eukaryotic mRNAs and there is increasing evidence that they act as *cis*-regulatory elements in eukaryotic gene expression at a post-transcriptional level (Wethmar, 2014). Although, uORFs are

generally thought to repress downstream translation, under distinct conditions they can enhance translation of the main protein coding sequence (CDS). Indeed, uORFs have drawn a lot of attention as versatile translational modifiers of gene expression. The regulatory impact of uORFs on gene expression is determined by several factors such as Kozak context of uAUGs, the length and number of uORFs, distance from CDS, overlap with CDS and secondary structure of mRNA (Wethmar, 2014). Lack of upstream initiation codons in leader sequences of H-1PV capsid mRNA (in contrast to MVMi) (Figure 14 and Supplementary Figure 1) suggests fundamental differences in translational regulation of the capsid mRNAs between these parvoviruses. Consequently, introduction of an upstream ORF by PM-III mutation could result in different outcomes in H-1PV (increased fitness) and MVMi (attenuation).

In addition to upstream AUGs, secondary structure of mRNA 5'-UTR sequence can modulate translation, in some cases by cooperation of protein factors *in trans* (Wethmar, 2014). In order to better understand the effects of PM-III mutation on the structure of mRNA 5'-UTR sequence, an *in-silico* model of structure prediction using RNAfold webserver was designed (Figure 15 and Supplementary Figure 2). The predicted models indicate that PM-III mutation could induce structural modifications including elimination of a large loop in an upstream region without creating downstream secondary structures such as stem-loops. On the other hand, the silent mutation was predicted to restore the mRNA structure to its wt configuration (Figure 15 and Supplementary Figure 2). Whether or not these subtle structural changes have any contribution to the diminished production of the capsid proteins is not clear.

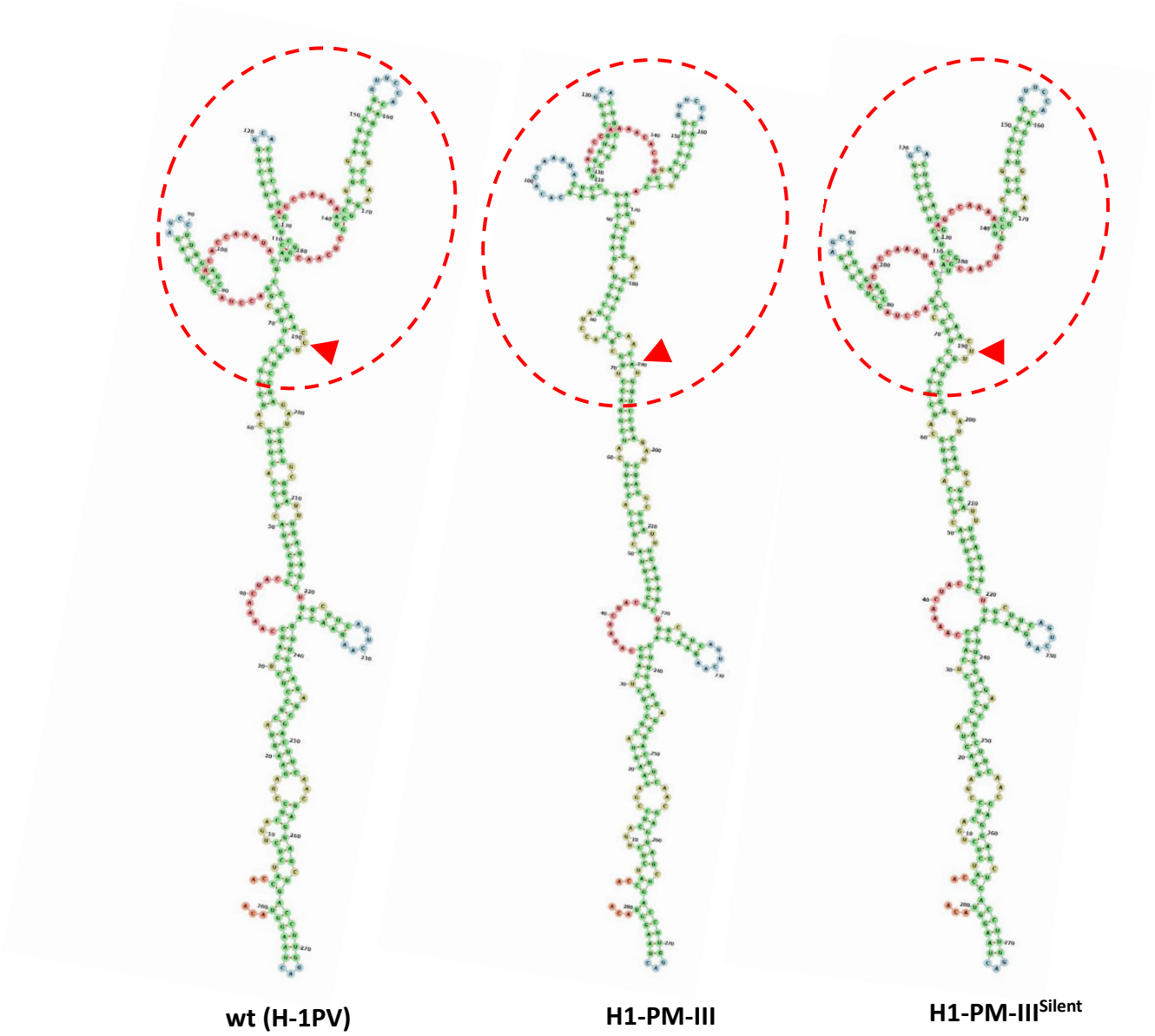

Figure 15. *In silico*-predicted secondary structure of 5' leader region from VP1 mRNA. Secondary structures of 5'-UTR sequences derived from wt (H-1PV), H1-PM-III and H1-PM-III^{Silent} viruses were predicted *in silico* using default settings of RNAfold webserver. A structure based on minimum free energy (MFE) is shown here. The region subject to structural modification is enclosed by a dashed red line, and the position of PM-III and PM-III^{Silent} mutations are indicated by an arrowhead. Colors indicate different types of structures (small or large loops, terminal loops and base-paired regions). For VP2 5'-UTR structures, see supplementary Figure 2.

5.1 Tyr595His Substitution in NS1 Enhances Virus Replication and Infectivity

The enhanced fitness of H1-DM mutant was shown by a large plaque phenotype and improved infectivity of the virus particles (Figure 1 and 2). As mentioned before, this virus carries both PM-I and PM-II mutations. PM-I introduces an amino acid

substitution in both NS1 (Y595H) and NS2 (L103P). To investigate the contribution of Y595H substitution in NS1 to virus replication in the absence of the NS2 mutation, NS2null derivatives were created in pH1 (wt) (see Figure 12), pH1-DM and pDelH1 DNA clones, in which NS2 expression was abolished by mutagenesis of the R2 mRNA splice acceptor site (see Materials and Methods, Section 2.3). Master stocks of NS2null viruses were produced by transfection of pH1-NS2null, pH1-DM-NS2null and pH1-Del-NS2null plasmids (Table 2.1) followed by virus purification (Section 2.5) and titration (Section 2.6). In order to evaluate virus replication and spread, $5x10^6$ NB-324K cells were infected at a MOI of 0.003 PFU/cell followed at day 5 post-infection by virus extraction and purification on Iodixanol gradients from cell pellets (cell-associated fraction). Also, the cell culture medium was clarified by centrifugation to quantify free virus particles. Total yield of genome-containing progeny particles and their infectivity were quantified by qPCR and plaque assay respectively (Section 2.6).

As shown in Figure 16A, although NS2null virus can complete its infectious cycle and generate infectious progeny in human cells, it replicates and spreads poorly forming small plaques in a plaque assay. However, H1-DM-NS2null and H1-Del-NS2null replicate and spread significantly better than H1-NS2null virus, as shown by the larger plaques of these viruses (Figure 16A), compared to the control. It is noteworthy that Y595H mutation in H1-DM and the deletion carried by DelH1PV (aa 587-624) reside in C-terminal domain of NS1 protein, which is essential for transactivation of the capsid promoter (Legendre and Rommelaere, 1994) via interaction with *tar* element and cellular transcription factors (Krady and Ward, 1995). Despite of the C-terminal position of Y559H mutation, no increased induction of VP and luciferase reporter was observed in a transient transfection assay using split vectors (see Materials and Methods, Section 2.10) (data not shown). This suggests other molecular mechanism(s) than transactivation is (are) responsible for the moderately higher accumulation of capsid proteins after infection of the cells with H1-DM mutant (Figure 5B and 6B), for instance, increased stability of VP1 and VP2 via post-translational modifications (e.g. phosphorylation).

Also, as depicted in Figure 16, H1-DM-NS2null mutant was not only able to generate higher titers of progeny full particles (Figure 16B) but also showed 2-fold lower particle to infectivity (P:I) ratio compared to wt H1-NS2null (Figure 16C and D). Indeed, total yield of progeny DNA-containing particles including both cell-associated and free particles, for wt H1-NS2null and H1-DM-NS2null was as following: wt H1-NS2null (cell-associated particles: $3.04x10^{11}$ VG/ml, free particles: $4x10^{10}$ VG/ml) and H1-DM-NS2null (cell-associated particles: $4.37x10^{11}$ VG/ml, free particles: $9.8x10^{10}$ VG/ml). Similarly, higher titers of infectious particles were obtained for H1-DM-NS2null virus compared to wt H1-NS2null, as following: wt H1-NS2null (cell-associated particles: $2.41x10^{7}$ PFU/ml, free particles: $7x10^{6}$ PFU/ml) and H1-DM-NS2null (cell-associated particles: $9.25x10^{7}$ VG/ml, free particles: $2.23x10^{7}$ PFU/ml). Altogether our results indicate that NS1-Y595H mutation contributes to the fitness phenotype of H1-DM mutant even in the absence of NS2 mutation. However, relative contribution of NS2 mutation (L103P) to the fitness phenotype of H1-DM and H1-PM-I mutants cannot be determined since the Y595H substitution of NS1 also modifies NS2.

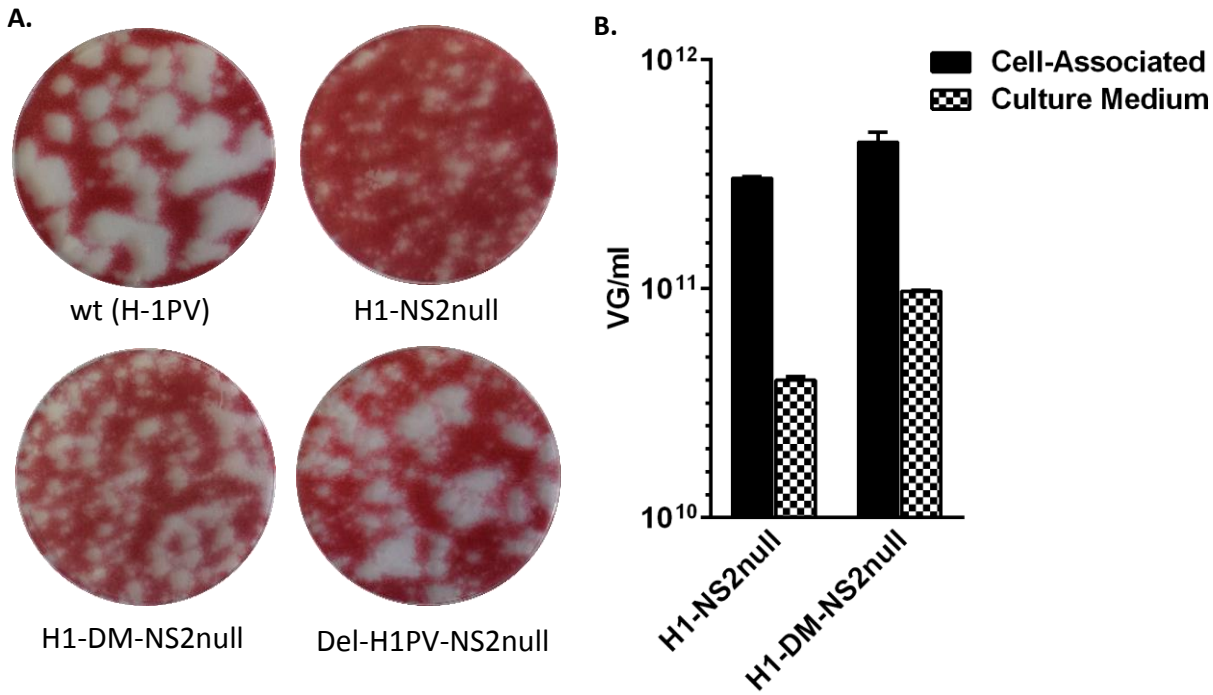

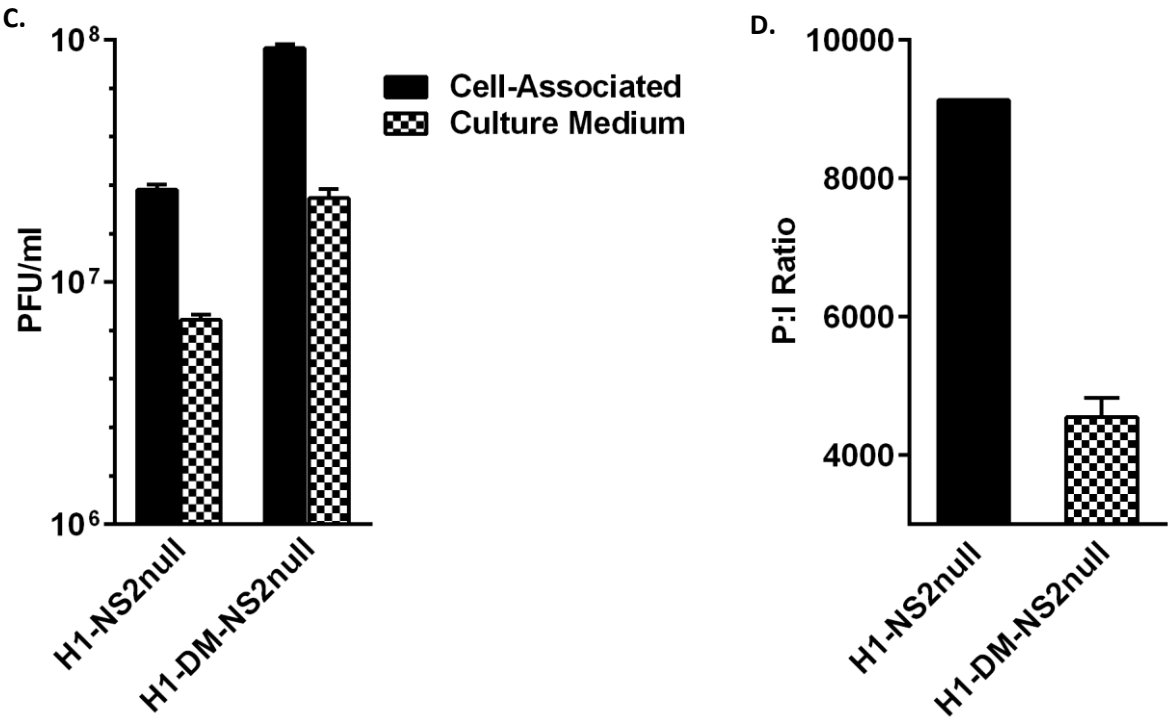

Figure 16. Effects of Y595H mutation in NS1 protein carried by H1-DM virus. The splice acceptor site of NS2 pre-mRNA was ablated by a point mutation to create NS2-null derivatives of wt (H-1PV), H1-DM and Del-H1PV mutants. Master virus stocks were prepared by transfection of the plasmids pH1-NS2null, pH1-DM-NS2null and pH1-Del-NS2null into $5x10^6$ 293-T cells and the viruses were isolated from the cells 72 h after transfection. The yield of progeny virions and their infectivity were determined after infection of $5x10^6$ NB-324K cells at a MOI of 0.003 PFU/cell and viruses were harvested 5 dpi from both culture medium and cell pellets. (A) Infectious virions were titrated by plaque assay in NB-324K cells. (B) Total yield of genome-containing particles was measured by qPCR and is presented as virus genome copies/ml (VG/ml). The culture medium was incubated with DNase I to degrade the replicative forms and partially packaged ssDNA. (C) Yield of infectious progeny is shown as PFU/ml. (D) Particle-to-infectivity (P:I) ratios of the virus stocks. Mean ± SD of three independent quantifications are shown.

5.2 Tyr595His Substitution in NS1 of H1-DM Does Not Remove a Phosphorylated Tyr Residue

As shown above (Figure 16), Y595H substitution in NS1, or deletion of a region spanning this residue, improved H-1PV replication and virus spread in human cells. Although DNA replication functions of NS1 in MVM are regulated by phosphorylation of serine and threonine residues, tyrosine phosphorylation was never observed in this protein (Nuesch et al., 2003; Nuesch et al., 1998a; Nuesch et al., 1998b), we were wondering whether this might happen in Tyr595 in H-1PV and, if so, whether removing (as in DelH1PV) or replacing Tyr595 in NS1 (as in H1-DM) would be responsible for the

enhanced replication and spread of H-1PV. For this the Tyr595 aa residue in NS1 protein was substituted in H-1PV by a nonphosphorylable, structural mimic, Phenylalanine (F), without altering NS2 amino acid sequence. Briefly, the mutation (Y595F) was introduced in pH1 plasmid by PCR mutagenesis (Section 2.3) using NS1-Y595F-F and NS1-Y595F-R primers listed in Table 2.8. A master virus stock was prepared by transfection of 293-T cells (Section 2.4) followed by virus purification (Section 2.5) and titration (Section 2.6). Virus particles were harvested from cell pellets and culture medium (after pretreatment with DNase I to degrade viral replicative forms) representing cell-associated and free particles, respectively. DNA-containing and infectious particles were quantified by qPCR (genome copies/ml) and plaque assay (PFU/ml) respectively. Figure 17A illustrates the plaques obtained with the virus carrying the Y595F modification and those from wt. The virus carrying Y595F mutation exhibited a plaque phenotype similar to wt. No difference was observed after infection of NB-324k cells with wt and the mutant Y595F regarding the titers of full progeny particles (Figure 17B), the infectious titers (Figure 17C) and the P:I ratio (Figure 17D).

A.

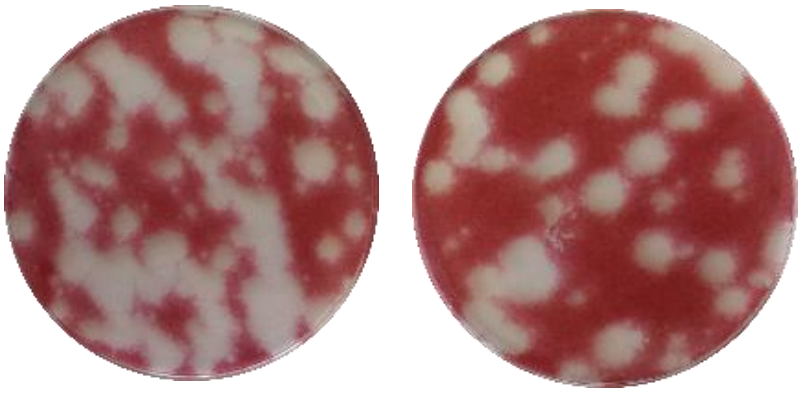

wt (H-1PV) H1-Y595F

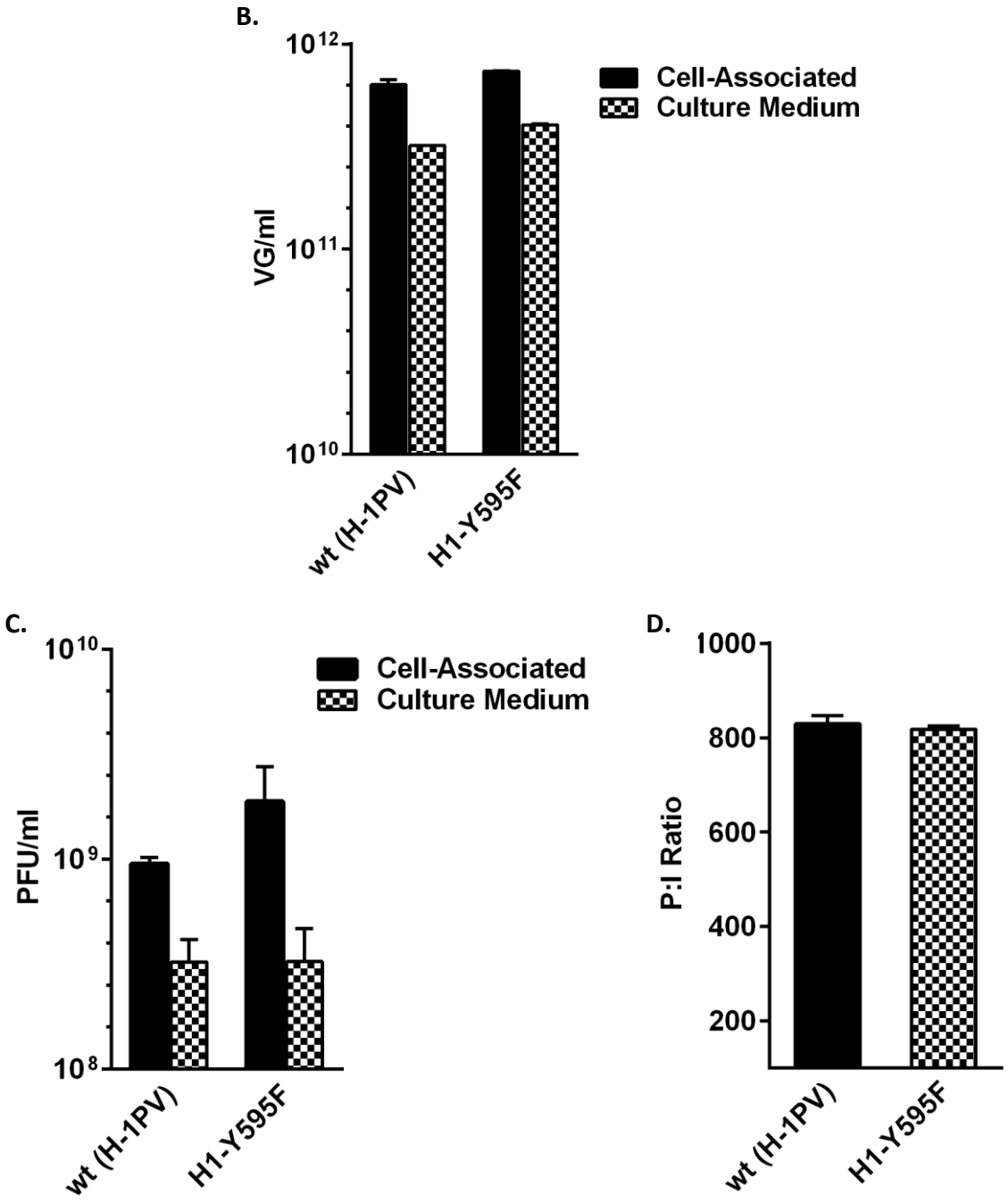

Figure 17. Replication and spread of H-1PV is not altered by Y595F substitution in NS1. $5x10^6$ NB-324K cells were infected at a MOI of 0.003 PFU/cell to allow several cycles of infection. 5 days after infection, cell-associated viruses and free particles in the cell culture medium were quantified. (A) plaque phenotype of wt (H-1PV) and H1-Y595F viruses in NB-324K cells. (B) Titer of DNA-containing particles was determined by qPCR and is presented as viral genome copies/ml (VG/ml). (C) Infectious particle titers in PFU/ml, determined by plaque assay. (D) Particle-to-infectivity (P:I) ratio of the viruses. Means ± SD of two independent duplicate titrations are shown.

This suggests that Tyr595 residue of NS1 is not subject to phosphorylation during the course of viral infection. Most likely, radical substitution of uncharged tyrosine by a positively charged histidine due to its imidazole functional group, somehow modulates NS1 structure resulting in enhanced performance of this protein during virus replication in the cells and subsequently increased yield of progeny particles. However, whether or not the overlapping NS2 mutation (L103P) in H1-PM-I and H1-DM mutants further contributes to the virus phenotype is unclear. Indeed, due to overlapping sequences of NS1 and NS2 proteins it is not possible to construct a mutant carrying a NS2 mutation at the position L103 without modifying NS1. However, another mutation in close proximity of this residue in NS2 (PM-II mutation: K96E) also increased the virus fitness, as indicated by enhanced replication and improved infectivity of the virus particles (Figure 2). This suggests that NS2 mutations in this region can enhance the virus fitness in the presence of a wt NS1 protein. Whether NS2 mutations such as K96E act directly or modulate NS1 functions for example those required for DNA replication, etc., via post-translational modifications (e.g. phosphorylation) is unclear.

5.3 Binding to the Cell Membrane is not Increased with the Fitness Mutants

In order to determine whether some early steps of the infection cycle were stimulated by the fitness mutants, we next analyzed virus entry and transport to the nucleus. During the course of infection, the first step for H-1 virus particles consists of the binding to (a) yet unidentified receptor(s) involving sialic acid residues on the cell membrane. To assess this step in our mutants, a confluent monolayer of NB-324K cells ($5x10^5$ cells) was inoculated with a MOI of 2225 virus genomes/cell at 4°C for 1 h of wt (H-1PV), H1-PM-I, H1-PM-II, H1-PM-III and H1-DM viruses to allow the adsorption but prevent internalization of the virus particles. Both free particles in the culture medium and cell-bound particles were quantified by qPCR as described before (Section 2.6). As shown in Figure 18, no significant difference was observed in the number of full particles that were recovered from the cell membranes between wt and mutant viruses. Interestingly, even H1-PM-III virus particles which showed a higher P:I ratio

than wt virus (Figure 2C), could bind to the cells as efficiently as wt. This shows that the fitness of H1-PM-I, H1-PM-II and H1-DM mutants is not caused by an increased binding capacity of the virus particles to the cells.

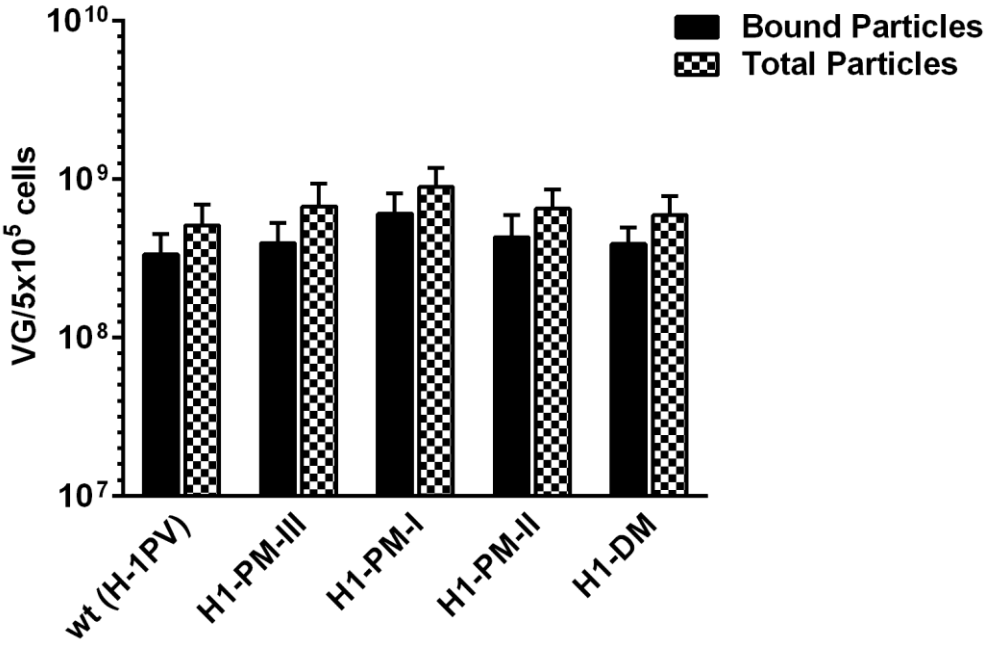

Figure 18. Cell binding of the mutant viruses. $5x10^5$ NB-324K cells were infected with wt (H-1PV) or H1-PM-III, H1-PM-I, H1-PM-II and H1-DM mutants at a MOI of 2225 genome copies/cell at 4°C to prevent virus internalization. After 1 h incubation at 4°C, both cell-bound and free particles were prepared as described in Materials and Methods (Section 3.1) and quantified by qPCR. Mean ± SD of three independent experiments are shown.

5.4 Mutant Viruses are Taken Up by the Cells More Efficiently than wt Virus

Although sialic acid residues on the cell membrane are required for infection of the host cells by H-1 virus (Allaume et al., 2012; Lopez-Bueno et al., 2006), the protein receptor(s) that mediates entry has (are) not been identified yet. Thus, further interaction(s) with proteins on the cellular membrane and probably are required for successful transport of the virus particles from the apical surface of plasma membrane to the cell interior. As shown in Figure 18, all the mutant viruses attached to the cells with similar efficiencies at 4°C. We next wanted to determine if further downstream steps of the virus infection cycle were modified in the mutants, for instance due to

altered post-translational modification(s) of the capsids. In order to analyze the virus entry, the viruses were allowed to bind to NB-324K cells at 4°C followed by incubation at 37°C for virus internalization. As shown in Figure 19, overall cell uptake of the fitness mutant particles was more efficient than of the wt virus, and this was more prominent for H1-PM-I mutant. Given the fact that none of the mutants described in this study contains any mutation in the capsid genes, this suggests that some post-translational modifications (e.g. phosphorylation) of the capsids may modulate their virus entry. As for cell binding (Figure 18), H1-PM-III mutant particles were taken up by the cells as efficiently as wt, showing that this step is not limiting in this mutant. Altogether, our data suggest that sialic acid interaction is not altered in these mutants and probably downstream interactions with the entry receptor(s) are modified, for instance due to post-translational modifications of the capsids (e.g. phosphorylation).

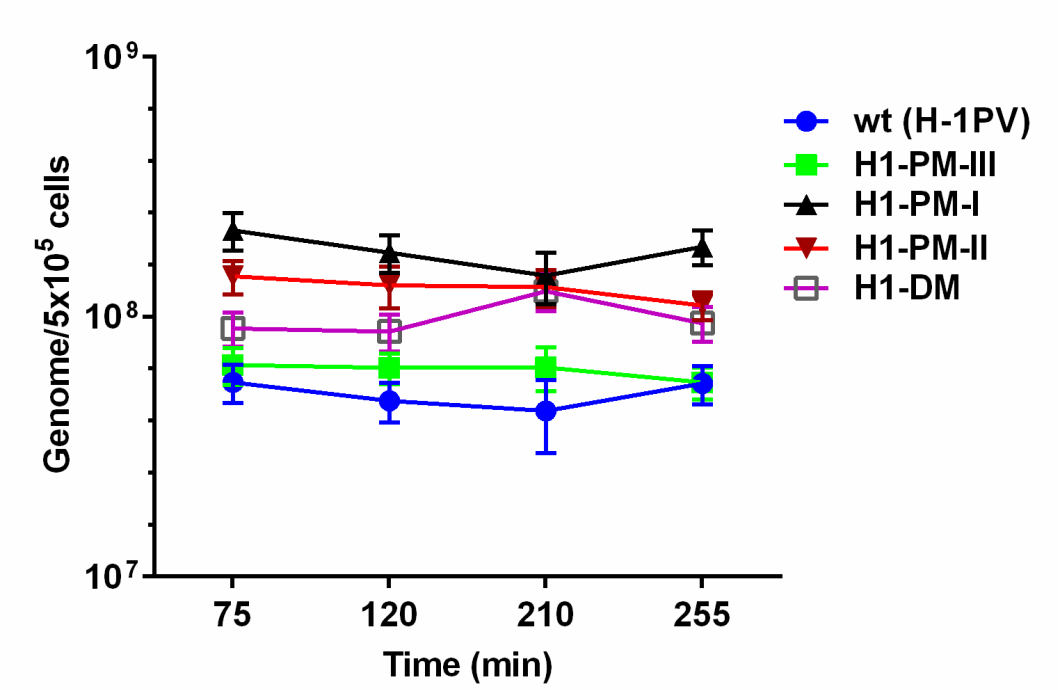

Figure 19. Cell uptake of the mutants. $5x10^5$ NB-324K cells were infected at 4°C with wt (H-1PV) or H1-PM-III, H1-PM-I, H1-PM-II and H1-DM mutants at a MOI of 2225 genome copies/cell and subsequently incubated at 37°C to allow virus uptake. At indicated time points, the cells were treated with trypsin-EDTA to discard cell membrane-associated particles and total viral DNA was extracted from the cells. Viral genomes internalized by the cells were quantified by qPCR. Mean ± SD of two independent experiments in duplicates are shown.

5.5 Nuclear Transport of Mutant Virions is Similar to wt Virus

Following entry, the virus particles traffic through endosomal compartment, from which they finally need to escape and translocate to the nucleus where conversion of ssDNA to dsDNA, DNA amplification and viral gene expression take place. In order to analyze this step, NB-324K cells were infected and subsequently cytoplasmic and nuclear fractions were collected and their viral load measured by qPCR of viral genomes (Section 3.2). In agreement with the virus uptake (Figure 19), in case of the mutants more viral genomes were recovered from both cytoplasmic (Figure 20A) and nuclear fractions (Figure 20B). However, only a minor fraction of the incoming particles (~20%) were recovered from the nuclear fraction and the viral load of this fraction was similar between wt and mutants (Figure 20C). This indicates that the mutant virus particles are transported to the nucleus as efficient as wt particles. The exponential increase in the viral DNA copies at 6-8 hpi (Figure 20B) indicates that DNA replication/amplification started, resulting in ~10-fold higher genome copies for H1-PM-I, H1-PM-II and H1-DM mutants compared to wt.

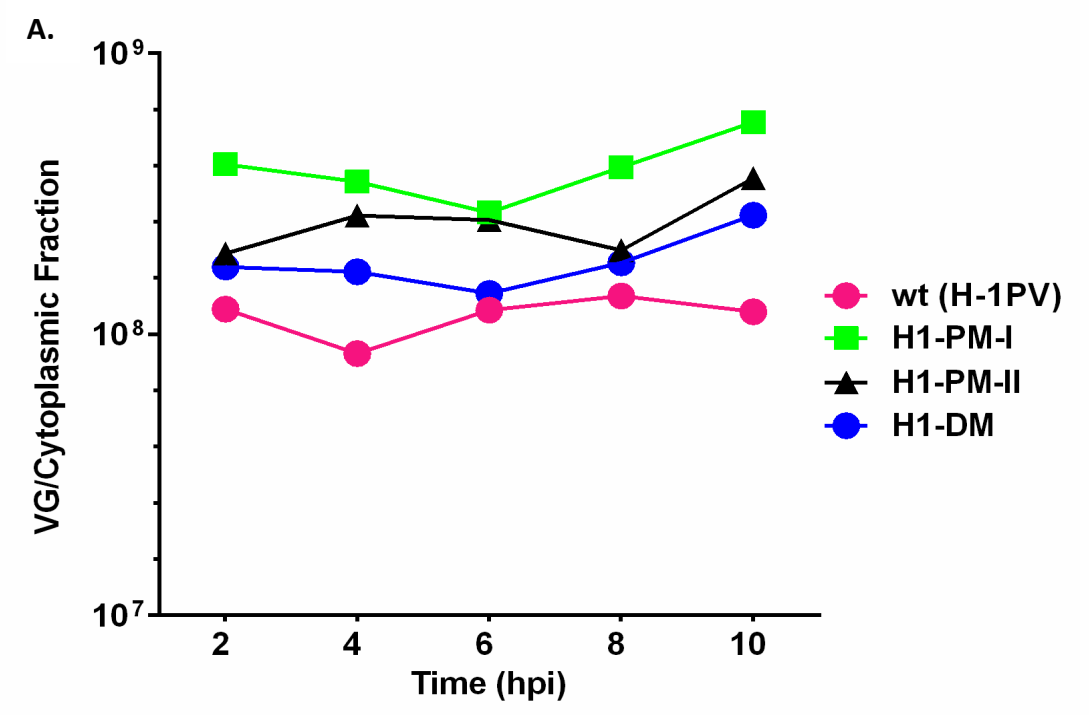

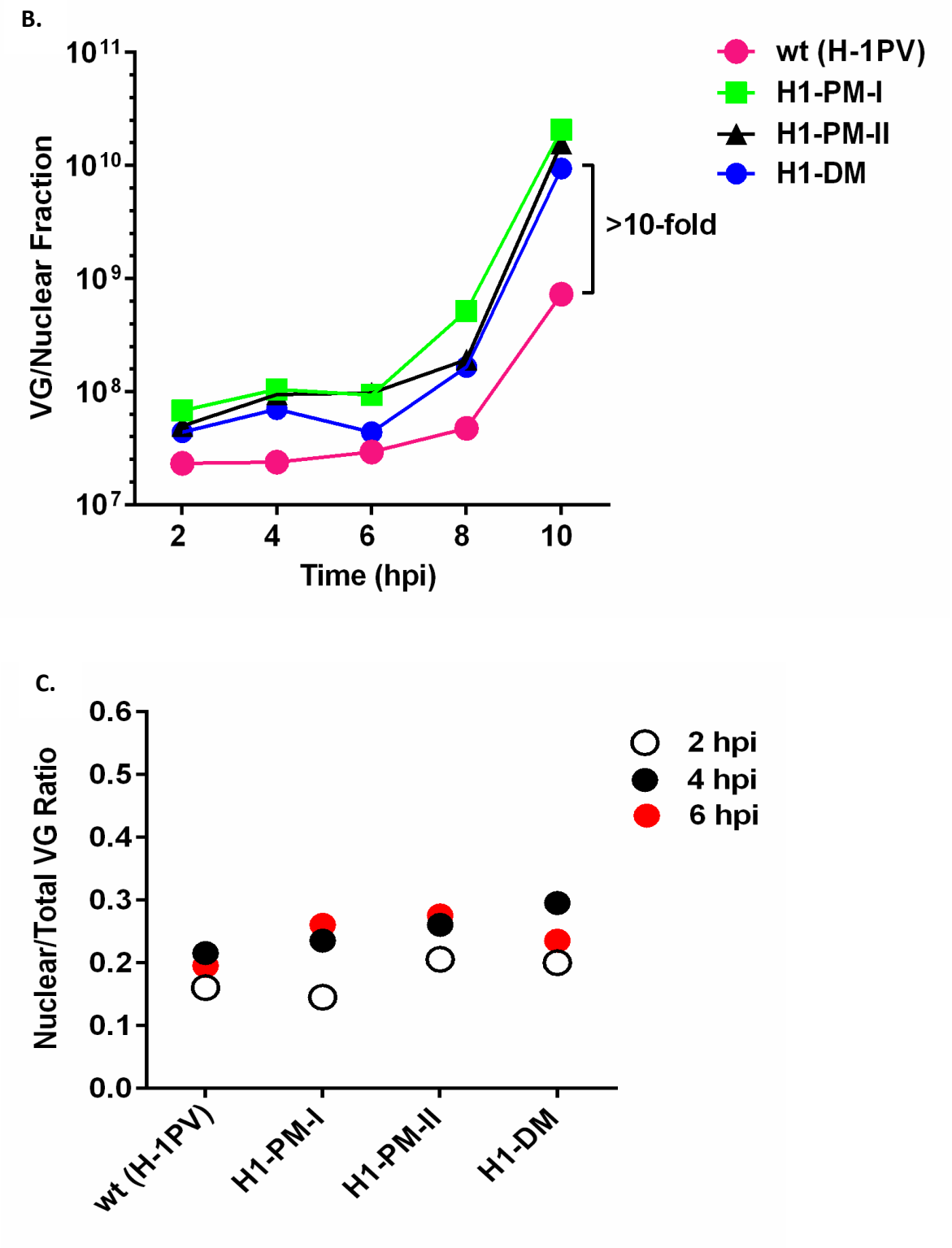

Figure 20. Kinetics of Cytoplasmic/Nuclear distribution of wt and mutant viruses. $5x10^5$ NB-324K cells were infected at 4°C with wt (H-1PV), H1-PM-I, H1-PM-II and H1-DM viruses at a MOI of 2225 VG/cell followed by incubation at 37°C. At progressive time points after infection, the viruses were isolated from cytoplasmic and nuclear fractions and their genomes were quantified by qPCR. Figures A and B show total load of the virus genomes recovered from the cytoplasmic and nuclear fractions

respectively. Figure C shows the ratio of nuclear to total virus genomes (Nuclear + cytoplasmic) 2,4 and 6 hpi. To exclude *de novo*-synthesized DNA, only samples collected 2,4 and 6 hpi are shown. Mean ± SD of two independent titrations in duplicates are shown.

Altogether our results show that, compared to wt, virus uptake of the mutants, but not their binding to the cell membrane, is enhanced. Downstream steps including endosomal escape and nuclear transport of the virions did not seem to be stimulated. Furthermore, in all the viruses tested, the DNA replication initiated 6-8 hpi as shown by exponential increase in the titers of the viral genomes in the nuclear fraction. However, the DNA replication progressed significantly faster for the H1-PM-I, H1-PM-II and H1-PM-III mutants than for wt, resulting in dramatically higher accumulation (∼10-fold) of viral DNA in the nucleus 10 h after infection.

5.6 Higher, But Not Faster, Pre-lytic Progeny Virus Release of the Mutants

Although like most non-enveloped DNA viruses, progeny parvovirus particles are mainly released passively after cell lysis, there is accumulating evidence showing an active pre-lytic egress of MVM virions (Maroto et al., 2004; Wolfisberg et al., 2016). A faster nuclear export of DelH1PV, compared with H-1PV was previously observed (Weiss et al., 2012). In order to investigate whether or not the fitness mutants egress from the nucleus more efficiently than wt virus prior to cell lysis, irrespective of the alterations in the early steps of the infection cycle (e.g. cellular uptake), NB-324K cells were infected with the same infectious units of wt (H-1PV), H1-PM-I, H1-PM-II and H1-DM viruses (1 PFU/cell) followed by addition of an anti-capsid neutralizing serum to the culture medium to prevent secondary rounds of infection. At progressive time points after infection, the viral load present in the cytoplasmic and nuclear fractions, and in the culture medium was quantified by qPCR as described before (Section 2.6). As shown in Figure 21A, the number of viral DNA copies measured in the nucleus was ∼2-fold higher after infection with H1-PM-I, H1-PM-II and H1-DM compared to wt at any time point tested (12-21 hpi). However, the kinetics of DNA replication were similar to wt. Also, more progeny particles were recovered from both cytoplasmic fraction

(Figure 21B) and (Figure 21C) culture medium after infection with the mutants compared to wt. Titration of H1-DM infectious virions in the cytoplasmic and nuclear fractions by plaque assay showed no increased cytoplasmic: nuclear PFU ratio compared to wt (Figure 21D). This is in contrast to the data reported previously for the deletion mutant (DelH-1PV) (Weiss et al., 2012), where nuclear egress of the progeny virions was significantly increased. Taken together, our data indicate that although the mutant viruses yield more progeny virions, their egress is not stimulated compared to wt virus.

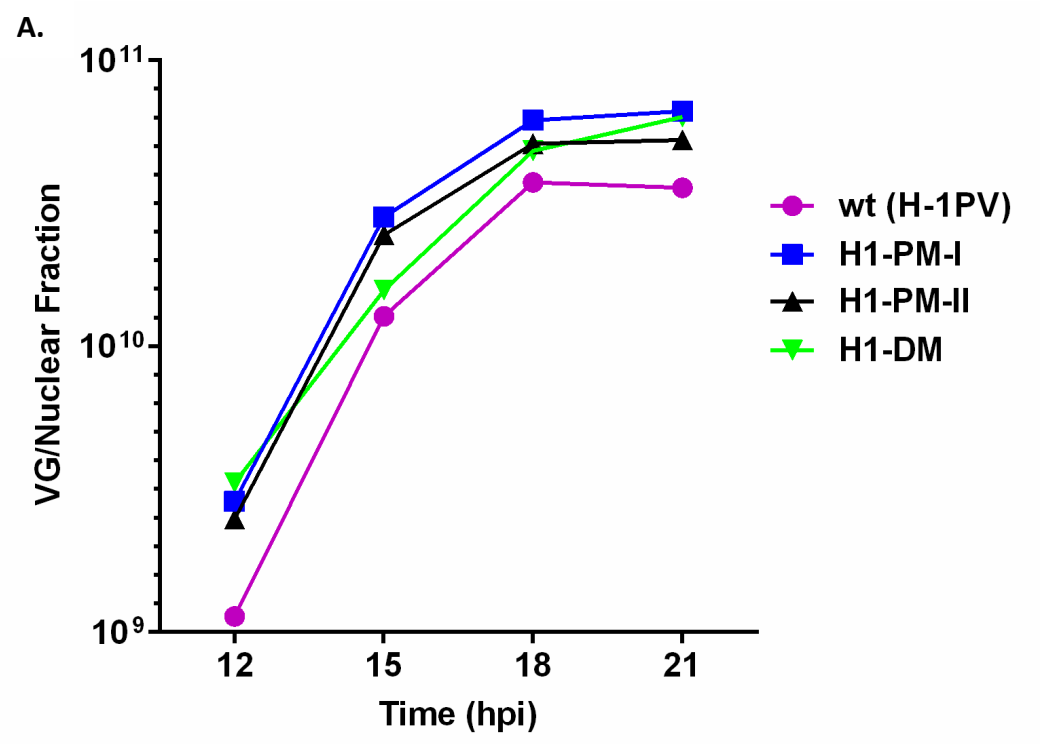

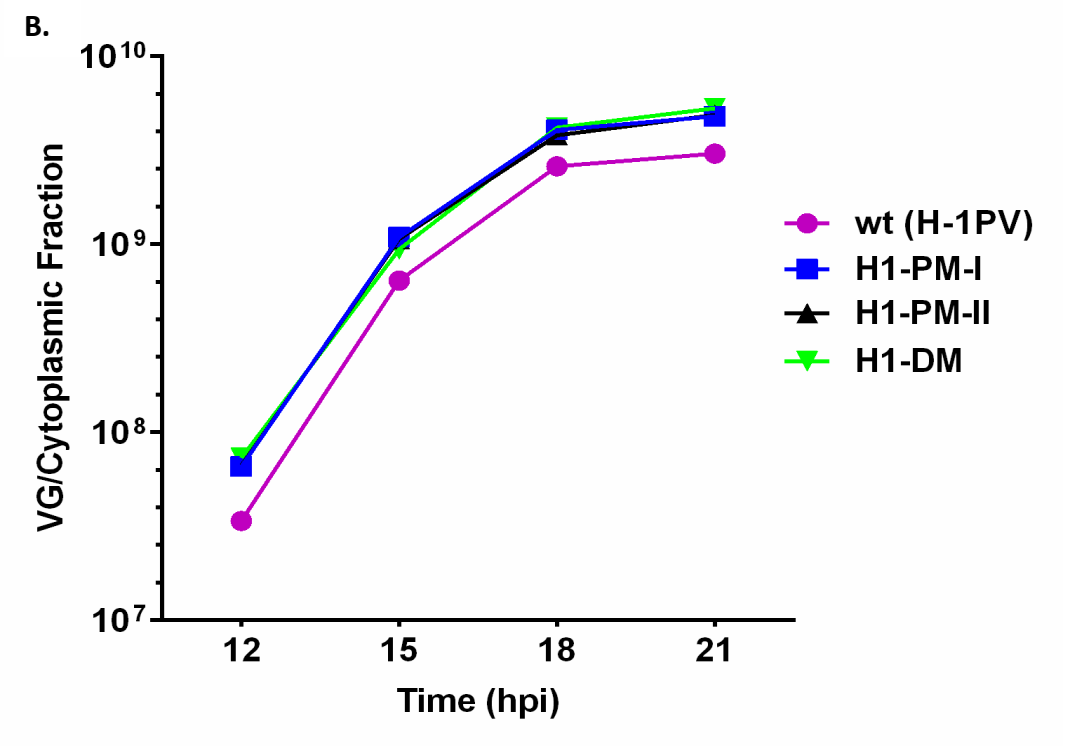
B.
VG/Cytoplasmic Fraction
10^10
10^9
10^8
10^7
12
15
18
21
Time (hpi)
wt (H-1PV)
H1-PM-I
H1-PM-II
H1-DM

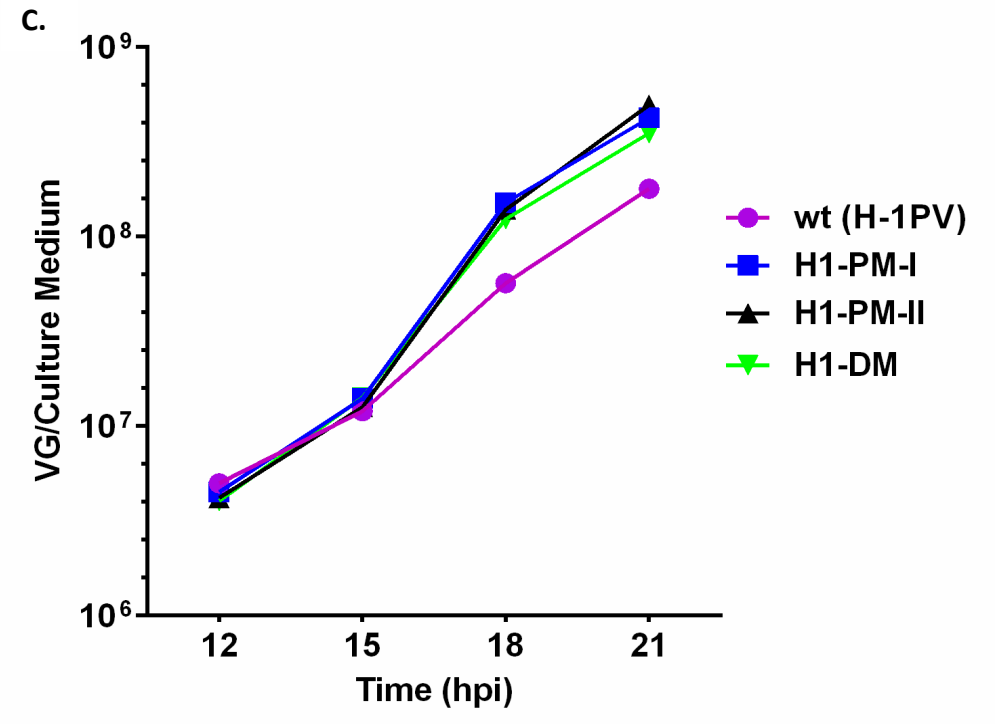
C.
VG/Culture Medium
10^9
10^8
10^7
10^6
12
15
18
21
Time (hpi)
wt (H-1PV)
H1-PM-I
H1-PM-II
H1-DM

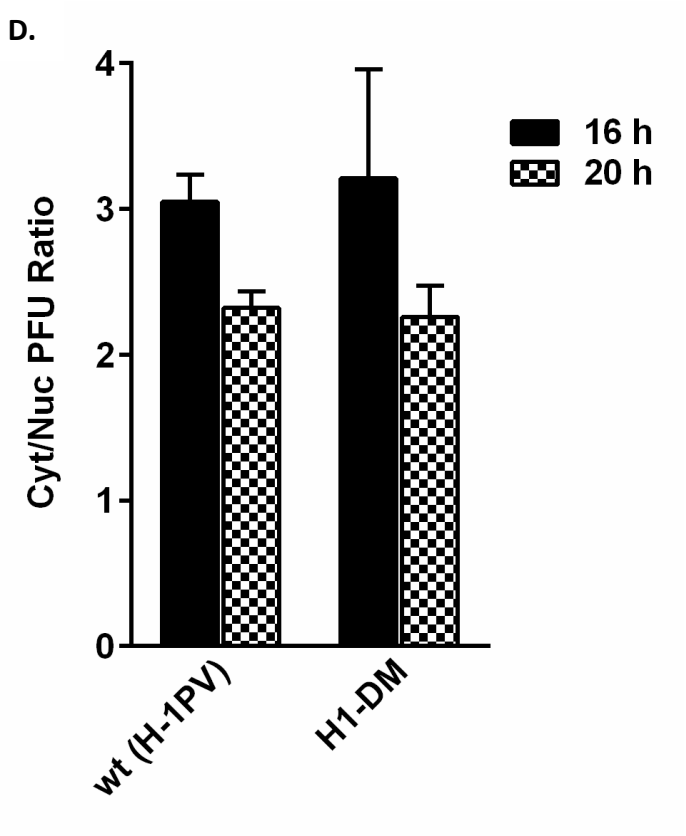

Figure 21. Cytoplasmic/Nuclear distribution of progeny virus particles. $1x10^5$ NB-324K cells were infected with wt or mutants at a MOI of 1 PFU/cell followed by addition of anti-capsid neutralizing serum. At indicated time points, culture medium and nuclear and cytoplasmic fractions were collected and their total load of DNA-containing particles was quantified by qPCR as for Figure 20. (A), (B) and (C) show the total load of viral DNA in the nucleus, cytoplasm and culture medium respectively. (D) The ratio of cytoplasmic: nuclear infectious viral loads (PFU) were determined by plaque assay. Mean ± SD of two independent titrations in duplicates are shown.

6. H-1PV with A Point Mutation in SAT Protein: A New Fitness Mutant?

A new variant emerged in the WT virus stock during virus replication in NB-324K cells. A point mutation affecting SAT protein (S18N), but not the overlapping capsid proteins, was identified in five isolated lysis plaques. This variant was characterized by a large plaque phenotype that was not observed from a lysis plaque control displaying a wt plaque phenotype. This mutation was introduced by molecular cloning into pH1PV, pH1-DM and pDelH-1PV plasmids (see Materials and Methods Table 2.1). Master virus stocks were produced by transfection of 293-T cells (Section 2.4) followed by Iodixanol purification (Section 2.5). The virus titers were determined for both DNA-containing (full) and infectious particles by qPCR and plaque assay, respectively, as described

before (Section 2.6). As shown in Figure 22, H-1 virus carrying SAT^{S18N} mutation (H1-SAT^{S18N}) replicates and spread more efficiently than wt virus, as indicated by the formation of significantly larger plaques (Figure 22A). However, the infectivity of the particles (P:I ratio about 3000, Figure 22C) was comparable to what has been frequently reported for wild-type H-1PV (not shown). Interestingly, when this mutation was introduced into H1-DM and DelH-1 mutants, not only H1-DM-SAT^{S18N} and Del-H1-SAT^{S18N} infection gave rise to a large plaque phenotype (Figure 22A), but the titers of progeny virions (Figure 22B) were significantly higher (~5x10^8 and 4x10^9 PFU/ml respectively) compared to wt virus carrying the SAT mutation (~6x10^7 PFU/ml). Moreover, their P:I ratio was dramatically reduced, 3- and 10-fold, respectively, compared to H1-SAT^{S18N} virus (Figure 22C). However, it appears that the SAT^{S18N} mutation enhanced the virus replication and spread regardless of its genomic background (encoding wild-type or mutant NS1/NS2 proteins) without improving the infectivity of the particles. The mechanism underlying enhanced replication and spread of H1-PV carrying SAT^{S18N} mutation requires further investigation of the virus cycle in a single round of infection.

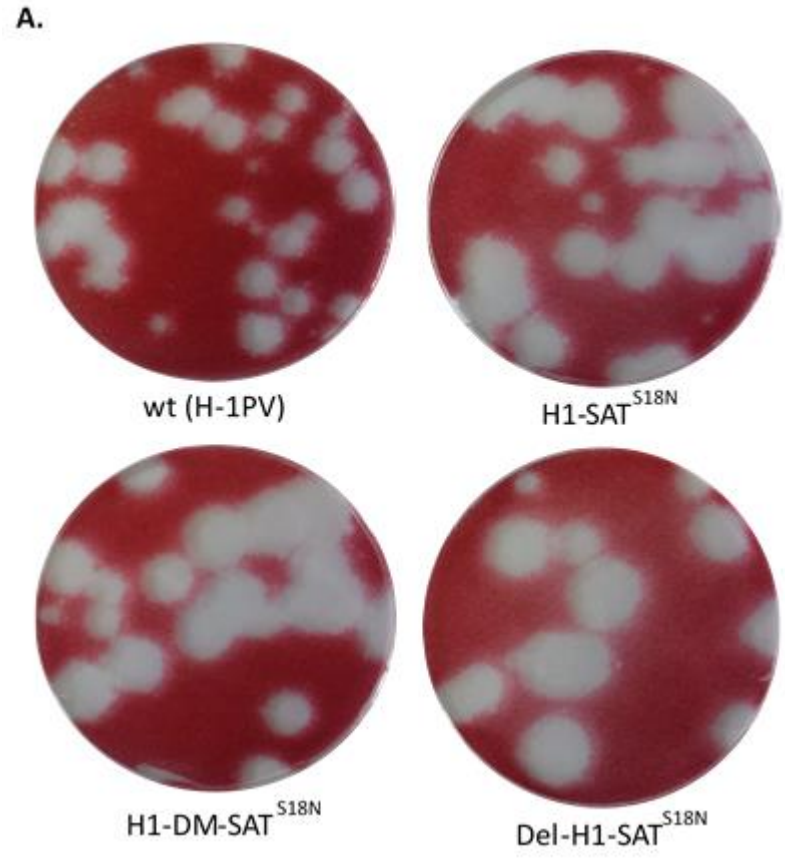

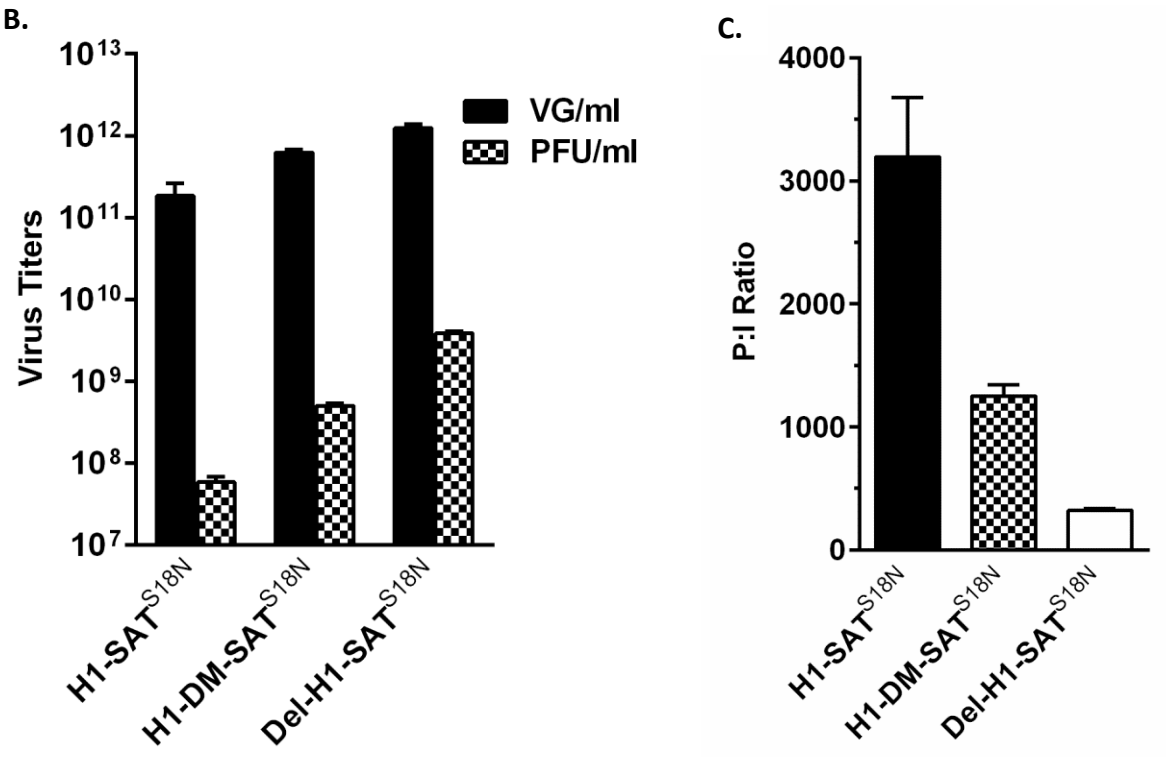

Figure 22. Titers and spread of wt (H-1PV), H1-DM and DelH1PV carrying SAT^{S18N} mutation. The SAT^{S18N} mutation was introduced into infectious DNA clones pH1, and pH1-DM and pDelH1. A master virus stock was prepared after transfection of 293-T cells followed by quantification of DNA-containing and infectious particles using qPCR and plaque assay respectively. (A) Plaque phenotype of wt (H-1PV), H1-DM and Del-H1PV viruses carrying SAT^{S18N} mutation. (B) Titers of progeny full and infectious particles shown as viral genomes/ml (VG/ml) and PFU/ml respectively. (C) Particle-to-infectivity (P:I) ratio of the virus stocks. Mean ± SD of two independent titrations in duplicates are shown.

Chapter 4

Discussion

4.1 Effects of Point Mutations in NS Coding Sequences on H-1PV Replication and Spread

Over the past decades, several viruses from different families of DNA and RNA viruses have been investigated as oncolytic biotherapeutics including reovirus, measles virus, vesicular stomatitis virus (VSV), adenovirus, herpesvirus and rat H-1 parvovirus (Russell et al., 2012a). Several strategies have been implemented to improve tumor selectivity or oncolytic potency of viruses through genetic reprograming including arming with cytotoxic suicide genes or immunostimulatory cytokines, surface targeting by insertion of tumor homing peptides or cleavage sites of tumor-specific proteases into the viral ligands and selection of fitness mutants using artificial mutagenesis and serial passage on cancer cells (Hermiston and Kuhn, 2002; Kaufman et al., 2015; Russell et al., 2012b; Seymour and Fisher, 2016; Yan et al., 2003). Due to their extremely small genome, parvoviruses are highly dependent on DNA replication machinery of the host cell which is fully active only during transition through S phase of the cell cycle (Cornelis et al., 1988; Deleu et al., 1999), a hallmark of transformed cells. Hence, in addition to apathogenicity in humans, rodent parvoviruses have an intrinsic tumor selectivity which makes them attractive tools for oncolytic virotherapy purposes. The rat parvovirus H-1PV has been subject to extensive research in our group which led to a phase I/IIa clinical trial, aiming at evaluating the efficacy of H-1PV for treatment of patients with recurrent glioblastoma multiforme (Geletneky et al., 2012) and more recently pancreatic adenocarcinoma (Angelova et al., 2015; Marchini et al., 2015). Previously in our lab, a fully infectious variant of H-1 virus designated H-1 dr, was isolated from stock of the standard H-1 virus strain during propagation in human NB-324K cell line (Faisst et al., 1995). This variant carried a large in-frame deletion in coding

sequences of nonstructural proteins NS1 and NS2, and outperformed the wt virus in cell culture (Faisst et al., 1995). In a follow-up study in our lab, a virus carrying this deletion, so-called DelH1-PV, was created from the parental wt strain by molecular cloning, which demonstrated an enhanced fitness in cell culture and a more potent oncolytic activity in human xenograft tumors in nude mice (Weiss et al., 2012). The deletion affected both NS1 and NS2 proteins (NS1 aa 587-624 and NS2 aa 96-133), and boosted some of early and late steps of the infection cycle, including virus entry and nuclear egress of the progeny particles (Weiss et al., 2012). The region subject to the deletion was further investigated in the current study using introduction of four point mutations (PM-I, PM-II, PM-III and DM) that were originally selected in mice inoculated with a lymphotropic strain of MVM (MVMi), a closely related mouse parvovirus (Lopez-Bueno et al., 2004). All these mutations stimulated virus replication and spread in cell culture, and rendered the virus more virulent *in vivo* (Lopez-Bueno et al., 2004). Due to overlapping coding sequences of NS1 and NS2 proteins, the point mutations affected NS1, NS2 or both. Three of the point mutations (PM-I, PM-II and DM) clustered in the deletion region, increased the fitness H-1PV in human cells. These mutants showed a large plaque phenotype and yielded higher titers of progeny particles with improved infectivity indicated by significantly lower (~4-fold) particle-to-infectivity (P:I) ratios compared to wt virus, characteristics that were also observed for DelH1-PV mutant (Weiss et al., 2012). In clear contrast, PM-III mutation which introduces an amino acid substitution in close proximity of 14.3.3 binding site of NS2 protein (L153M) without affecting NS1 coding sequence, compromised the virus replication and spread. This virus generated small plaques and yielded lower titers of progeny particles. Furthermore, particle-to-infectivity (P:I) ratio of the virus particles was significantly higher (~4-fold) compared to wt.

4.2 Point Mutations in NS Coding Sequences Modulate Viral Late Gene Expression

Upon parvovirus infection, the early P4 promoter drives the expression of two nonstructural proteins: NS1 and NS2. The large nonstructural protein, NS1, binds to *tar* element upstream of P38 promoter and induces expression of the capsid proteins

through further interaction with cellular transcription factors (Krady and Ward, 1995; Legendre and Rommelaere, 1994). Although the small nonstructural protein, NS2, is not required for transcription of P38-driven genes, several studies speak for a post-transcriptional role for NS2 in viral late gene expression in host cells. A study using MVM mutants carrying nonsense mutations in different regions of NS2 open reading frame, showed that NS2 is required for efficient translation of viral transcripts in mouse cells but not human cells (Naeger et al., 1993). Similar observations were reported by Li *et al*. using a NS2-null derivative of H-1PV in rat fibroblasts in which the splice acceptor site of the second exon in NS2 was abolished by mutagenesis (Li and Rhode, 1991). The authors showed that protein expression (both NS1 and VP) after infection of rat cells but not human cells by this mutant, was severely diminished while viral transcripts were generated at wt levels and were highly translatable in vitro using rabbit reticulocyte lysates. A follow-up study by the same group indicated that NS2-dependent translation of viral transcripts in rat cells is mediated by their common 3'-UTR sequence (Li and Rhode, 1993). Also, a full-length viral 5'-UTR sequence was required for maximal reporter gene expression, but in a NS2-indepdnent manner (Li and Rhode, 1993). In human cells, however, NS2 was largely dispensable for viral protein expression. In our present study, when PM-III mutation was introduced into 5'-UTR of luciferase reporter expressed from a H1-based vector under the control of the P38 promoter, lower reporter signals were obtained compared to a wt construct. A NS2-null derivative of H-1 virus was created in this study and viral protein expression was analyzed after infection of human cells. In agreement with what was previously reported for a NS2null derivative of MVM (Cotmore et al., 1997), capsid proteins were expressed very efficiently after infection of human cells by a NS2-null H-1PV. These data further supported that NS2 protein is not required for viral late gene expression in human cells, therefore, it seems unlikely that lower capsid expression by PM-III mutant is caused by L153M substitution in NS2. Cotmore *et al*. further analyzed the role of NS2 in expression and assembly of MVM capsids, and demonstrated that when mouse cells were infected with NS2-null MVM, VP1 and VP2 proteins were synthesized normally but there was a major primary defect in the folding or assembly processes

required for effective capsid production (Cotmore et al., 1997). In agreement with this, our results showed that capsid proteins accumulate efficiently after infection of human cells with a NS2-null derivative of H-1PV, confirming that NS2 is not required for capsid protein synthesis in human cells. However, significantly lower titers of progeny virions were obtained, indicating that NS2 is important for optimal production of progeny virions in human cells. In contrast to this, H-1PV carrying PM-III mutation (L153M) in NS2 protein, exhibited a strong defect in expression of the capsid proteins VP1 and VP2 (more prominently VP1), while the steady-state level of NS1, the protein required for induction of P38 promoter (Krady and Ward, 1995; Legendre and Rommelaere, 1994), was not altered. Furthermore, NS1/2 expression cassette derived from PM-III mutant was fully capable of inducing wt levels of the capsid proteins or a luciferase reporter under the control of the P38 promoter. Indeed, expression of NS2 carrying L153M substitution did not interfere with the accumulation of capsid proteins, which further reduces the possibility that NS2 mutation could have a *trans* effect on capsid expression, for instance due to an impaired interaction with 3'-UTR of the capsid mRNAs. The diminished expression of capsid proteins was also observed when an infectious DNA clone of PM-III mutant was transfected into the cells, in an attempt to circumvent early steps preceding viral gene expression, including binding and entry, nuclear transport, uncoating and conversion of ssDNA to dsDNA (transcription template). Hence, the reduced accumulation of capsid proteins after infection with this mutant could not be ascribed to an early defect in the virus cycle.

Analysis of steady-state accumulation of viral proteins after infection with equal number of full particles showed a general increase in all viral proteins by PM-I, PM-II and DM mutants. The large nonstructural protein NS1 serves as a transcription factor which induces the expression of capsid proteins via its acidic C-terminal domain (Krady and Ward, 1995; Legendre and Rommelaere, 1994) while it binds to so-called *tar* element in viral DNA via its N-terminal domain in an ATP-dependent manner (Lorson et al., 1996). To analyze viral gene expression independent of P:I ratios, steady-state levels of viral proteins were also investigated post-infection with the same dose of

infectious (PFU) viruses . A moderate increase in the accumulation of the capsid proteins was observed after infection with PM-I and DM mutants, the latter carrying both PM-I and PM-II mutations. Similarly, more capsid proteins were synthesized when an infectious DNA clone of DM mutant was introduced into the cells by transfection.

Expression of the capsid proteins by DelH-1PV was also increased, as previously reported by Weiss *et al*. (Weiss et al., 2012) which suggests similar effects of the deletion and the point mutations in NS1/NS2 proteins on steady-state levels of the capsid proteins. As mentioned earlier, PM-I and DM both carry a point mutation at C-terminal region of NS1, part of the protein required for induction of P38 promoter. However, using a split vector co-transfection system, NS1 derived from DM mutant induced capsid and reporter expression similar to wt NS1 (data not shown). This suggests that increased accumulation of the capsid proteins in this mutant compared to wt virus, is a post-translational event, related to enhanced stability of the capsid proteins for instance due to some post-translational modifications (e.g. phosphorylation) of these proteins. Since DM mutant carries amino acid substitutions in both NS1 (Y595H) and NS2 (L103P and K96E) proteins, it is not clear which mutation(s) is responsible for this phenomenon. Ablation of NS2 expression in H1-DM virus (H1-DM-NS2null virus) by mutagenesis showed that NS1 mutation (Y595H) contributes to virus replication and spread, as shown by formation of larger plaques, higher yields of progeny particles and improved P:I ratio of the virus stock compared to a NS2-null variant of wt virus. Similarly, a NS2-null virus carrying a deletion in this region (H1-Del-NS2null) exhibited the same plaque phenotype as the H1-DM-NS2null virus. However, it is not clear whether improved replication and spread of H1-PM-I and H1-DM viruses is solely due to NS1 mutation or if NS2 substitution (L103P) also contributes to their phenotype. The small nonstructural protein NS2 is rapidly degraded by proteasomes in a ubiquitination-independent manner, resulting in relatively short half-life (~1 h) of this protein (Miller and Pintel, 2001). Pulse chase experiments using metabolic ^{35}S-labelling of proteins after infection, showed that *de novo* synthesis of del-NS2 protein encoded by DelH-1PV mutant was increased

followed by its faster degradation, leading to significantly diminished steady-state levels of this protein compared to native protein encoded by wt virus (Weiss et al., 2012). In contrast to this, introduction of point mutation(s) (K96E and/or L103P) in the same region of NS2 did not compromise the steady-state levels of this protein and even a slight increase was observed in DM compared to wt infection. Our data indicates that the region of NS2 subject to deletion, participate in affecting the stability of NS2.

4.3 Strong *Cis* Effects of PM-III Mutation on Capsid Synthesis

As mentioned hereinabove (Section 4.2), NS2 substitution (L153M) carried by PM-III mutant did not have a *trans* effect on accumulation of the capsid proteins. Due to overlapping position of NS coding sequences at the C-terminus, with 5'-UTR region of P38-driven capsid transcripts (R3 mRNA), we explored cis effects of PM-III mutation on VP expression. For this purpose, split vectors were created to express P4-NS and P38-VP cassettes from separate constructs. By using these vectors, a strong *cis* effect of PM-III mutation (C-to-A) on the expression of the capsid proteins was observed. Upon infection with the virus and transfection with infectious DNA clone of PM-III, overall production of both VP1 and VP2 was decreased, with a more striking effect on VP1, which resulted in increased ratio of VP2:VP1 compared to wt. In MVM, VP1:VP2 are synthesized and assembled in pro-capsids in 1:5 molar ratio, and this is regulated mainly by the splicing rate of the R3 messengers (Jongeneel et al., 1986; Morgan and Ward, 1986; Schoborg and Pintel, 1991). Indeed, a small intron flanked by the so-called D1-A1 splice junctions of the capsid pre-mRNA is excised out more efficiently to make the predominant mRNA species encoding the major capsid component VP2 (Clemens and Pintel, 1988; Schoborg and Pintel, 1991). In our study, RT-PCR quantification data showed no decrease in accumulation of total capsid mRNA transcribed from P38-VP cassette derived from PM-III mutant, indicating a post-transcriptional effect of PM-III mutation. For example, it is speculated that PM-III mutation could interfere with splicing of VP1 pre-mRNA, although the primers used in mRNA quantification could not distinguish unspliced VP1 premRNA from mature spliced mRNA. It has been previously reported that introduction of stop codons in NS2 exons can inhibit the splicing of MVM

RNA *in cis* (Naeger et al., 1992). It is known that in addition to the core elements involved in splicing such as donor/acceptor sites, branch point and polypyrimidine tract (PPT), other sequences in pre-mRNA sequence such as exonic/intronic splicing enhancers and silencers can regulate this process *in-cis* or through binding of proteins *in trans* (Matera and Wang, 2014; Matlin et al., 2005; Wang and Burge, 2008). Thus, it is conceivable that PM-III mutation located 125 nucleotides upstream of VP1 splice donor site (so-called D2) may interfere with VP1 pre-mRNA splicing. Another possible mechanism with respect to the effects of PM-III mutation on splicing, could be the creation of a non-canonical splice donor site in 5'-UTR of the capsid transcripts, thereby interfering with optimal splicing of D1-A1 and D2-A2 small introns. However, even in the absence of VP1/VP2 small introns, luciferase gene expression was downregulated under a P38-Gluc cassette carrying PM-III mutation. Hence, this negative cis effect of PM-III mutation on the expression of P38-driven genes, in the absence of splicing, is probably caused by a different mechanism, for instance creation of an upstream AUG in an optimal Kozak context in 5'-UTR of the capsid mRNAs (AAC**C**UGG to AAC**A**UGG). A silent mutation maintaining amino acid sequence of NS2 protein at this position and eliminating the initiating AUG (AAC**A**UGG to AAC**U**UGG) not only restored the virus replication and spread (the silent sequence is then identical as in wt MVM), but also removed the *cis* effect of PM-III mutation on both VP1/VP2 and luciferase reporter expression. There is now compelling evidence that several elements within noncoding regions of genes regulate gene expression at transcriptional or post-transcriptional level. While promoters, enhancers and silencers exert their functions at the transcription level, several elements in 5'-UTR region of mRNA including cap, internal ribosome entry sites (IRES) and other secondary structures (e.g. stem-loops, G-quadruplets) and upstream AUGs, and miRNA binding sites (typically in 3'-UTR) regulate mRNA expression post-transcriptionally (Barrett et al., 2012). In contrast to regulatory mechanisms mediated by 3'-UTR region of mRNAs, for instance through interaction with microRNAs and cellular factors like poly A-binding protein (PABP), very little is known about post-transcriptional gene regulation by 5'-UTR region interactions. Also, regulation by protein–RNA interactions in the 5'-UTR is surprisingly

rare with, to the best of our knowledge, only one well-studied example, ferritin mRNAs. However, *cis* elements in 5'-UTR sequence can influence translation of mRNA. In a recent study, Johnstone *et al*. systematically analyzed translation and function of upstream open reading frames (uORFs) in vertebrate mRNAs using high-resolution ribosome footprinting (Johnstone et al., 2016). By using reporter experiments they showed repression of down-stream translation by uORFs. Also, the magnitude of translation downregulation was mostly dependent on factors such as number of uORFs, intercistronic distance and nucleotide context of upstream AUG. As mentioned before, PM-III mutation was originally identified in MVMi as a fitness mutation under selective pressure of anti-capsid neutralizing antibodies in mice where it replicated and spread better *in vitro* and *in vivo* (Lopez-Bueno et al., 2004). Bioinformatic analysis showed that the 5'-UTR regions of capsid mRNA from H-1PV and MVMi are slightly different (10% and 14% for VP2 and VP1 mRNA respectively), leading to slightly different *in silico*-predicted secondary structures. As mentioned hereinabove, VP1 expression is more dramatically affected by PM-III mutation compared to VP2 and this results in increased ratio of VP2:VP1. However, PM-III mutation introduces the same structural modification in 5'-UTR of VP1 and VP2 mRNAs. Furthermore, PM-III mutation does not introduce stable structures such as stem-loops in 5'-UTR. Therefore, it seems unlikely that impaired translation of the capsid mRNAs in PM-III mutant could be caused by subtle structural changes in 5'-UTR. Additionally, more striking effects of PM-III mutation on VP1 expression compared to VP2, cannot be explained by a common structural modification in the two mRNAs. Interestingly, sequence alignment of the capsid mRNA 5'-UTR derived from H-1PV and MVMi showed that there is no uORF in the capsid mRNA from H-1PV whereas two AUG initiation codons in VP1 and three in VP2 (one AUG in a strong Kozak context) are found in MVMi. This probably indicates differences in regulation of the capsid mRNA translation in MVMi and H-1PV.

4.4 Viral DNA Replication and Packaging is Modified by NS1/NS2 Mutations

Although NS1 is, due to its enzymatic activities such as ATP-dependent DNA-binding, DNA helicase and nickase activities, the main player in DNA replication, NS2 is also

important for DNA replication, generation of ssDNA and consequently progeny virions in rodent host cells. However, it is largely dispensable for virus replication in human cells (Cotmore et al., 1997; Li and Rhode, 1991). As mentioned before, PM-III replicates and spread poorly in cell culture, resulting in small plaques (see Section 4.1). Analysis of PM-III mutant DNA replication after infection and also after transfection of an infectious DNA clone, showed that replicative intermediate forms (mRF and dRF) accumulate efficiently in the cells but production of ssDNA is severely diminished. Furthermore, the production of capsid proteins was severely diminished (see Section 4.2). During the course of infection by protoparvoviruses, empty capsids (procapsids) are assembled in the nucleus and subsequently package progeny ssDNA generated from monomeric replicative form (mRF) by helicase and nickase activities of NS1 protein in cooperation (though poorly understood) with NS2. In other words, generation of progeny ssDNA after infection is tightly connected to accessibility of preassembled empty capsids (procapsids) in the nucleus. Hence, decreased generation of ssDNA and subsequently progeny virions by PM-III mutant is mainly due to decreased amounts of capsid proteins. Unlike AAVs, where small Rep proteins physically interact with capsids (Dubielzig et al., 1999) and initiate DNA packaging via their helicase activity (King et al., 2001), this step is rather poorly understood in protoparvoviruses and it is not known how exactly NS1 and NS2 proteins cooperate and interact with the DNA replicative forms and preassembled capsids. As a matter of fact, empty procapsids and DNA replicative forms (esp. monomeric RF) are always produced in excess, and mRF duplexes are only partially processed to unit-length progeny ssDNA which is concomitantly packaged into preformed capsids. Hence, it is speculated that in PM-I, PM-II and DM mutants, not only the DNA replication functions of nonstructural proteins (carried mainly by NS1) but also their packaging machinery might work more efficiently than wt, leading to increased yield of progeny virions in a single cycle of infection. Since the main DNA replicating functions of NS1 protein are regulated via phosphorylation by specific isoforms of cellular protein kinase C (PKC) (Nuesch et al., 2003), we suggest that NS mutations could modulate post-translational modifications of this protein and enhance DNA replication and packaging. In the

present study, a stronger viral DNA replication was observed after infection with PM-I and DM mutants, both carrying Y595H substitution at C-terminal region of NS1. However, the deletion in DelH-1PV did not enhance the viral DNA replication. As mentioned earlier, PM-I mutation also introduces an amino acid substitution in NS2 (L103P). To investigate the contribution of NS1 mutation to virus replication in the absence of NS2 mutation, a NS2-null variant of DM virus was created in which R2 mRNA splice acceptor site was abolished by mutagenesis. This virus was able to replicate and spread better than a NS2-null virus encoding a wt NS1 protein, indicated by large plaques and higher yield of progeny virions with slightly improved infectivity. Interestingly, the same phenotype was obtained with a NS2-null DelH-1PV virus. This indicates that either radical substitution of tyr595 by histidine or deletion of this region, boosts viral replication and spread. However, it is unclear whether or not this is due to an enhanced DNA replication. Furthermore, it cannot be excluded that NS2 mutation (L103P) could also contribute to improved virus replication. As mentioned hereinabove, NS1 is subject to phosphorylation during the course of infection. However, NS1 functions in DNA replication of MVM are regulated by serine and threonine phosphorylations (Nuesch et al., 2003) and no tyrosine phosphorylation has been shown in this protein. In this study, when Tyr595 was substituted by phenylalanine, a nonphosphorylable structural mimic of tyrosine, without changing amino acid sequence of NS2, a wt phenotype was obtained. This indicated that the enhanced virus fitness achieved with Y595H mutation was not due to elimination of a phosphorylation site and probably caused by radical substitution of tyrosine by a positively charged histidine.

4.5 Point Mutations in NS1/NS2 Modulate Early Steps of Viral Infection Cycle

There is accumulating data, supporting a role of NS2 protein in modulating infectivity of the progeny particles, probably through post-translational modification of the capsids before or after assembly. Previously Weiss *et al*. showed that infection with DelH-1PV substantially improved infectivity of the virus particles. This was reflected, in particular, by a significant increase in binding and entry of the virus particles (Weiss et

al., 2012). In this study, we showed that PM-I, PM-II and DM mutations did not modify binding of the progeny virus particles, but enhanced their internalization, and this was more prominently observed for PM-I mutant. Also, PM-III mutant virus particles were capable of binding and entering human cells as efficient as wt strain. Although the attachment of PM-I, PM-II and DM mutant particles to host cells at 4°C was comparable to wt virus, their uptake was more efficient. Several parvoviruses attach to their target cells via binding to glycan receptors (Huang et al., 2014). For example, human parvovirus B19 uses gangliosides (Cooling et al., 1995), AAV2 uses heparan sulfate proteoglycan (HSPG) (Kern et al., 2003) and protoparvoviruses including porcine parvovirus (Boisvert et al., 2010), MVM (Nam et al., 2006) and rat H-1 parvovirus (Allaume et al., 2012) bind to sialic acid residues. Sialic acid is a monosaccharide derived from neuraminic acid that decorates all eukaryotic cell surfaces, capping different glycoproteins and glycolipids (Varki, 2008). In fact, sialic acid-containing glycans linked to either a protein or lipid serve as a receptor for many viruses including several human pathogens (Neu et al., 2011; Stencel-Baerenwald et al., 2014). Interestingly, large-plaque variants of MVM were identified that carried amino acid substitutions in the sialic acid binding pocket of the capsid leading to lower binding affinity of the virus to host cells (Lopez-Bueno et al., 2006; Rubio et al., 2005). Upon inoculation of mice, these viruses were more virulent as shown by more efficient dissemination to other organs and higher mortality rates. It is worth noting that in our study, the adsorption of the virus particles was tested below the physiological temperature (4°C), hence, low and high affinity binders were not distinguishable. Similarly, for internalization experiments the cells were incubated at 4°C for 1 h to allow the virus attachment before a temperature shift to 37°C. Our data indicated that not all the adsorbed particles are successfully taken up by the cells and the efficiency of the internalization can be enhanced independent of whether or not the binding step is stimulated. Although sialic acid is essential for primary adsorption of MVM (Nam et al., 2006) and H-1PV (Allaume et al., 2012) to the host cells, the protein receptor(s) mediating entry of the virus is not known. Garcin *et al*. employed a siRNA library screening approach in host cells in an attempt to find the entry receptor for MVM

(Garcin et al., 2013; Garcin et al., 2015). They found that galectin-3 is necessary for efficient MVMp cell entry and infection, but not for cell binding (Garcin et al., 2015). These findings strongly suggest that the virus particles are first nonspecifically adsorbed to glycans containing sialic acid, but, for successful translocation of the virion from the apical side of plasma membrane to the cell interior, capsids require to engage in further specific interactions with plasma membrane proteins. Consequently, structural determinants of the capsid involved in virus adsorption to cell surface sialic acid and subsequent entry are probably different. In case of PM-I, PM-II and DM mutants, while there was no difference in attachment of the virus particles to the cells compared to wt, but the mutants were taken up more efficiently. This indicates that adsorption of the capsids to sialic acid residues is not affected by the mutations, but subsequent interaction with the entry receptor(s) is modified, for instance due to alterations in post-translational modifications of the capsids. In rodent parvoviruses MVM and H-1PV, phosphorylation of the capsid proteins has been reported (Maroto et al., 2000) and it is not clear whether or not the capsids undergo other kind of modifications, in contrast to AAVs where ubiquitination (Yan et al., 2002) or SUMOylation of the capsids can affect viral transduction efficiency (Holscher et al., 2015). It has been shown that MVM capsids are not only phosphorylated at VP2 N-terminus but also further on the surface during a late maturation step in the nucleus, which makes the capsids competent to egress from the nucleus prior to cell death (Wolfisberg et al., 2016). During the course of infection by MVM, VP1 and VP2 are synthesized in cytoplasm and form trimeric complexes that are subject to phosphorylation by mitogen-activated protein kinase (MAPK) signaling pathway kinases such as Raf-1 kinase, followed by nuclear translocation (Riolobos et al., 2010). Once inside the nucleus they assemble to empty capsids (procapsids) and subsequently package progeny ssDNA and go through further surface phosphorylation steps collectively known as “maturation step”, which plays an important role in nuclear egress of the progeny virions prior to cell death (Wolfisberg et al., 2016). The nuclear egress of the mutants is further discussed in Section 4.6.

The role of post-translational modifications in early steps of the viral infection cycle such as binding, endocytosis, trafficking through endosomal compartment and nuclear transport is not understood. Following endocytosis, parvoviral capsids traffic through endosomes where they are exposed to low pH and lysosomal hydrolases. Under these conditions, conformational rearrangements occur in the capsids, for instance VP2 N-terminus which is exposed on the surface of genome-containing capsids is proteolytically cleaved to VP3 (Mani et al., 2006; Paradiso, 1984; Tattersall et al., 1977; Tullis et al., 1992), and VP1 N-terminus deploys its PLA2 activity which is required for breaching through the endosomal membrane and escape of virus into the cytoplasm (Farr et al., 2005; Girod et al., 2002; Zadori et al., 2001). It is still not clear how the genomes enter the nucleus, but in addition to mechanisms involving nuclear pore complex (NPC), passing through the nuclear envelope by induction of transient disruptions has also been proposed (Cohen et al., 2006; Cohen and Pante, 2005). In this study, using cellular fractionation we showed that only a minor proportion (~20% of total particles) of the virus particles (both wt and mutants) are recovered from the nuclear fraction after infection. However, there was no significant difference between wt and mutants in this regard. In order to initiate DNA replication and gene expression, viral genome needs to be released. Currently, very little is known about uncoating step and genome release after parvoviral infection. It has been shown that viral genomes can be released *in vitro* by certain physicochemical treatments (e.g. heating, acidic pH and EDTA) of virions without capsid degradation (Cotmore et al., 2010; Ros et al., 2006). Viral DNA replication initiated 6 hpi with PM-I, PM-II and DM mutants, similar to wt virus, but it progressed significantly faster than wt virus, resulting in ~10-fold higher DNA copies within 4 hours (10 hpi). In other words, the viral DNA replication was significantly faster after infection with the mutants compared to wt virus. It is unclear whether uncoating of the capsids is affected by these mutations, but DNA replication during the course of infection (6-10 hpi) is accelerated with the mutants.

Although NS2 has no enzymatic function but it has been shown to interact with at least some members of cellular 14-3-3 protein family when it is phosphorylated at threonine

149 (Brockhaus et al., 1996). The 14-3-3 proteins are ubiquitous small (28–33 kDa) polypeptides with several isoforms that occur as homo- or heterodimers and function as adaptors in diverse physiological pathways including signal transduction, cell cycle regulation and apoptosis (Aitken, 2006; Morrison, 2009). The phosphorylated form of NS2 is only found in the cytoplasm of infected cells (Cotmore and Tattersall, 1990a) where it interacts with cellular 14-3-3 proteins (Brockhaus et al., 1996). However, mutagenesis of T149A in NS2 protein (located upstream of PM-III mutation L153M) from MVM did not affect the virus replication and spread either in mouse or human cells (Dr. Nathalie Salome' unpublished data). Similar results were obtained in the current study by a H-1PV mutant (T149A) in human cells (data not shown). Hence, it is very unlikely that PM-III phenotype could be due to a loss of function in NS2 which affects interaction of this protein with cellular 14-3-3 protein family. Various biological functions of the large nonstructural protein NS1 including DNA replication functions and cytotoxic properties are subject to regulation by phosphorylation (Corbau et al., 2000; Corbau et al., 1999; Daeffler et al., 2003; Dettwiler et al., 1999; Nuesch et al., 2003; Nuesch et al., 1998b) and also acetylation (Li et al., 2013). It has been reported previously that the so-called hyperphosphorylated band of NS1, a slow migrating form of the protein on denaturing gels, is significantly decreased after infection by a NS2-null derivative of H-1 virus (Li and Rhode, 1991). This suggests that NS2 can influence post-translational modifications of NS1, although a direct physical interaction between the two proteins has not been demonstrated. Similarly, a deletion in nonstructural proteins of H-1PV modified phosphorylation pattern of NS1 after infection of human cells as shown by 2D phosphopeptide mapping of ^{32}P-labeled protein (Nadine Weiss, Ph.D. Thesis).

4.6 The Nuclear Egress of Mutants is Not Stimulated by NS1/2 Mutations

Although enhanced DNA replication and also slightly increased accumulation of the capsids in DM mutant boosted overall production of progeny virions, but progeny virions egressed from the nucleus with similar efficiency as wt virus. It is well known that progeny particles are generated in the nucleus by packaging of ssDNA pre-

assembled capsids in the nucleus. Although it is generally believed that parvoviruses, like many other nonenveloped DNA viruses (e.g. adenoviruses) are released when the cells collapse, there is increasing evidence of a pre-lytic phase of parvoviral egress (Maroto et al., 2004; Wolfisberg et al., 2016). Weiss *et al*. showed that nuclear egress of progeny virions was stimulated in cells infected with DelH-1PV (Weiss et al., 2012). Although the underlying mechanism was not described, post-translational modification of the capsids was suggested to be altered due to NS mutation. A recent study identified two distinct populations of MVM particles in the nucleus using anion exchange chromatography (Wolfisberg et al., 2016). The different anion exchange profile of these particles was found to be linked to degrees of surface phosphorylation of the capsids. Interestingly, capsids with more extensive phosphorylations on the surface were preferentially allowed to egress from the nucleus prior to cell lysis and those lacking these maturation determinants were released passively after cell death (Wolfisberg et al., 2016). The cellular kinase(s) involved in this process were not reported but it was proposed to occur in the nucleus during maturation of the virus particles. Also, these late phosphorylations of the capsid surface had no effect on cellular binding or internalization of the virions, and these two virus populations showed similar plaque phenotypes. In the current study, PM-I, PM-II and DM mutants were more efficiently taken up by the cells but progeny virions egressed from the nucleus with similar kinetics as wt virus. Taken together, these data suggest that capsid phosphorylation determinants that are involved in binding and entry are different from those defining nuclear egress of these viruses. However, this needs to be verified by infecting the cells with phosphatase-treated capsids and also further by 2D phosphopeptide mapping of the capsids.

The small nonstructural protein, NS2, is the only protein in protoparvoviruses known to directly interact with nuclear export machinery of the cells (Ohshima et al., 1999) and mediate nuclear egress of MVM progeny virions from mouse cells prior to cell lysis (Eichwald et al., 2002; Miller and Pintel, 2002a). This has been shown by inhibition of the NS2 interaction with Exportin 1 also known as chromosomal region maintenance 1

(CRM1) using leptomycin B and mutagenesis of CRM1-binding site in NS2 (Eichwald et al., 2002; Miller and Pintel, 2002a). CRM1 is a well characterized member of nuclear transport machinery involved in trafficking of several cellular proteins and mRNAs (Cautain et al., 2015). An extensively studied viral interaction partner of CRM1 is HIV Rev protein which is required for nuclear export of partially spliced and unspliced viral mRNAs via selective binding to a cis element called Rev Response Element (RRE) on these transcripts (Pollard and Malim, 1998). This interaction is mediated by a leucine-rich nuclear export signal (**L**PP**L**ER**L**T**L**) on Rev protein. Similarly, MVM NS2 protein contains a supraphysiological nuclear export signal (**M**TKK**F**GT**L**T**I)** which tightly binds to CRM1 (Engelsma et al., 2008), but a role for nuclear export of viral mRNAs or proteins has not been identified. Also, Eichwald *et al.* showed proficient synthesis of viral proteins after infection of human and mouse cells with MVM mutants expressing NS2 proteins with abolished CRM1 interaction (Eichwald et al., 2002). The NS2-CRM1 interaction is however important for nuclear egress of MVM particles in mouse cells but not in human transformed cells (NB-324K cell line), resulting in nuclear retention of the viruses and subsequently poor spread in cell culture as demonstrated a by small plaque phenotype (Eichwald et al., 2002). Considering the fact that no physical interaction between NS2 and assembled capsids have been demonstrated so far (e.g. by pull-down assays), a more likely scenario is that the NS2-CRM1 interaction is required for regulation of a cellular protein that is involved in nuclear export of virus. The CRM1-binding site of NS2 protein spans residues 82-91, upstream of the region where point mutations described in this study are clustered (PM-I: L103P and PM-II: K96E). As demonstrated in this study, nuclear egress of DM virions carrying PM-I and PM-II mutations in NS2, was comparable to wt. This is in contrast to the deletion mutation described by Weiss *et al.* where nuclear egress of the progeny virions was significantly improved (Weiss et al., 2012). The point mutations described in MVMi, did not compromise NS2 binding to CRM1 protein and in some cases (DM mutant) enhanced this interaction as shown by co-immunoprecipitation assay. Furthermore, by immunofluorescence staining, the authors showed an enhanced cytoplasmic sequestration of CRM1 protein and better nuclear release of the viruses after infection

with these mutants (Lopez-Bueno et al., 2004). In our study, the nuclear egress of the mutants was not enhanced and therefore the effects of NS2 mutation on CRM1 interaction was not analyzed. However, the indirect impacts of NS2-CRM1 interaction and its cytoplasmic sequestration, on nucleocytoplasmic trafficking of the viral proteins during the course of infection deserves further investigation.

4.7 Outlook

Taken together, our data along with the study reported previously (Weiss et al., 2012), points out different steps of the virus life cycle including both early and late steps that can be improved by mutagenesis of H-1PV nonstructural proteins. Increased fitness of the virus by introduction of point mutations in the deletion region further clarified functions of NS2 in the deletion region, which affect virus replication and spread in transformed human cells. It is tempting to introduce random peptide libraries into this region to create a toolbox of mutants with different phenotypes and test their performance against different tumor entities. Furthermore, these mutations can be employed to enhance the performance of replication-deficient H-1 vectors expressing anti-tumor transgenes (e.g. antiangiogenic or immunostimulatory chemokines).

Supplementary Figure 1.

PM-III Mutation

M	V	R	D	R	G	G	F	E	S	L	L	Q	S	R	T
AUG	GUC	CGA	GAU	CGA	GGC	GGA	UUU	GAG	AGC	UUG	CUU	CAG	UCA	AGA	ACA

V	G	E	R	L	Q	R	G	A	D	L	G	L	R	P	E
GUU	GGA	GAG	CGA	CUU	CAA	CGA	GGA	GCU	GAC	CUU	GGA	CUA	AGG	CCU	GAA

I	T	W	F	#							M	S	D
AUC	ACU	UGG	UUC	UAG	GUU	GGG	UGC	CUC	.....	CAA	UGA	GUG	AUG

Figure 1. (Top panel) Nucleotide Sequence alignment of wt 5'-UTR region of the VP2 mRNA of MVMi and H-1PV. The nucleotide sequences were aligned using default settings of Clustal Omega online tool. Identical regions are shown with asterisks. Three AUGs located upstream of VP2 initiation codon in MVMi are shown in red letters. The AUG flanked by a favorable Kozak context is underlined with -3 (A) and +4 (G) nucleotides (relative to A in AUG as +1 nt) in italic. The blue box encloses the position of PM-III mutation where CUG in wt is mutated to AUG. (Bottom Panel) A small ORF is created by PM-III upstream of VP2 initiation codon, indicated by AUG (enclosed by a blue rectangle) and stop codon (#). The C-terminal peptide derived from NS2 protein (NS2P isoform) encoded by this ORF is shown. The VP2 ORF at the end of the sequence is underlined (frame +3). The VP2 initiation codon is located 395 nt downstream (395 nt) of the PM-III ORF stop codon. The intervening sequence is shown by a dotted line.

Supplementary Figure 2.

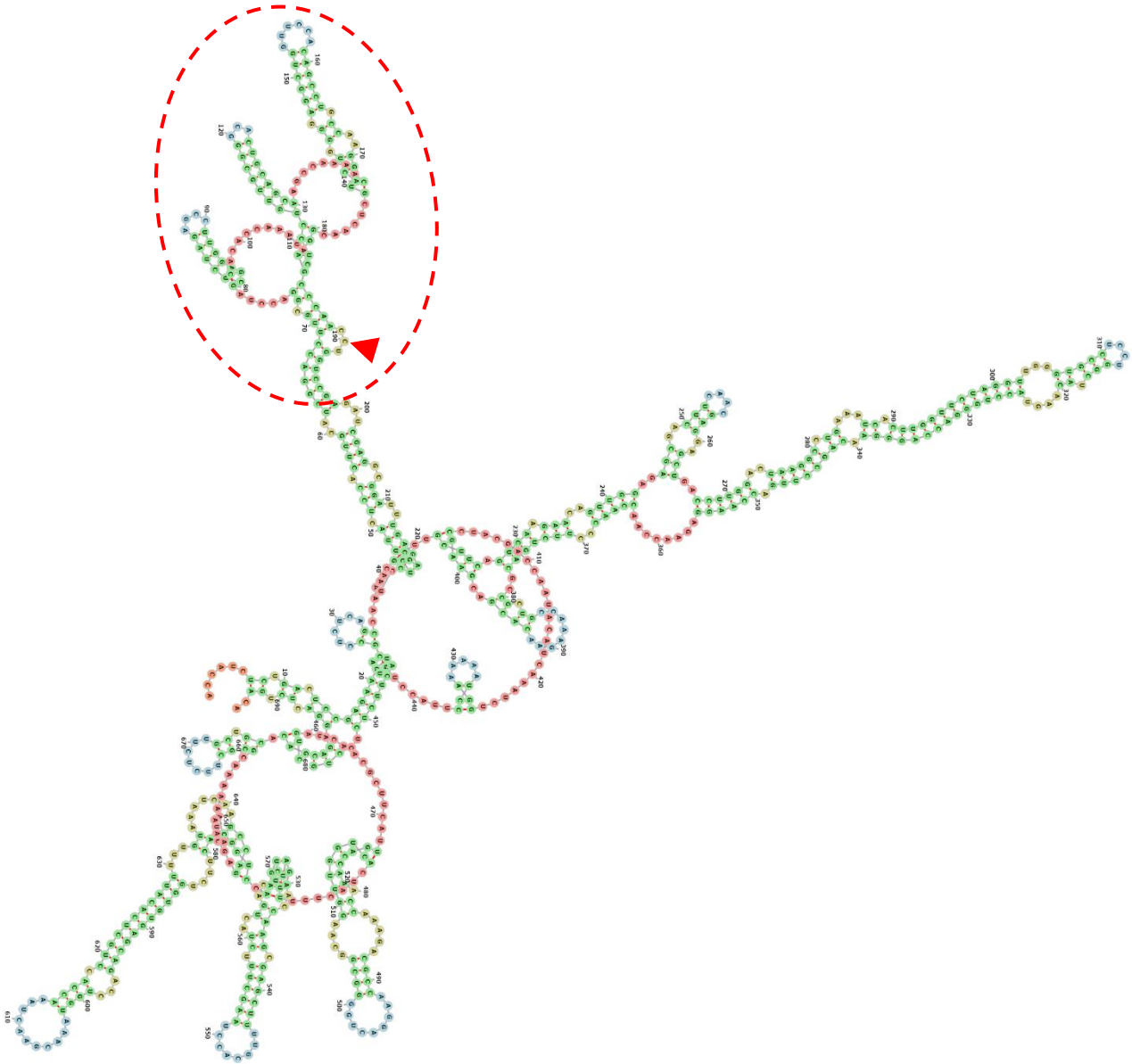

wt (H-1PV)

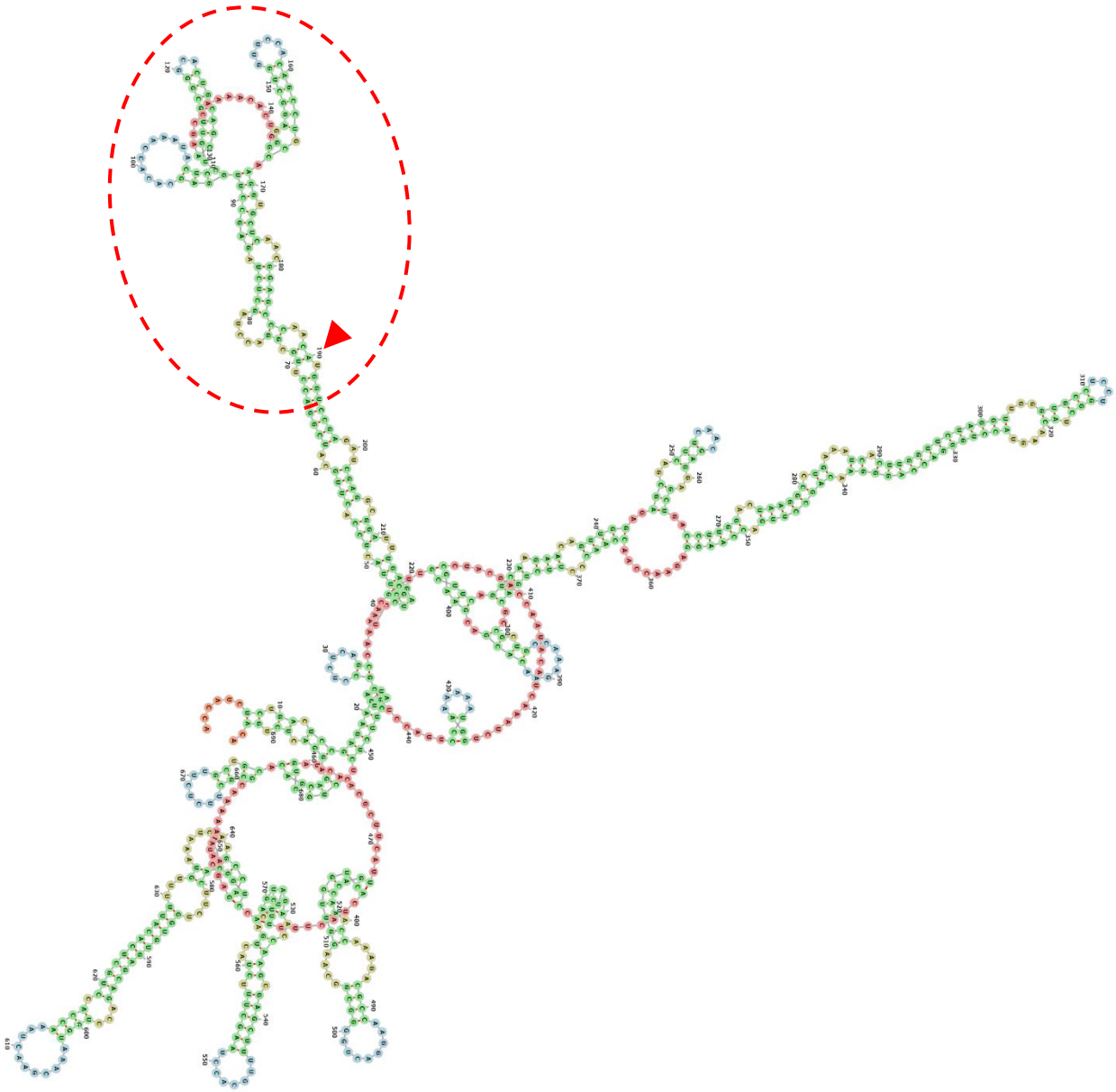

H1-PM-III

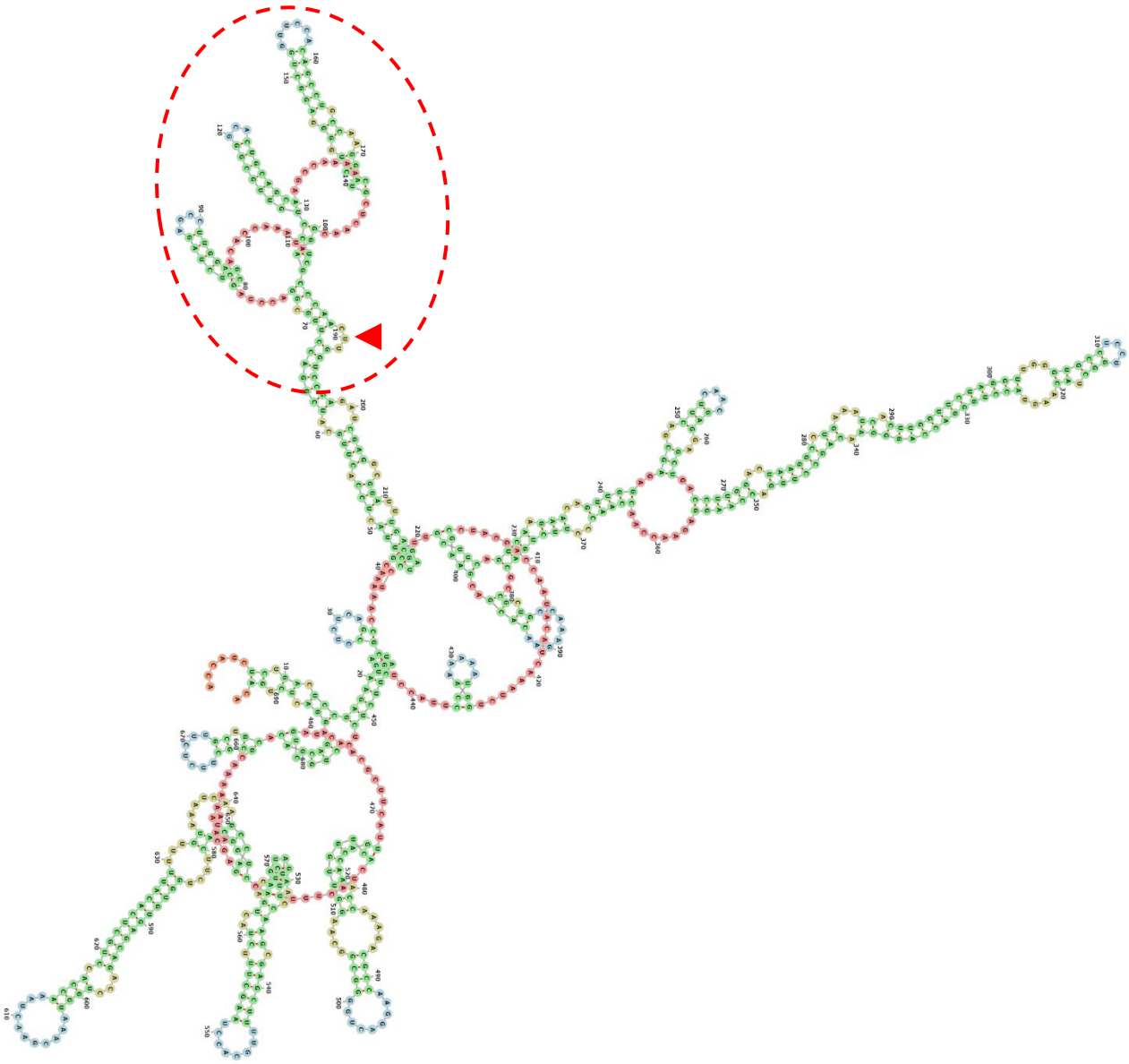

H1-PM-III^{Silent}

Figure 2. *In silico*-predicted secondary structure of 5'-UTR region from VP2 mRNA. Secondary structures of 5'-UTR sequences derived from wt (H-1PV), H1-PM-III and H1-PM-III^{Silent} viruses were predicted *in silico* using default settings of RNAfold webserver. A structure based on minimum free energy (MFE) is shown here. The region subject to structural modification is enclosed by a dashed red line, and the position of PM-III and PM-III^{Silent} mutations are indicated by an arrowhead. Colors indicate different types of structures (small or large loops, terminal loops and base-paired regions). For VP1 5'-UTR structures, see Figure 15 in Chapter 3.

Supplementary Figure 3.

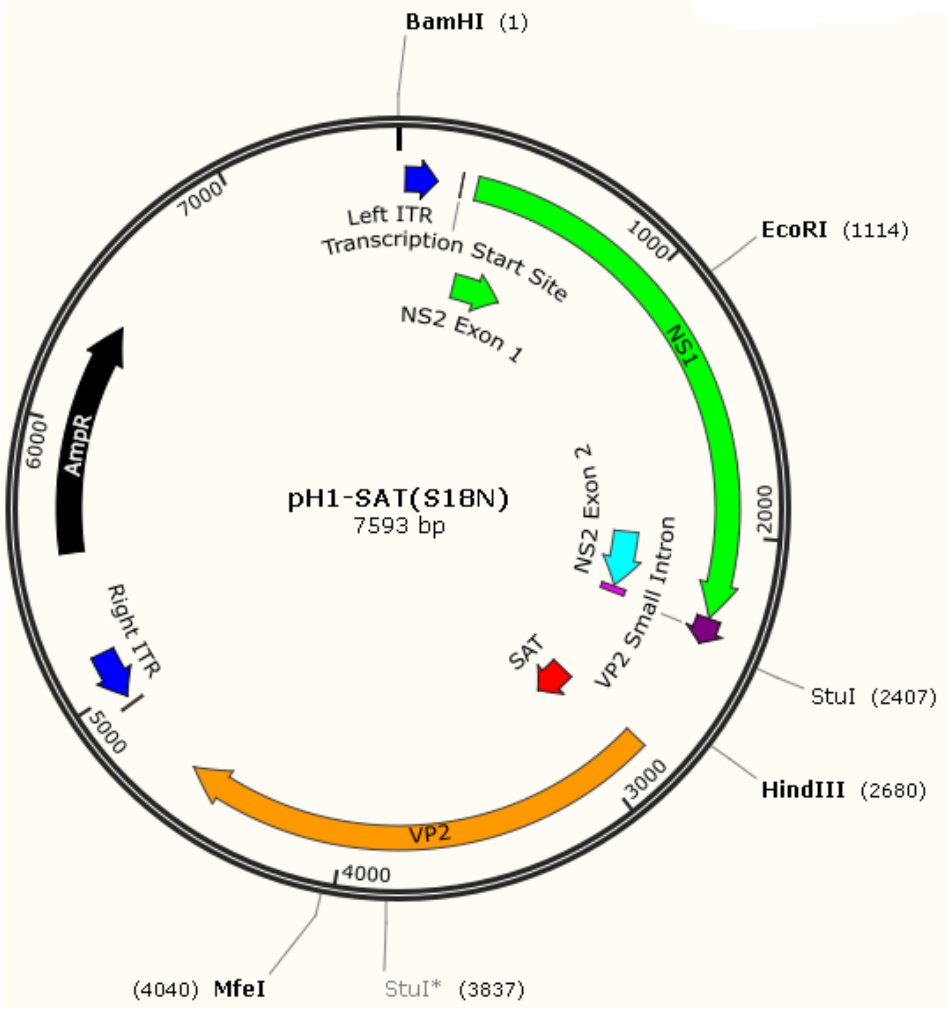

GGATCCAAACTCCCTGAACCGCTTATCATTTTTAGAAACTGACCAACCATGTTCACGCTAGT
GACGTGATGACGCGCGCTGCGCGCGCTGCCTTCGGCAGTCACACGTCACTAGCGTTTCACAT
GGTTGGTCAGTTCTAAAAATGATAAGCGGTTCAGAGAGTTTGAAACCAAGGCGGGAAACGGA
AGTGGGCGTGGCTAACTGTATATAAGCAGTCACTCTGGTCGGTTACTCACTCTGCTTTCATT
TCTGAGTTTGTGAGACACAGGAGCGAGACTAACCAACTAACCATGGCTGGAAACGCTTACTC
CGATGAGGTTTTGGGAGTAACCAACTGGCTGAAGGACAAAAGTAGCCAGGAGGTGTTCTCAT
TTGTTTTTAAAAATGAAAACGTCCAACTAAATGGAAAGGACATCGGTTGGAATAGTTACAGA
AAGGAGCTACAAGATGACGAGCTGAAGTCTCTACAACGAGGGGCGGAGACCACTTGGGACCA
AAGCGAGGACATGGAATGGGAGAGCGCAGTGGATGACATGACCAAAAAGCAAGTATTTATTT
TTGATTCTTTGGTTAAGAAGTGTTTGTTTGAAGTGCTCAGCACAAAGAACATAGCTCCTAGT
AATGTTACTTGGTTCGTGCAGCATGAATGGGGAAAGGACCAAGGCTGGCACTGTCATGTGCT
GATTGGAGGCAAGGACTTTAGTCAACCTCAAGGAAAATGGTGGAGAAGGCAGCTAAATGTGT
ACTGGAGTAGATGGTTGGTGACTGCCTGTAATGTTCAACTAACACCAGCTGAAAGAATTAAA
CTGAGAGAAATAGCAGAGGACAGTGAATGGGTCACTTTGCTTACCTATAAGCATAAGCACAC
CAAGAAGGACTATACCAAGTGTGTTCTTTTTGGAAACATGATTGCTTATTACTTTTTAAGCA
AAAAGAAAATATGTACCAGTCCACCAAGGGACGGAGGCTATTTTCTTAGCAGTGACTCTGGC
TGGAAAACTAACTTTTTGAAAGAGGGCGAGCGCCATCTAGTGAGCAAACTGTATACTGATGA

GATGAAACCAGAAACGGTCGAGACCACAGTGACCACTGCACAGGAAGCTAAGCGCGGCAGAA
TTCAAACTAGAAAGGAGGTCTCGATTAAAACCACACTCAAAGAGTTGGTACATAAAAGAGTA
ACCTCACCAGAAGACTGGATGATGATGCAGCCAGACAGTTACATTGAAATGATGGCTCAACC
AGGTGGAGAAAACTTGCTTAAAAATACACTAGAGATCTGTACACTGACTCTAGCAAGAACCA
AAACAGCCTTTGACTTGATTCTGGAAAAAGCTGAAACCAGCAAACTAGCCAACTTTTCCATG
GCTAGCACCAGAACCTGTAGAATCTTTGCTGAGCATGGCTGGAACTATATTAAAGTCTGCCA
TGCCATCTGTTGTGTGCTGAATAGACAAGGAGGCAAAAGGAACACTGTGCTCTTTCACGGAC
CAGCCAGCACAGGCAAATCTATTATTGCACAAGCCATAGCACAAGCAGTTGGTAATGTTGGT
TGTTACAATGCTGCCAATGTGAACTTTCCATTTAATGACTGTACCAACAAAAACTTGATTTG
GGTGGAAGAAGCTGGTAACTTTGGCCAGCAAGTAAACCAATTCAAAGCTATTTGTTCTGGCC
AAACCATACGCATTGATCAAAAAGGAAAAGGCAGCAAACAGATTGAACCAACACCAGTTATT
ATGACCACCAACGAGAACATTACCGTGGTTAGAATAGGCTGTGAGGAAAGACCAGAACACAC
TCAACCAATCAGAGACAGAATGCTCAACATTCACCTGACACGTACACTACCTGGTGACTTTG
GTTTGGTGGATAAGCACGAATGGCCTCTGATCTGTGCTTGGTTGGTGAAGAATGGTTACCAA
TCTACCATGGCTTGTTACTGTGCTAAATGGGGCAAAGTTCCTGATTGGTCAGAGGACTGGGC
GGAGCCGAAGCTAGACACTCCTATAAATTCGCTAGGTTCAATGCGCTCACCATCTCTGACTC
CGAGAAGTACGCCTCTCAGCCAAAACTACGCTCTTACTCCACTTGCATCGGACCTTGCGGAC
CTAGCTCTAGAGCCTTGGAGCACACCAAATACTCCTGTTGCGGGCACTGCAGCAAGCCAAAA
CACTGGGGAGGCTGGTTCCACAGCCTGCCAAGGTGCTCAACGGAGCCCAACCTGGTCCGAGA
TCGAGGCGGATTTGAGAGCTTGCTTCAGTCAAGAACAGTTGGAGAGCGACTTCAACGAGGAG
CTGACCTTGGACTAAGGTACAATGGCACCTCCAGCTAAAAGAGCTAAAAGAGGTAAGGGGCT
AAGGGATGGTTGGTTGGTGGGGTACTAATGTATGACTACCTGTTTTACAGGCCTGAAATCAC
TTGGTTCTAGGTTGGGTGCCTCCTGGCTACAAGTACCTGGGACCAGGGAACAGCCTTGACCA
AGGAGAACCAACCAACCCTTCTGACGCCGCTGCCAAAGAACACGACGAAGCCTACGACCAAT
ACATCAAATCTGGAAAAAATCCTTACCTGTACTTCTCTCCTGCTGATCAACGCTTCATTGAC
CAAACCAAAGACGCCAAGGACTGGGGCGGCAAGGTTGGTCACTACTTTTTTAGAACCAAGCG
AGCTTTTGCACCTAAGCTTTCTACTGACTCTGAACCTGGCACTTCTGGTGTGAGCAGACCTG
GTAAACGAACTAAACCACCTGCTCACATTTTTGTAAATCAAGCCAGAGCTAAAAAAAAACGC
GCTTCTCTTGCTGCACAGCAGAGGACTCTGACAATGAGTG**ATGGCACCGAAACAAACCAACC**
AGACACTGGAATCGCTAATGCTAGAGTTGAACGATCAGCTGACGGAGGTGGAAGCTCTGGGG
GTGGGGGCTCTGGCGGGGGTGGGATTGGTGTTTCTACTGGGACTTATGATAATCAAACGACT
TATAAGTTTTTGGGAGATGGATGGGTAGAAATAACTGCACATGCTTCTAGACTTTTGCACTT
GGGAATGCCTCCTTCAGAAAACTACTGCCGCGTCACCGTTCACAATAATCAAACAACAGGAC
ACGGAACTAAGGTAAAGGGAAACATGGCCTATGATGACACACATCAACAAATTTGGACACCA
TGGAGCTTGGTAGATGCTAATGCTTGGGGAGTTTGGTTCCAACCAAGTGACTGGCAGTTCAT
TCAAAACAGCATGGAATCGCTGAATCTTGACTCATTGAGCCAAGAACTATTTAATGTAGTAG
TCAAAACAGTCACTGAACAACAAGGAGCTGGCCAAGATGCCATTAAAGTCTATAATAATGAC
TTGACGGCCTGTATGATGGTTGCTCTGGATAGTAACAACATACTGCCTTACACACCTGCAGC
TCAAACATCAGAAACACTTGGTTTCTACCCATGGAAACCAACCGCACCAGCTCCTTACAGAT
ACTACTTTTTCATGCCTAGACAACTCAGTGTAACCTCTAGCAACTCTGCTGAAGGAACTCAA
ATCACAGACACCATTGGAGAGCCACAGGCACTAAACTCTCAATTTTTTACTATTGAGAACAC
CTTGCCTATTACTCTCCTGCGCACAGGTGATGAGTTTACAACTGGCACCTACATCTTTAACA
CTGACCCACTTAAACTTACTCACACATGGCAAACCAACAGACACTTGGGCATGCCTCCAAGA
ATAACTGACCTACCAACATCAGATACAGCAACAGCATCACTAACTGCAAATGGAGACAGATT
TGGATCAACACAAACACAGAATGTGAACTATGTCACAGAGGCTTTGCGCACCAGGCCTGCTC
AGATTGGCTTCATGCAACCTCATGACAACTTTGAAGCAAACAGAGGTGGCCCATTTAAGGTT
CCAGTGGTACCGCTAGACATAACAGCTGGCGAGGACCATGATGCAAACGGAGCCATACGATT
TAACTATGGCAAACAACATGGCGAAGATTGGGCCAAACAAGGAGCAGCACCAGAAAGGTACA

CATGGGATGCAATTGATAGTGCAGCTGGGAGGGACACAGCTAGATGCTTTGTACAAAGTGCA
CCAATATCTATTCCACCAAACCAAAACCAGATCTTGCAGCGAGAAGACGCCATAGCTGGCAG
AACTAACATGCATTATACTAATGTTTTTAACAGCTATGGTCCACTTAGTGCATTTCCTCATC
CAGATCCCATTTATCCAAATGGACAAATTTGGGACAAAGAATTGGACCTGGAACACAAACCT
AGACTACACGTAACTGCACCATTTGTTTGTAAAAACAACCCACCAGGTCAACTATTTGTTCG
CTTGGGGCCTAATCTGACTGACCAATTTGACCCAAACAGCACAACTGTTTCTCGCATTGTTA
CATATAGCACTTTTTACTGGAAGGGTATTTTGAAATTCAAAGCCAAACTAAGACCAAATCTG
ACCTGGAATCCTGTATACCAAGCAACCACAGACTCTGTTGCCAATTCTTACATGAATGTTAA
GAAATGGCTCCCATCTGCAACTGGCAACATGCACTCTGATCCATTGATTTGTAGACCTGTGC
CTCACATGACATACTAACCAACCAACTATGTTTCTCTGTTTGCTTCACATAATACTTAAACT
AACTAGACTACAACATAAAAATATACACTTAATAATAGATTATAAAAATAACATAATATGGT
ATTGGTTAACTGTAAAAAATAATAGAACTTTTGGAATAAATATAGTTAGTTGGTTAATGTTA
GATAGAATATAAAAAGATTTTGTATTTTAAAATAAATATAGTTAGTTGGTTAATGTTAGATA
GAATATAAGAAGATTTTGTATTTGGGGAATAAAGAGGGTGGTTGGGTGGTTGGTTGGTACTC
CCTTAGACTGAATGTTAGGGACCAAAAAAATAATAAAATAATTAAAATGAACAAGGACTACT
GTCTATTCAGTTGACCAACTGAACCTATAGTATCACTATGTTTTTAGGGTGGGGGGGTGGGA
GATACATACGTTCGCTATGGACCAAGTGGTACCGGTTGGTTGCGCTCAACCAACCGGACCGG
CTTAGCCGGTCCGGTTGGTTCGAGCTTAGCAACCAACCGGTACCACTTGGTCCATAGCGAAC
ATATGGTGCACTCTCAGTACAATCTGCTCTGATGCCGCATAGTTAAGCCAGCCCCGACACCC
GCCAACACCCGCTGACGCGCCCTGACGGGCTTGTCTGCTCCCGGCATCCGCTTACAGACAAG
CTGTGACCGTCTCCGGGAGCTGCATGTGTCAGAGGTTTTCACCGTCATCACCGAAACGCGCG
AGACGAAAGGGCCTCGTGATACGCCTATTTTTATAGGTTAATGTCATGATAATAATGGTTTC
TTAGACGTCAGGTGGCACTTTTCGGGGAAATGTGCGCGGAACCCCTATTTGTTTATTTTTCT
AAATACATTCAAATATGTATCCGCTCATGAGACAATAACCCTGATAAATGCTTCAATAATAT
TGAAAAAGGAAGAGTATGAGTATTCAACATTTCCGTGTCGCCCTTATTCCCTTTTTTGCGGC
ATTTTGCCTTCCTGTTTTTGCTCACCCAGAAACGCTGGTGAAAGTAAAAGATGCTGAAGATC
AGTTGGGTGCACGAGTGGGTTACATCGAACTGGATCTCAACAGCGGTAAGATCCTTGAGAGT
TTTCGCCCCGAAGAACGTTTTCCAATGATGAGCACTTTTAAAGTTCTGCTATGTGGCGCGGT
ATTATCCCGTATTGACGCCGGGCAAGAGCAACTCGGTCGCCGCATACACTATTCTCAGAATG
ACTTGGTTGAGTACTCACCAGTCACAGAAAAGCATCTTACGGATGGCATGACAGTAAGAGAA
TTATGCAGTGCTGCCATAACCATGAGTGATAACACTGCGGCCAACTTACTTCTGACAACGAT
CGGAGGACCGAAGGAGCTAACCGCTTTTTTGCACAACATGGGGGATCATGTAACTCGCCTTG
ATCGTTGGGAACCGGAGCTGAATGAAGCCATACCAAACGACGAGCGTGACACCACGATGCCT
GTAGCAATGGCAACAACGTTGCGCAAACTATTAACTGGCGAACTACTTACTCTAGCTTCCCG
GCAACAATTAATAGACTGGATGGAGGCGGATAAAGTTGCAGGACCACTTCTGCGCTCGGCCC
TTCCGGCTGGCTGGTTTATTGCTGATAAATCTGGAGCCGGTGAGCGTGGGTCTCGCGGTATC
ATTGCAGCACTGGGGCCAGATGGTAAGCCCTCCCGTATCGTAGTTATCTACACGACGGGGAG
TCAGGCAACTATGGATGAACGAAATAGACAGATCGCTGAGATAGGTGCCTCACTGATTAAGC
ATTGGTAACTGTCAGACCAAGTTTACTCATATATACTTTAGATTGATTTAAAACTTCATTTT
TAATTTAAAAGGATCTAGGTGAAGATCCTTTTTGATAATCTCATGACCAAAATCCCTTAACG
TGAGTTTTCGTTCCACTGAGCGTCAGACCCCGTAGAAAAGATCAAAGGATCTTCTTGAGATC
CTTTTTTTCTGCGCGTAATCTGCTGCTTGCAAACAAAAAAACCACCGCTACCAGCGGTGGTT
TGTTTGCCGGATCAAGAGCTACCAACTCTTTTTCCGAAGGTAACTGGCTTCAGCAGAGCGCA
GATACCAAATACTGTTCTTCTAGTGTAGCCGTAGTTAGGCCACCACTTCAAGAACTCTGTAG
CACCGCCTACATACCTCGCTCTGCTAATCCTGTTACCAGTGGCTGCTGCCAGTGGCGATAAG
TCGTGTCTTACCGGGTTGGACTCAAGACGATAGTTACCGGATAAGGCGCAGCGGTCGGGCTG
AACGGGGGGTTCGTGCACACAGCCCAGCTTGGAGCGAACGACCTACACCGAACTGAGATACC
TACAGCGTGAGCTATGAGAAAGCGCCACGCTTCCCGAAGGGAGAAAGGCGGACAGGTATCCG

GTAAGCGGCAGGGTCGGAACAGGAGAGCGCACGAGGGAGCTTCCAGGGGGAAACGCCTGGTA
TCTTTATAGTCCTGTCGGGTTTCGCCACCTCTGACTTGAGCGTCGATTTTTGTGATGCTCGT
CAGGGGGGCGGAGCCTATGGAAAAACGCCAGCAACGCGGCCTTTTTACGGTTCCTGGCCTTT
TGCTGGCCTTTTGCTCACATGTTCTTTCCTGCGTTATCCCCTGATTCTGTGGATAACCGTAT
TACCGCCTTTGAGTGAGCTGATACCGCTCGCCGCAGCCGAACGACCGAGCGCAGCGAGTCAG
TGAGCGAGGAAGCGGAAGAGCGCCCAATACGCAAACCGCCTCTCCCCGCGCGTTGGCCGATT
CATTAATGCAGCTGGCACGACAGGTTTCCCGACTGGAAAGCGGGCAGTGAGCGCAACGCAAT
TAATGTGAGTTAGCTCACTCATTAGGCACCCCAGGCTTTACACTTTATGCTTCCGGCTCGTA
TGTTGTGTGGAATTGTGAGCGGATAACAATTTCACACAGGAAACAGCTATGACCATGATTAC
GCCAAGCTAGCTTGCATGCCTGCAGGTCG

SAT ORF and SAT^{S18N} Mutation:

M	A	P	K	Q	T	N	Q	T	L	E	S	L	M	L
ATG	GCA	CCG	AAA	CAA	ACC	AAC	CAG	ACA	CTG	GAA	TCG	CTA	ATG	CTA

E	L	N	D	Q	L	T	E	V	E	A	L	G	V	G
GAG	TTG	AAC	GAT	CAG	CTG	ACG	GAG	GTG	GAA	GCT	CTG	GGG	GTG	GGG

A	L	A	G	V	G	L	V	F	L	L	G	L	M	I
GCT	CTG	GCG	GGG	GTG	GGA	TTG	GTG	TTT	CTA	CTG	GGA	CTT	ATG	ATA

I	K	R	L	I	S	F	W	E	M	D	G	#
ATC	AAA	CGA	CTT	ATA	AGT	TTT	TGG	GAG	ATG	GAT	GGG	TAG

Figure 3. (Top Figure) Genetic Map of pH1-SAT^{S18N} plasmid. VP1 coding sequence is not shown on the map. SAT initiation codon starts 7 nucleotides downstream of VP2 AUG. (Middle Figure) Nucleotide sequence of pH1-SAT^{S18N} plasmid. SAT open reading frame (ORF) is underlined and G2883A mutation corresponding to SAT^{S18N} amino acid substitution is shown in red letter. (Bottom Figure) SAT ORF and amino acid sequence. The N18 residue is shown in red letter.

References

Adeyemi, R.O., Landry, S., Davis, M.E., Weitzman, M.D., Pintel, D.J., 2010. Parvovirus Minute Virus of Mice Induces a DNA Damage Response That Facilitates Viral Replication. PLoS pathogens 6.

Adeyemi, R.O., Pintel, D.J., 2014. The ATR Signaling Pathway Is Disabled during Infection with the Parvovirus Minute Virus of Mice. Journal of virology 88, 10189-10199.

Agbandje-McKenna, M., Llamas-Saiz, A.L., Wang, F., Tattersall, P., Rossmann, M.G., 1998. Functional implications of the structure of the murine parvovirus, minute virus of mice. Struct Fold Des 6, 1369-1381.

Ahn, J.K., Gavin, B.J., Kumar, G., Ward, D.C., 1989. Transcriptional analysis of minute virus of mice P4 promoter mutants. Journal of virology 63, 5425-5439.

Aitken, A., 2006. 14-3-3 proteins: A historic overview. Semin Cancer Biol 16, 162-172.

Allaume, X., El-Andaloussi, N., Leuchs, B., Bonifati, S., Kulkarni, A., Marttila, T., Kaufmann, J.K., Nettelbeck, D.M., Kleinschmidt, J., Rommelaere, J., Marchini, A., 2012. Retargeting of Rat Parvovirus H-1PV to Cancer Cells through Genetic Engineering of the Viral Capsid. Journal of virology 86, 3452-3465.

Angelova, A.L., Geletneky, K., Nuesch, J.P., Rommelaere, J., 2015. Tumor Selectivity of Oncolytic Parvoviruses: From in vitro and Animal Models to Cancer Patients. Frontiers in bioengineering and biotechnology 3, 55.

Anouja, F., Wattiez, R., Mousset, S., CailletFauquet, P., 1997. The cytotoxicity of the parvovirus minute virus of mice nonstructural protein NS1 is related to changes in the synthesis and phosphorylation of cell proteins. Journal of virology 71, 4671-4678.

Bar, S., Rommelaere, J., Nuesch, J.P., 2013. Vesicular transport of progeny parvovirus particles through ER and Golgi regulates maturation and cytolysis. PLoS pathogens 9, e1003605.

Barrett, L.W., Fletcher, S., Wilton, S.D., 2012. Regulation of eukaryotic gene expression by the untranslated gene regions and other non-coding elements. Cell Mol Life Sci 69, 3613-3634.

Bashir, T., Romelaere, J., Cziepluch, C., 2001. In vivo accumulation of cyclin A and cellular replication factors in autonomous parvovirus minute virus of mice-associated replication bodies. Journal of virology 75, 4394-4398.

Boisvert, M., Fernandes, S., Tijssen, P., 2010. Multiple Pathways Involved in Porcine Parvovirus Cellular Entry and Trafficking toward the Nucleus. Journal of virology 84, 7782-7792.

Brockhaus, K., Plaza, S., Pintel, D.J., Rommelaere, J., Salome, N., 1996. Nonstructural proteins NS2 of minute virus of mice associate in vivo with 14-3-3 protein family members. Journal of virology 70, 7527-7534.

Burnett, E., Tattersall, P., 2003. Reverse genetic system for the analysis of parvovirus telomeres reveals interactions between transcription factor binding sites in the hairpin stem. Journal of virology 77, 8650-8660.

Canaan, S., Zadori, Z., Ghomashchi, F., Bollinger, J., Sadilek, M., Moreau, M.E., Tijssen, P., Gelb, M.H., 2004. Interfacial enzymology of parvovirus phospholipases A(2). Journal of Biological Chemistry 279, 14502-14508.

Cautain, B., Hill, R., Pedro, N., Link, W., 2015. Components and regulation of nuclear transport processes. Febs J 282, 445-462.

Chapman, M.S., Rossmann, M.G., 1993. Structure, Sequence, and Function Correlations among Parvoviruses. Virology 194, 491-508.

Christensen, J., Cotmore, S.F., Tattersall, P., 1997. A novel cellular site-specific DNA-Binding protein cooperates with the viral NS1 polypeptide to initiate parvovirus DNA replication. Journal of virology 71, 1405-1416.

Christensen, J., Tattersall, P., 2002. Parvovirus initiator protein NS1 and RPA coordinate replication fork progression in a reconstituted DNA replication system. Journal of virology 76, 6518-6531.

Clemens, K.E., Pintel, D.J., 1988. The two transcription units of the autonomous parvovirus minute virus of mice are transcribed in a temporal order. Journal of virology 62, 1448-1451.

Cohen, S., Behzad, A.R., Carroll, J.B., Pante, N., 2006. Parvoviral nuclear import: bypassing the host nuclear-transport machinery. Journal of General Virology 87, 3209-3213.

Cohen, S., Marr, A.K., Garcin, P., Pante, N., 2011. Nuclear envelope disruption involving host caspases plays a role in the parvovirus replication cycle. Journal of virology 85, 4863-4874.

Cohen, S., Pante, N., 2005. Pushing the envelope: microinjection of Minute virus of mice into Xenopus oocytes causes damage to the nuclear envelope. Journal of General Virology 86, 3243-3252.

Cooling, L.L.W., Koerner, T.A.W., Naides, S.J., 1995. Multiple Glycosphingolipids Determine the Tissue Tropism of Parvovirus B19. J Infect Dis 172, 1198-1205.

Corbau, R., Duverger, V., Rommelaere, L., Nuesch, J.P.F., 2000. Regulation of MVM NS1 by protein kinase C: Impact of mutagenesis at consensus phosphorylation sites on replicative functions and cytopathic effects. Virology 278, 151-167.

Corbau, R., Salom, N., Rommelaere, J., Nuesch, J.P., 1999. Phosphorylation of the viral nonstructural protein NS1 during MVMp infection of A9 cells. Virology 259, 402-415.

Cornelis, J.J., Becquart, P., Duponchel, N., Salome, N., Avalosse, B.L., Namba, M., Rommelaere, J., 1988. Transformation of Human-Fibroblasts by Ionizing-Radiation, a Chemical Carcinogen, or Simian Virus-40 Correlates with an Increase in Susceptibility to the Autonomous Parvoviruses H-1 Virus and Minute Virus of Mice. Journal of virology 62, 1679-1686.

Cotmore, S.F., Agbandje-McKenna, M., Chiorini, J.A., Mukha, D.V., Pintel, D.J., Qiu, J., Soderlund-Venermo, M., Tattersall, P., Tijssen, P., Gatherer, D., Davison, A.J., 2014. The family Parvoviridae. Archives of virology 159, 1239-1247.

Cotmore, S.F., Christensen, J., Nuesch, J.P., Tattersall, P., 1995. The NS1 polypeptide of the murine parvovirus minute virus of mice binds to DNA sequences containing the motif [ACCA]2-3. Journal of virology 69, 1652-1660.

Cotmore, S.F., D'Abramo, A.M., Ticknor, C.M., Tattersall, P., 1999. Controlled conformational transitions in the MVM virion expose the VP1 N-terminus and viral genome without particle disassembly. Virology 254, 169-181.

Cotmore, S.F., DAbramo, A.M., Carbonell, L.F., Bratton, J., Tattersall, P., 1997. The NS2 polypeptide of parvovirus MVM is required for capsid assembly in murine cells. Virology 231, 267-280.

Cotmore, S.F., Gottlieb, R.L., Tattersall, P., 2007. Replication initiator protein NS1 of the parvovirus minute virus of mice binds to modular divergent sites distributed throughout duplex viral DNA. Journal of virology 81, 13015-13027.

Cotmore, S.F., Hafenstein, S., Tattersall, P., 2010. Depletion of virion-associated divalent cations induces parvovirus minute virus of mice to eject its genome in a 3'-to-5' direction from an otherwise intact viral particle. Journal of virology 84, 1945-1956.

Cotmore, S.F., Tattersall, P., 1988. The NS-1 polypeptide of minute virus of mice is covalently attached to the 5' termini of duplex replicative-form DNA and progeny single strands. Journal of virology 62, 851-860.

Cotmore, S.F., Tattersall, P., 1989. A genome-linked copy of the NS-1 polypeptide is located on the outside of infectious parvovirus particles. Journal of virology 63, 3902-3911.

Cotmore, S.F., Tattersall, P., 1990a. Alternate Splicing in a Parvoviral Nonstructural Gene Links a Common Amino-Terminal Sequence to Downstream Domains Which Confer Radically Different Localization and Turnover Characteristics. Virology 177, 477-487.

Cotmore, S.F., Tattersall, P., 1990b. Alternate splicing in a parvoviral nonstructural gene links a common amino-terminal sequence to downstream domains which confer radically different localization and turnover characteristics. Virology 177, 477-487.

Cotmore, S.F., Tattersall, P., 2005a. Encapsidation of minute virus of mice DNA: Aspects of the translocation mechanism revealed by the structure of partially packaged genomes. Virology 336, 100-112.

Cotmore, S.F., Tattersall, P., 2005b. Genome packaging sense is controlled by the efficiency of the nick site in the right-end replication origin of parvoviruses minute virus of mice and LuIII. Journal of virology 79, 2287-2300.

Cotmore, S.F., Tattersall, P., 2007. Parvoviral host range and cell entry mechanisms. Advances in virus research 70, 183-232.

Cotmore, S.F., Tattersall, P., 2014. Parvoviruses: Small Does Not Mean Simple. Annual Review of Virology, Vol 1 1, 517-+.

Cziepluch, C., Lampel, S., Grewenig, A., Grund, C., Lichter, P., Rommelaere, J., 2000. H-1 parvovirus-associated replication bodies: A distinct virus-induced nuclear structure. Journal of virology 74, 4807-4815.

Daeffler, L., Horlein, R., Rommelaere, J., Nuesch, J.P.F., 2003. Modulation of minute virus of mice cytotoxic activities through site-directed mutagenesis within the NS coding region. Journal of virology 77, 12466-12478.

De Beeck, A.O., Sobczak-Thepot, J., Sirma, H., Bourgain, F., Brechot, C., Caillet-Fauquet, P., 2001. NS1- and minute virus of mice-induced cell cycle arrest: Involvement of p53 and p21(cip1). Journal of virology 75, 11071-11078.

DeBeeck, A.O., CailletFauquet, P., 1997. The NS1 protein of the autonomous parvovirus minute virus of mice blocks cellular DNA replication: A consequence of lesions to the chromatin? Journal of virology 71, 5323-5329.

Deleu, L., Pujol, A., Faisst, S., Rommelaere, J., 1999. Activation of promoter P4 of the autonomous parvovirus minute virus of mice at early S phase is required for productive infection. Journal of virology 73, 3877-3885.

Dempe, S., Stroh-Dege, A.Y., Schwarz, E., Rommelaere, J., Dinsart, C., 2010. SMAD4: a predictive marker of PDAC cell permissiveness for oncolytic infection with parvovirus H-1PV. International journal of cancer 126, 2914-2927.

Dettwiler, S., Rommelaere, J., Nuesch, J.P.F., 1999. DNA unwinding functions of minute virus of mice NS1 protein are modulated specifically by the lambda isoform of protein kinase C. Journal of virology 73, 7410-7420.

Di Piazza, M., Mader, C., Geletneky, K., Calle, M.H.Y., Weber, E., Schlehofer, J., Deleu, L., Rommelaere, J., 2007. Cytosolic activation of cathepsins mediates parvovirus H-1-induced killing of cisplatin and TRAIL-resistant glioma cells. Journal of virology 81, 4186-4198.

Dubielzig, R., King, J.A., Weger, S., Kern, A., Kleinschmidt, J.A., 1999. Adeno-associated virus type 2 protein interactions: Formation of pre-encapsidation complexes. Journal of virology 73, 8989-8998.

Eichwald, V., Daeffler, L., Klein, M., Rommelaere, J., Salome, N., 2002. The NS2 proteins of parvovirus minute virus of mice are required for efficient nuclear egress of progeny virions in mouse cells. Journal of virology 76, 10307-10319.

Engelsma, D., Valle, N., Fish, A., Salome, N., Almendral, J.M., Fornerod, M., 2008. A supraphysiological nuclear export signal is required for parvovirus nuclear export. Molecular biology of the cell 19, 2544-2552.

Faisst, S., Faisst, S.R., Dupressoir, T., Plaza, S., Pujol, A., Jauniaux, J.C., Rhode, S.L., Rommelaere, J., 1995. Isolation of a Fully Infectious Variant of Parvovirus H-1 Supplanting the Standard Strain in Human-Cells. Journal of virology 69, 4538-4543.

Farr, G.A., Zhang, L.G., Tattersall, P., 2005. Parvoviral virions deploy a capsid-tethered lipolytic enzyme to breach the endosomal membrane during cell entry. Proceedings of the National Academy of Sciences of the United States of America 102, 17148-17153.

Fuks, F., Deleu, L., Dinsart, C., Rommelaere, J., Faisst, S., 1996. ras oncogene-dependent activation of the P4 promoter of minute virus of mice through a proximal P4 element interacting with the Ets family of transcription factors. Journal of virology 70, 1331-1339.

Garcin, P., Cohen, S., Terpstra, S., Kelly, I., Foster, L.J., Pante, N., 2013. Proteomic analysis identifies a novel function for galectin-3 in the cell entry of parvovirus. J Proteomics 79, 123-132.

Garcin, P.O., Nabi, I.R., Pante, N., 2015. Galectin-3 plays a role in minute virus of mice infection. Virology 481, 63-72.

Garijo, R., Hernandez-Alonso, P., Rivas, C., Diallo, J.S., Sanjuan, R., 2014. Experimental Evolution of an Oncolytic Vesicular Stomatitis Virus with Increased Selectivity for p53-Deficient Cells. Plos One 9.

Geletneky, K., Huesing, J., Rommelaere, J., Schlehofer, J.R., Leuchs, B., Dahm, M., Krebs, O., Doeberitz, M.V., Huber, B., Hajda, J., 2012. Phase I/IIa study of intratumoral/intracerebral or intravenous/intracerebral administration of Parvovirus H-1 (ParvOryx) in patients with progressive primary or recurrent glioblastoma multiforme: ParvOryx01 protocol. Bmc Cancer 12.

Geletneky, K., Nuesch, J.P., Angelova, A., Kiprianova, I., Rommelaere, J., 2015. Double-faceted mechanism of parvoviral oncosuppression. Current opinion in virology 13, 17-24.

Gil-Ranedo, J., Hernando, E., Riolobos, L., Dominguez, C., Kann, M., Almendral, J.M., 2015. The Mammalian Cell Cycle Regulates Parvovirus Nuclear Capsid Assembly. PLoS pathogens 11.

Girod, A., Wobus, C.E., Zadori, Z., Ried, M., Leike, K., Tijssen, P., Kleinschmidt, J.A., Hallek, M., 2002. The VP1 capsid protein of adeno-associated virus type 2 is carrying a phospholipase A2 domain required for virus infectivity. Journal of General Virology 83, 973-978.

Gu, M.L., Chen, F.X., Rhode, S.L., 1992. Parvovirus H-1 P38 Promoter Requires the Transactivation Region (Tar), an Sp1 Site, and a Tata Box for Full Activity. Virology 187, 10-17.

Gu, Z., Plaza, S., Perros, M., Cziepluch, C., Rommelaere, J., Cornelis, J.J., 1995. NF-Y controls transcription of the minute virus of mice P4 promoter through interaction with an unusual binding site. Journal of virology 69, 239-246.

Halder, S., Nam, H.J., Govindasamy, L., Vogel, M., Dinsart, C., Salome, N., McKenna, R., Agbandje-McKenna, M., 2013. Structural Characterization of H-1 Parvovirus: Comparison of Infectious Virions to Empty Capsids. Journal of virology 87, 5128-5140.

Harbison, C.E., Chiorini, J.A., Parrish, C.R., 2008. The parvovirus capsid odyssey: from the cell surface to the nucleus. Trends in microbiology 16, 208-214.

Hermiston, T.W., Kuhn, I., 2002. Armed therapeutic viruses: strategies and challenges to arming oncolytic viruses with therapeutic genes. Cancer Gene Ther 9, 1022-1035.

Hernando, E., Llamas-Saiz, A.L., Foces-Foces, C., McKenna, R., Portman, I., Agbandje-McKenna, M., Almendral, J.M., 2000. Biochemical and physical characterization of parvovirus minute virus of mice virus-like particles. Virology 267, 299-309.

Holscher, C., Sonntag, F., Henrich, K., Chen, Q.X., Beneke, J., Matula, P., Rohr, K., Kaderali, L., Beil, N., Erfle, H., Kleinschmidt, J.A., Muller, M., 2015. The SUMOylation Pathway Restricts Gene Transduction by Adeno-Associated Viruses. PLoS pathogens 11.

Hristov, G., Kramer, M., Li, J.W., El-Andaloussi, N., Mora, R., Daeffler, L., Zentgraf, H., Rommelaere, J., Marchini, A., 2010. Through Its Nonstructural Protein NS1, Parvovirus H-1 Induces Apoptosis via Accumulation of Reactive Oxygen Species. Journal of virology 84, 5909-5922.

Huang, L.Y., Halder, S., Agbandje-McKenna, M., 2014. Parvovirus glycan interactions. Current opinion in virology 7, 108-118.

J. SZELEI, Z.Z., AND P. TIJSSEN, 2006. Porcine parvovirus, in: Jonathan R. Kerr, S.F.C., Marshall E. Bloom, R. Michael Linden, Colin R. Parrish (Ed.), Parvoviruses. Edward Arnold (Publishers) Ltd, pp. 435-443.

Jackson, S.P., Bartek, J., 2009. The DNA-damage response in human biology and disease. Nature 461, 1071-1078.

Johnstone, T.G., Bazzini, A.A., Giraldez, A.J., 2016. Upstream ORFs are prevalent translational repressors in vertebrates. The EMBO journal 35, 706-723.

Jongeneel, C.V., Sahli, R., McMaster, G.K., Hirt, B., 1986. A precise map of splice junctions in the mRNAs of minute virus of mice, an autonomous parvovirus. Journal of virology 59, 564-573.

Kaelber, J.T., Demogines, A., Harbison, C.E., Allison, A.B., Goodman, L.B., Ortega, A.N., Sawyer, S.L., Parrish, C.R., 2012. Evolutionary reconstructions of the transferrin receptor of Caniforms supports canine parvovirus being a re-emerged and not a novel pathogen in dogs. PLoS pathogens 8, e1002666.

Kantola, K., Hedman, L., Arthur, J., Alibeto, A., Delwart, E., Jartti, T., Ruuskanen, O., Hedman, K., Soderlund-Venermo, M., 2011. Seroepidemiology of Human Bocaviruses 1-4. J Infect Dis 204, 1403-1412.

Kaufman, H.L., Kohlhapp, F.J., Zloza, A., 2015. Oncolytic viruses: a new class of immunotherapy drugs. Nature Reviews Drug Discovery 14, 642-+.

Ke n n eth I . B e rn s , C.o.l.i.n.R.P.a.r., 2013. Parvoviridae, in: David M. Knipe, P.M.H. (Ed.), Fields Virology, Sixth Edition ed. Lippincott Williams & Wilkins, Philadelphia, pp. 1768-1791.

Kern, A., Schmidt, K., Leder, C., Muller, O.J., Wobus, C.E., Bettinger, K., Von der Lieth, C.W., King, J.A., Kleinschmidt, J.A., 2003. Identification of a heparin-binding motif on adeno-associated virus type 2 capsids. Journal of virology 77, 11072-11081.

Kestler, J., Neeb, B., Struyf, S., Van Damme, J., Cotmore, S.F., D'Abramo, A., Tattersall, P., Rommelaere, J., Dinsart, C., Cornelis, J.J., 1999a. cis requirements for the efficient production of recombinant DNA vectors based on autonomous parvoviruses. Hum Gene Ther 10, 1619-1632.

Kestler, J., Neeb, B., Struyf, S., Van Damme, J., Cotmore, S.F., D'Abramo, A., Tattersall, P., Rommelaere, J., Dinsart, C., Cornelis, J.J., 1999b. cis requirements for the efficient production of recombinant DNA vectors based on autonomous parvoviruses. Hum Gene Ther 10, 1619-1632.

King, J.A., Dubielzig, R., Grimm, D., Kleinschmidt, J.A., 2001. DNA helicase-mediated packaging of adeno-associated virus type 2 genomes into preformed capsids. Embo Journal 20, 3282-3291.

Kontou, M., Govindasamy, L., Nam, H.J., Bryant, N., Llamas-Saiz, A.L., Foces-Foces, C., Hernando, E., Rubio, M.P., McKenna, R., Almendral, J.M., Agbandje-McKenna, M., 2005. Structural determinants of tissue tropism and in vivo pathogenicity for the parvovirus minute virus of mice. Journal of virology 79, 10931-10943.

Kotterman, M.A., Schaffer, D.V., 2014. Engineering adeno-associated viruses for clinical gene therapy. Nature Reviews Genetics 15, 445-451.

Kozak, M., 2002. Pushing the limits of the scanning mechanism for initiation of translation. Gene 299, 1-34.

Krady, J.K., Ward, D.C., 1995. Transcriptional Activation by the Parvoviral Nonstructural Protein Ns-1 Is Mediated Via a Direct Interaction with Sp1. Molecular and Cellular Biology 15, 524-533.

Legendre, D., Rommelaere, J., 1994. Targeting of promoters for trans activation by a carboxy-terminal domain of the NS-1 protein of the parvovirus minute virus of mice. Journal of virology 68, 7974-7985.

Li, J., Bonifati, S., Hristov, G., Marttila, T., Valmary-Degano, S., Stanzel, S., Schnolzer, M., Mougin, C., Aprahamian, M., Grekova, S.P., Raykov, Z., Rommelaere, J., Marchini, A., 2013. Synergistic combination of valproic acid and oncolytic parvovirus H-1PV as a potential therapy against cervical and pancreatic carcinomas. EMBO molecular medicine 5, 1537-1555.

Li, X., Rhode, S.L., 1991. Nonstructural Protein Ns2 of Parvovirus H-1 Is Required for Efficient Viral Protein-Synthesis and Virus Production in Rat-Cells Invivo and Invitro. Virology 184, 117-130.

Li, X., Rhode, S.L., 1993. The Parvovirus H-1 Ns2 Protein Affects Viral Gene-Expression through Sequences in the 3' Untranslated Region. Virology 194, 10-19.

Lindahl, T., Barnes, D.E., 2000. Repair of endogenous DNA damage. Cold Spring Harbor Symposia on Quantitative Biology 65, 127-133.

Llamas-Saiz, A.L., Agbandje-McKenna, M., Parker, J.S., Wahid, A.T., Parrish, C.R., Rossmann, M.G., 1996. Structural analysis of a mutation in canine parvovirus which controls antigenicity and host range. Virology 225, 65-71.

Lombardo, E., Ramirez, J.C., Garcia, J., Almendral, J.M., 2002. Complementary roles of multiple nuclear targeting signals in the capsid proteins of the parvovirus minute virus of mice during assembly and onset of infection. Journal of virology 76, 7049-7059.

Lopez-Bueno, A., Rubio, M.P., Bryant, N., McKenna, R., Agbandje-McKenna, M., Almendral, J.M., 2006. Host-selected amino acid changes at the sialic acid binding pocket of the parvovirus capsid modulate cell binding affinity and determine virulence. Journal of virology 80, 1563-1573.

Lopez-Bueno, A., Valle, N., Gallego, J.M., Perez, J., Almendral, J.M., 2004. Enhanced cytoplasmic sequestration of the nuclear export receptor CRM1 by NS2 mutations developed in the host regulates parvovirus fitness. Journal of virology 78, 10674-10684.

Lorson, C., Burger, L.R., Mouw, M., Pintel, D.J., 1996. Efficient transactivation of the minute virus of mice P38 promoter requires upstream binding of NS1. Journal of virology 70, 834-842.

Lou, S., Luo, Y., Cheng, F., Huang, Q.F., Shen, W.R., Kleiboeker, S., Tisdale, J.F., Liu, Z.W., Qiu, J.M., 2012. Human Parvovirus B19 DNA Replication Induces a DNA Damage Response That Is Dispensable for Cell Cycle Arrest at Phase G(2)/M. Journal of virology 86, 10748-10758.

Macara, I.G., 2001. Transport into and out of the nucleus. Microbiology and Molecular Biology Reviews 65, 570-+.

Maija Vihinen-Ranta, C.R.P., 2006. Cell infection processes of autonomous parvoviruses, in: Jonathan R. Kerr, S.F.C., Marshall E. Bloom, R. Michael Linden, Colin R. Parrish (Ed.), Parvoviruses. Edward Arnold (Publishers) Ltd, pp. 1567-1162.

Mani, B., Baltzer, C., Valle, N., Almendral, J.M., Kempf, C., Ros, C., 2006. Low pH-dependent endosomal processing of the incoming parvovirus minute virus of mice virion leads to externalization of the VP1N-terminal sequence (N-VP1), N-VP2 cleavage, and uncoating of the full-length genome. Journal of virology 80, 1015-1024.

Marchini, A., Bonifati, S., Scott, E.M., Angelova, A.L., Rommelaere, J., 2015. Oncolytic parvoviruses: from basic virology to clinical applications. Virol J 12.

Maroto, B., Ramirez, J.C., Almendral, J.M., 2000. Phosphorylation status of the parvovirus minute virus of mice particle: Mapping and biological relevance of the major phosphorylation sites. Journal of virology 74, 10892-10902.

Maroto, B., Valle, N., Saffrich, R., Almendral, J.M., 2004. Nuclear export of the nonenveloped parvovirus virion is directed by an unordered protein signal exposed on the capsid surface. Journal of virology 78, 10685-10694.

Matera, A.G., Wang, Z.F., 2014. A day in the life of the spliceosome. Nat Rev Mol Cell Bio 15, 108-121.
Matlin, A.J., Clark, F., Smith, C.W.J., 2005. Understanding alternative splicing: Towards a cellular code. Nat Rev Mol Cell Bio 6, 386-398.

Miller, C.L., Pintel, D.J., 2001. The NS2 protein generated by the parvovirus minute virus of mice is degraded by the proteasome in a manner independent of ubiquitin chain elongation or activation. Virology 285, 346-355.

Miller, C.L., Pintel, D.J., 2002a. Interaction between parvovirus NS2 protein and nuclear export factor Crm1 is important for viral egress from the nucleus of murine cells. Journal of virology 76, 3257-3266.

Miller, C.L., Pintel, D.J., 2002b. Interaction between parvovirus NS2 protein and nuclear export factor Crm1 is important for viral egress from the nucleus of murine cells. Journal of virology 76, 3257-3266.

Morgan, W.R., Ward, D.C., 1986. Three splicing patterns are used to excise the small intron common to all minute virus of mice RNAs. Journal of virology 60, 1170-1174.

Morrison, D.K., 2009. The 14-3-3 proteins: integrators of diverse signaling cues that impact cell fate and cancer development. Trends Cell Biol 19, 16-23.

Naeger, L.K., Cater, J., Pintel, D.J., 1990. The Small Nonstructural Protein (Ns2) of the Parvovirus Minute Virus of Mice Is Required for Efficient DNA-Replication and Infectious Virus Production in a Cell-Type-Specific Manner. Journal of virology 64, 6166-6175.

Naeger, L.K., Salome, N., Pintel, D.J., 1993. Ns2 Is Required for Efficient Translation of Viral Messenger-Rna in Minute Virus of Mice-Infected Murine Cells. Journal of virology 67, 1034-1043.

Naeger, L.K., Schoborg, R.V., Zhao, Q., Tullis, G.E., Pintel, D.J., 1992. Nonsense mutations inhibit splicing of MVM RNA in cis when they interrupt the reading frame of either exon of the final spliced product. Genes & development 6, 1107-1119.

Nam, H.J., Gurda-Whitaker, B., Gan, W.Y., Ilaria, S., McKenna, R., Mehta, P., Alvarez, R.A., Agbandje-McKenna, M., 2006. Identification of the sialic acid structures recognized by minute virus of mice and the role of binding affinity in virulence adaptation. Journal of Biological Chemistry 281, 25670-25677.

Neu, U., Bauer, J., Stehle, T., 2011. Viruses and sialic acids: rules of engagement. Curr Opin Struc Biol 21, 610-618.

Nuesch, J.P., Lachmann, S., Corbau, R., Rommelaere, J., 2003. Regulation of minute virus of mice NS1 replicative functions by atypical PKClambda in vivo. Journal of virology 77, 433-442.

Nuesch, J.P., Rommelaere, J., 2006. NS1 interaction with CKII alpha: novel protein complex mediating parvovirus-induced cytotoxicity. Journal of virology 80, 4729-4739.

Nuesch, J.P., Rommelaere, J., 2007. A viral adaptor protein modulating casein kinase II activity induces cytopathic effects in permissive cells. Proceedings of the National Academy of Sciences of the United States of America 104, 12482-12487.

Nuesch, J.P.F., Corbau, R., Tattersall, P., Rommelaere, J., 1998a. Biochemical activities of minute virus of mice nonstructural protein NS1 are modulated in vitro by the phosphorylation state of the polypeptide. Journal of virology 72, 8002-8012.

Nuesch, J.P.F., Cotmore, S.F., Tattersall, P., 1992. Expression of Functional Parvoviral Ns1 from Recombinant Vaccinia Virus - Effects of Mutations in the Nucleotide-Binding Motif. Virology 191, 406-416.

Nuesch, J.P.F., Dettwiler, S., Corbau, R., Rommelaere, J., 1998b. Replicative functions of minute virus of mice NS1 protein are regulated in vitro by phosphorylation through protein kinase C. Journal of virology 72, 9966-9977.

Nuesch, J.P.F., Lacroix, J., Marchini, A., Rommelaere, J., 2012. Molecular Pathways: Rodent Parvoviruses-Mechanisms of Oncolysis and Prospects for Clinical Cancer Treatment. Clinical Cancer Research 18, 3516-3523.

Nuesch, J.P.F., Tattersall, P., 1993. Nuclear Targeting of the Parvoviral Replicator Molecule Ns1 - Evidence for Self-Association Prior to Nuclear Transport. Virology 196, 637-651.

Ohshima, T., Nakajima, T., Oishi, T., Imamoto, N., Yoneda, Y., Fukamizu, A., Yagami, K., 1999. CRM1 mediates nuclear export of nonstructural protein 2 from parvovirus minute virus of mice. Biochem Bioph Res Co 264, 144-150.

Palermo, L.M., Hueffer, K., Parrish, C.R., 2003. Residues in the apical domain of the feline and canine transferrin receptors control host-specific binding and cell infection of canine and feline parvoviruses. Journal of virology 77, 8915-8923.

Paradiso, P.R., 1984. Identification of multiple forms of the noncapsid parvovirus protein NCVP1 in H-1 parvovirus-infected cells. Journal of virology 52, 82-87.

Perros, M., Deleu, L., Vanacker, J.M., Kherrouche, Z., Spruyt, N., Faisst, S., Rommelaere, J., 1995. Upstream CREs participate in the basal activity of minute virus of mice promoter P4 and in its stimulation in ras-transformed cells. Journal of virology 69, 5506-5515.

Pollard, V.W., Malim, M.H., 1998. The HIV-1 Rev protein. Annu Rev Microbiol 52, 491-532.

Polo, S.E., Jackson, S.P., 2011. Dynamics of DNA damage response proteins at DNA breaks: a focus on protein modifications. Genes & development 25, 409-433.

Porwal, M., Cohen, S., Snoussi, K., Popa-Wagner, R., Anderson, F., Dugot-Senant, N., Wodrich, H., Dinsart, C., Kleinschmidt, J.A., Pante, N., Kann, M., 2013. Parvoviruses Cause Nuclear Envelope Breakdown by Activating Key Enzymes of Mitosis. PLoS pathogens 9.

Previsani, N., Fontana, S., Hirt, B., Beard, P., 1997. Growth of the parvovirus minute virus of mice MVMp3 in EL4 lymphocytes is restricted after cell entry and before viral DNA amplification: cell-specific differences in virus uncoating in vitro. Journal of virology 71, 7769-7780.

Qiu Jianming, Y.Y., GREGORY TULLIS, AND DAVID J. PINTEL, 2006. Parvovirus RNA processing strategies, in: Jonathan R. Kerr, S.F.C., Marshall E. Bloom, R. Michael Linden, Colin R. Parrish (Ed.), Parvoviruses. Edward Arnold (Publishers) Ltd, pp. 253-270.

Rayet, B., Lopez-Guerrero, J.A., Rommelaere, J., Dinsart, C., 1998. Induction of programmed cell death by parvovirus H-1 in U937 cells: connection with the tumor necrosis factor alpha signalling pathway. Journal of virology 72, 8893-8903.

Riolobos, L., Reguera, J., Mateu, M.G., Almendral, J.M., 2006. Nuclear transport of trimeric assembly intermediates exerts a morphogenetic control on the icosahedral parvovirus capsid. J Mol Biol 357, 1026-1038.

Riolobos, L., Valle, N., Hernando, E., Maroto, B., Kann, M., Almendral, J.M., 2010. Viral Oncolysis That Targets Raf-1 Signaling Control of Nuclear Transport. Journal of virology 84, 2090-2099.

Rommelaere, J., Geletneky, K., Angelova, A.L., Daeffler, L., Dinsart, C., Kiprianova, I., Schlehofer, J.R., Raykov, Z., 2010. Oncolytic parvoviruses as cancer therapeutics. Cytokine & Growth Factor Reviews 21, 185-195.

Ros, C., Baltzer, C., Mani, B., Kempf, C., 2006. Parvovirus uncoating in vitro reveals a mechanism of DNA release without capsid disassembly and striking differences in encapsidated DNA stability. Virology 345, 137-147.

Ros, C., Burckhardt, C.J., Kempf, C., 2002. Cytoplasmic trafficking of minute virus of mice: Low-pH requirement, routing to late endosomes, and proteasome interaction. Journal of virology 76, 12634-12645.

Ros, C., Kempf, C., 2004. The ubiquitin-proteasome machinery is essential for nuclear translocation of incoming minute virus of mice. Virology 324, 350-360.

Rubio, M.P., Lopez-Bueno, A., Almendral, J.M., 2005. Virulent variants emerging in mice infected with the apathogenic prototype strain of the parvovirus minute virus of mice exhibit a capsid with low avidity for a primary receptor. Journal of virology 79, 11280-11290.

Ruiz, Z., D'Abramo, A., Tattersall, P., 2006. Differential roles for the C-terminal hexapeptide domains of NS2 splice variants during MVM infection of murine cells. Virology 349, 382-395.

Russell, S.J., Peng, K.W., Bell, J.C., 2012a. Oncolytic virotherapy. Nature biotechnology 30, 658-670.

Russell, S.J., Peng, K.W., Bell, J.C., 2012b. Oncolytic virotherapy. Nature biotechnology 30, 658-670.

Schoborg, R.V., Pintel, D.J., 1991. Accumulation of Mvm Gene-Products Is Differentially Regulated by Transcription Initiation, Rna Processing and Protein Stability. Virology 181, 22-34.

Seymour, L.W., Fisher, K.D., 2016. Oncolytic viruses: finally delivering. British journal of cancer 114, 357-361.

Sonntag, F., Bleker, S., Leuchs, B., Fischer, R., Kleinschmidt, J.A., 2006. Adeno-associated virus type 2 capsids with externalized VP1/VP2 trafficking domains are generated prior to passage through the cytoplasm and are maintained until uncoating occurs in the nucleus. Journal of virology 80, 11040-11054.

Stencel-Baerenwald, J.E., Reiss, K., Reiter, D.M., Stehle, T., Dermody, T.S., 2014. The sweet spot: defining virus-sialic acid interactions. Nat Rev Microbiol 12, 739-749.

Suikkanen, S., Aaltonen, T., Nevalainen, M., Valilehto, O., Lindholm, L., Vuento, M., Vihinen-Ranta, M., 2003a. Exploitation of microtubule cytoskeleton and dynein during parvoviral traffic toward the nucleus. Journal of virology 77, 10270-10279.

Suikkanen, S., Antila, M., Jaatinen, A., Vihinen-Ranta, M., Vuento, M., 2003b. Release of canine parvovirus from endocytic vesicles. Virology 316, 267-280.

Tattersall, P., Shatkin, A.J., Ward, D.C., 1977. Sequence homology between the structural polypeptides of minute virus of mice. J Mol Biol 111, 375-394.

Tsao, J., Chapman, M.S., Agbandje, M., Keller, W., Smith, K., Wu, H., Luo, M., Smith, T.J., Rossmann, M.G., Compans, R.W., et al., 1991. The three-dimensional structure of canine parvovirus and its functional implications. Science 251, 1456-1464.

Tullis, G.E., Burger, L.R., Pintel, D.J., 1992. The Trypsin-Sensitive Rver Domain in the Capsid Proteins of Minute Virus of Mice Is Required for Efficient Cell Binding and Viral-Infection but Not for Proteolytic Processing Invivo. Virology 191, 846-857.

Tullis, G.E., Burger, L.R., Pintel, D.J., 1993. The Minor Capsid Protein Vp1 of the Autonomous Parvovirus Minute Virus of Mice Is Dispensable for Encapsidation of Progeny Single-Stranded-DNA but Is Required for Infectivity. Journal of virology 67, 131-141.

Varki, A., 2008. Sialic acids in human health and disease. Trends Mol Med 14, 351-360.

Vihinen-Ranta, M., Wang, D., Weichert, W.S., Parrish, C.R., 2002. The VP1 N-terminal sequence of canine parvovirus affects nuclear transport of capsids and efficient cell infection. Journal of virology 76, 1884-1891.

Vihinen-Ranta, M., Yuan, W., Parrish, C.R., 2000. Cytoplasmic trafficking of the canine parvovirus capsid and its role in infection and nuclear transport. Journal of virology 74, 4853-4859.

Wang, Z.F., Burge, C.B., 2008. Splicing regulation: From a parts list of regulatory elements to an integrated splicing code. Rna 14, 802-813.

Weiss, N., Stroh-Dege, A., Rommelaere, J., Dinsart, C., Salome, N., 2012. An In-Frame Deletion in the NS Protein-Coding Sequence of Parvovirus H-1PV Efficiently Stimulates Export and Infectivity of Progeny Virions. Journal of virology 86, 7554-7564.

Wethmar, K., 2014. The regulatory potential of upstream open reading frames in eukaryotic gene expression. Wiley interdisciplinary reviews. RNA 5, 765-778.

Wiethoff, C.M., Wodrich, H., Gerace, L., Nemerow, G.R., 2005. Adenovirus protein VI mediates membrane disruption following capsid disassembly. Journal of virology 79, 1992-2000.

Willwand, K., Hirt, B., 1993. The major capsid protein VP2 of minute virus of mice (MVM) can form particles which bind to the 3'-terminal hairpin of MVM replicative-form DNA and package single-stranded viral progeny DNA. Journal of virology 67, 5660-5663.

Wilson, G.M., Jindal, H.K., Yeung, D.E., Chen, W., Astell, C.R., 1991. Expression of Minute Virus of Mice Major Nonstructural Protein in Insect Cells - Purification and Identification of Atpase and Helicase Activities. Virology 185, 90-98.

Wolfisberg, R., Kempf, C., Ros, C., 2016. Late Maturation Steps Preceding Selective Nuclear Export and Egress of Progeny Parvovirus. Journal of virology 90, 5462-5474.

Wrzesinski, C., Tesfay, L., Salome, N., Jauniaux, J.C., Rommelaere, J., Cornelis, J., Dinsart, C., 2003. Chimeric and pseudotyped parvoviruses minimize the contamination of recombinant stocks with replication-competent viruses and identify a DNA sequence that restricts parvovirus H-1 in mouse cells. Journal of virology 77, 3851-3858.

Xie, Q., Chapman, M.S., 1996. Canine parvovirus capsid structure, analyzed at 2.9 A resolution. J Mol Biol 264, 497-520.

Yan, W., Kitzes, G., Dormishian, F., Hawkins, L., Sampson-Johannes, A., Watanabe, J., Holt, J., Lee, V., Dubensky, T., Fattaey, A., Hermiston, T., Balmain, A., Shen, Y.Q., 2003. Developing novel oncolytic adenoviruses through bioselection. Journal of virology 77, 2640-2650.

Yan, Z.Y., Zak, R., Luxton, G.W.G., Ritchie, T.C., Bantel-Schaal, U., Engelhardt, J.F., 2002. Ubiquitination of both adeno-associated virus type 2 and 5 capsid proteins affects the transduction efficiency of recombinant vectors. Journal of virology 76, 2043-2053.

Young, P.J., Jensen, K.T., Burger, L.R., Pintel, D.J., Lorson, C.L., 2002. Minute virus of mice NS1 interacts with the SMN protein, and they colocalize in novel nuclear bodies induced by parvovirus infection. Journal of virology 76, 3892-3904.

Zadori, Z., Szelei, J., Lacoste, M.C., Li, Y., Gariepy, S., Raymond, P., Allaire, M., Nabi, I.R., Tijssen, P., 2001. A viral phospholipase A2 is required for parvovirus infectivity. Developmental cell 1, 291-302.

Zadori, Z., Szelei, J., Tijssen, P., 2005. SAT: a late NS protein of porcine parvovirus. Journal of virology 79, 13129-13138.

AAV2: Aden-associated virus 2

APAR body: Autonomous parvovirus-associated replication body

ATM: Ataxia-Telangiectasia mutated

CKII: Casein kinase II

CMV: Cytomegalovirus

CPE: Cytopathic effect

CPV: Canine parvovirus

CRM-1: Chromosome region maintenance 1

Cyp.luc: Cypridina luciferase

DDR: DNA damage response

DM: Double mutant

DNA: Deoxyribonucleic acid

dRF: Dimeric Replicative form

dsDNA: Double-stranded DNA

FPV: Feline panleukopenia virus

GAPDH: Glyceraldehyde 3-phosphate dehydrogenase

Gluc: *Gaussia* luciferase

H-1PV: H-1 Parvovirus

HRP: Horse radish peroxidase

ITR: Inverted terminal repeat

MOI: Multiplicity of infection

MPV-1: Mouse parvovirus 1

mRF: Monomeric replicative form

mRNA: Messenger ribonucleic acid

MVMi: Immunosuppressive strain of minute virus of mice

MVMp: Prototype strain of minute virus of mice

NES: Nuclear export signal

NLS: Nuclear localization signal

NPC: Nuclear pore complex

NS1: Non-structural protein 1

NS2: Non-structural protein 2

ORF: Open reading frame

PCNA: Proliferating cell nuclear antigen

PCR: Polymerase chain reaction

PFU: Plaque forming unit

PIF: Parvovirus initiation factor

PKC: Protein kinase C

PLA2: Phospholipase A2

PM-I: Parvovirus mutant 1

pm-II: Parvovirus mutant 2

PM-III: Parvovirus mutant 3

PPV: Porcine parvovirus

qPCR: Quantitative polymerase chain reaction

qRT-PCR: Quantitative reverse transcriptase polymerase chain reaction

RLU: Relative light unit

RNA: Ribonucleic acid

ROS: Reactive oxygen species

RPA: replication protein A

SAT: small alternatively translated protein

SCID: Severe combined immunodeficiency

siRNA: Small interfering RNA

SMN: survival motor neuron

ssDNA: Single-stranded DNA

SUMO: Small ubiquitin-like modifiers

SV40: Simian virus 40

Tar: Transactivation response element

uORF: Upstream open reading frame

UTR: Untranslated region